MR Spectroscopic Imaging

M. Albert Thomas
Professor
Department of Radiological Sciences
University of California Los Angeles (UCLA)
athomas@mednet.ucla.edu

David Geffen School of Medicine

M219: Introduction to Magnetic Resonance Imaging 03/12/25

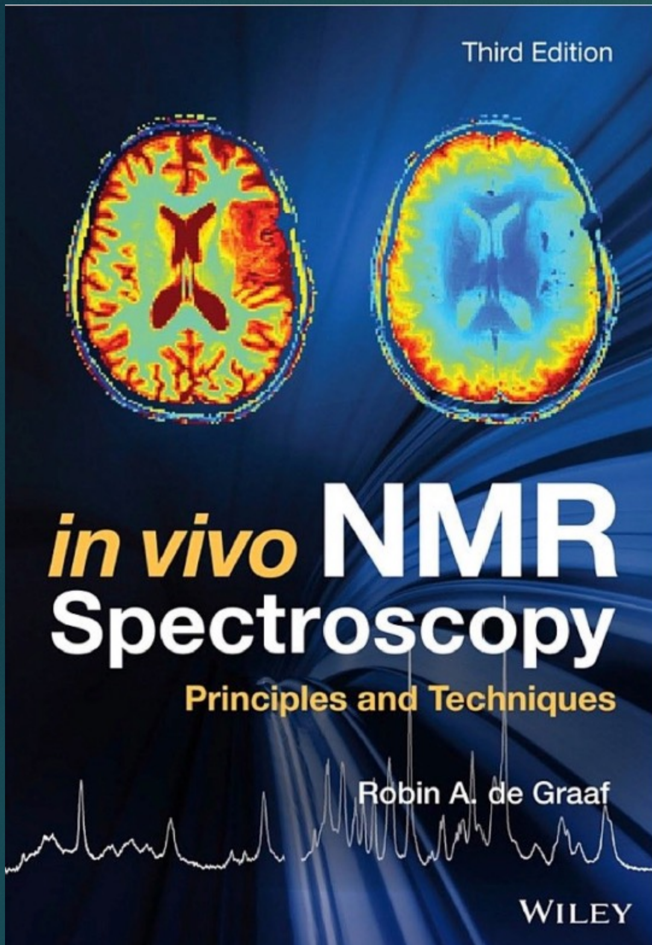
Third Edition
in vivo NMR Spectroscopy
Principles and Techniques
Robin A. de Graaf
WILEY

Contents

Important Nuclei for Biomedical MR

Nucleus	Spin	γ, MHz/T	Natural Abundance	Relative Sensitivity
^{1}H	1/2	42.576	99.985	100
^{2}H	1	6.536	0.015	0.96
^{3}He	1/2	32.433	.00013	44
^{13}C	1/2	10.705	1.108	1.6
^{17}O	3/2	5.772	0.037	2.9
^{19}F	1/2	40.055	100	83.4
^{23}Na	3/2	11.262	100	9.3
^{31}P	1/2	17.236	100	6.6
^{39}K	3/2	1.987	93.08	.05

Spin Basics

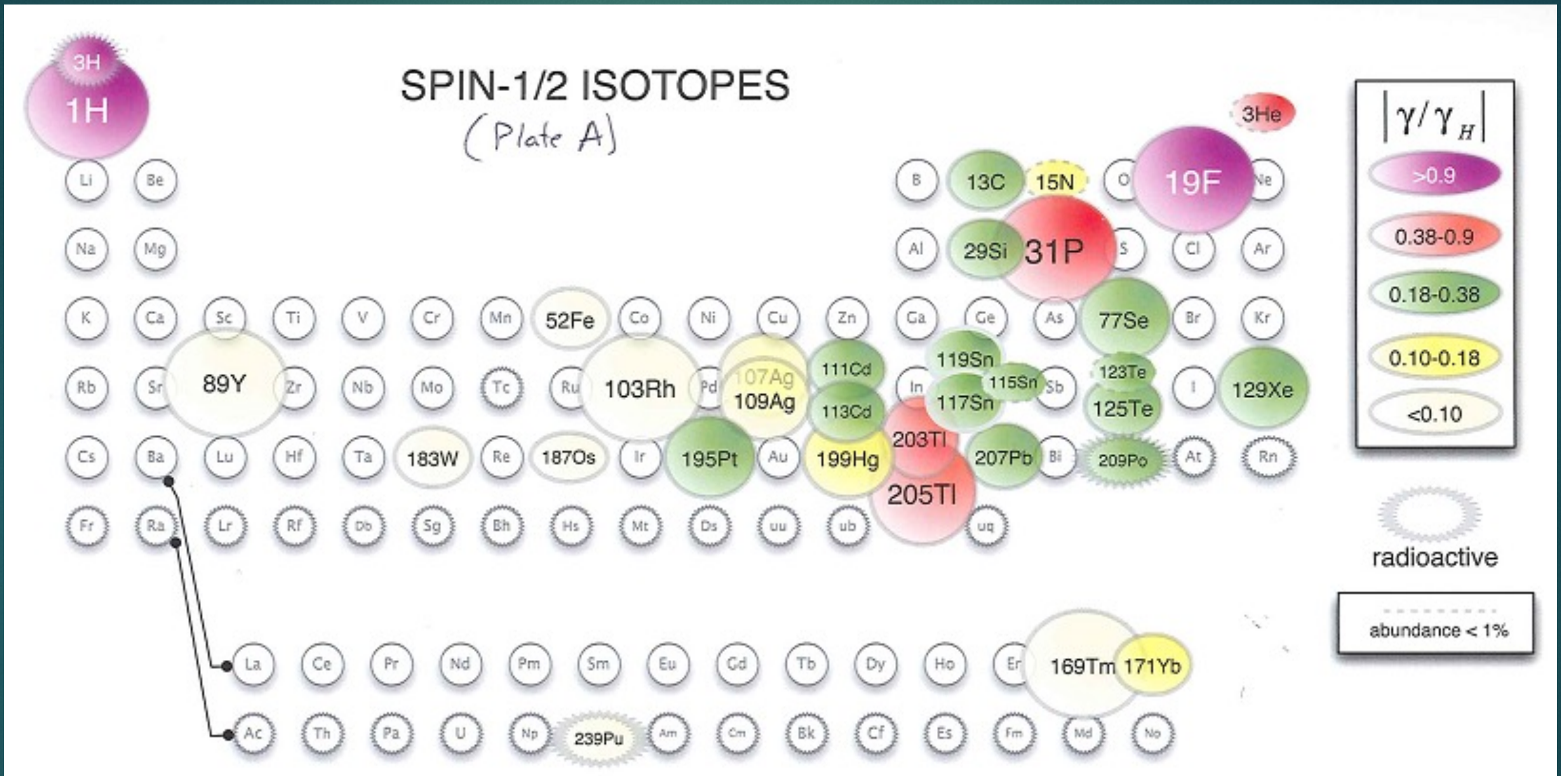

SPIN-1/2 ISOTOPES
(Plate A)
3H
1H
3He
13C
15N
19F
29Si
31P
52Fe
77Se
89Y
103Rh
107Ag
109Ag
111Cd
113Cd
119Sn
115Sn
117Sn
123Te
125Te
129Xe
183W
187Os
195Pt
199Hg
203Tl
205Tl
207Pb
209Po
169Tm
171Yb
239Pu
$|\gamma/\gamma_H|$
>0.9
0.38-0.9
0.18-0.38
0.10-0.18
<0.10
radioactive
abundance < 1%

Spin Basics

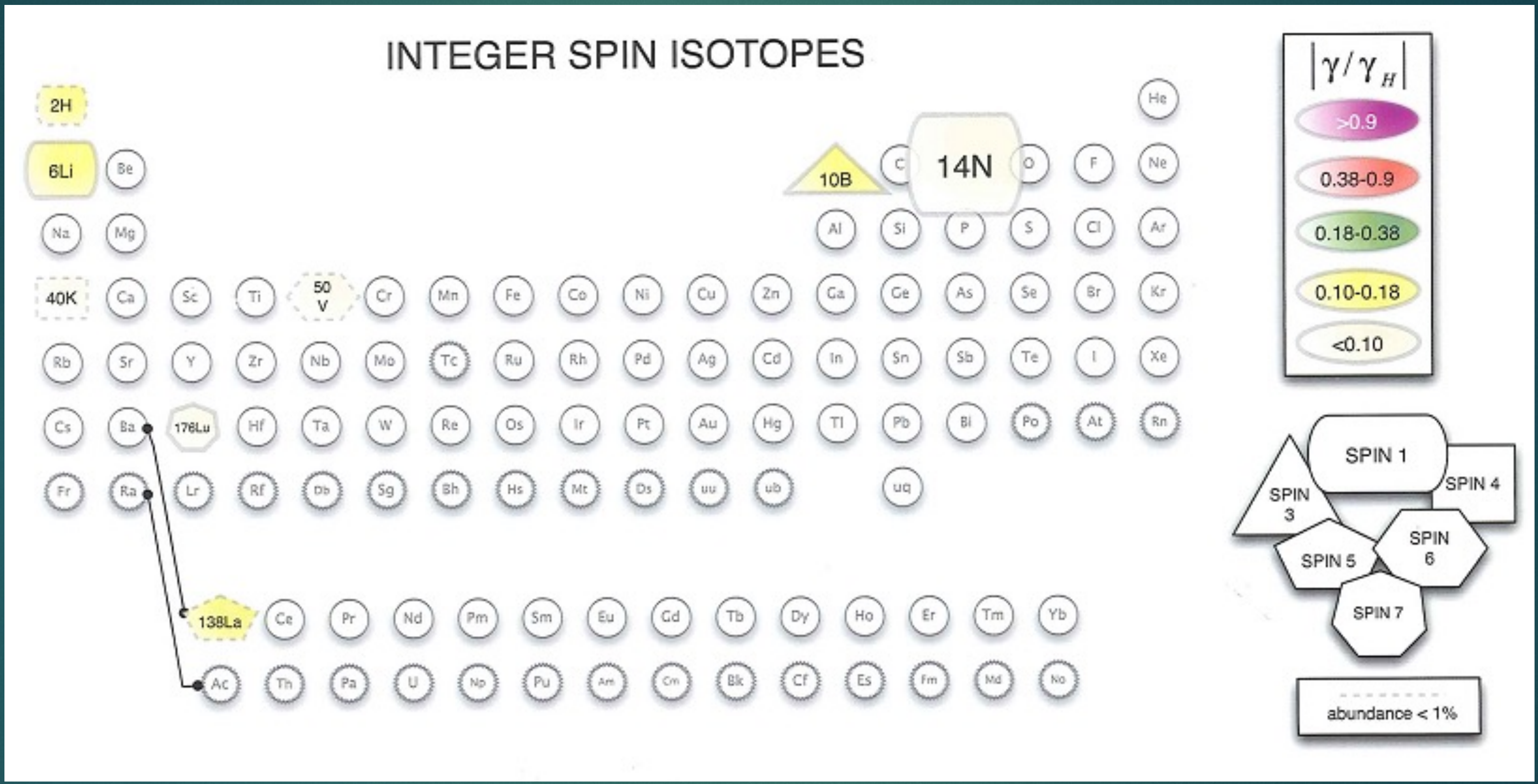

INTEGER SPIN ISOTOPES
2H
6Li
40K
50 V
10B
14N
176Lu
138La
|γ/γ_H|
>0.9
0.38-0.9
0.18-0.38
0.10-0.18
<0.10
SPIN 1
SPIN 3
SPIN 4
SPIN 5
SPIN 6
SPIN 7
abundance < 1%

Spin Basics

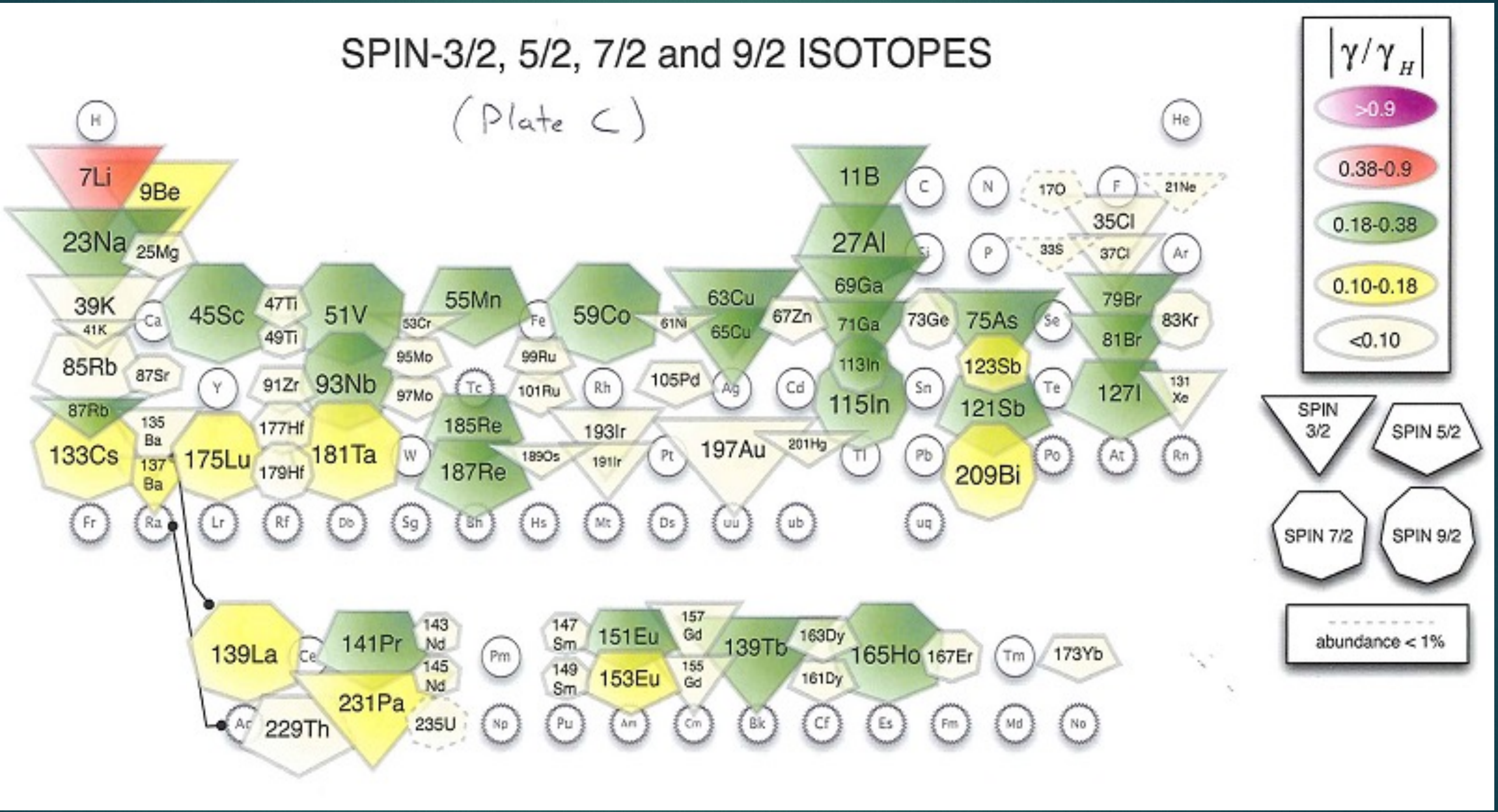
SPIN-3/2, 5/2, 7/2 and 9/2 ISOTOPES
(Plate C)
|γ/γ_H|
>0.9
0.38-0.9
0.18-0.38
0.10-0.18
<0.10
SPIN 3/2
SPIN 5/2
SPIN 7/2
SPIN 9/2
abundance < 1%
7Li
9Be
23Na
25Mg
39K
41K
85Rb
87Sr
87Rb
133Cs
135 Ba
137 Ba
45Sc
47Ti
49Ti
51V
53Cr
93Nb
95Mo
97Mo
91Zr
175Lu
177Hf
179Hf
181Ta
55Mn
185Re
187Re
59Co
99Ru
101Ru
189Os
193Ir
191Ir
61Ni
63Cu
65Cu
105Pd
197Au
67Zn
201Hg
11B
27Al
69Ga
71Ga
113In
115In
73Ge
75As
123Sb
121Sb
209Bi
17O
21Ne
35Cl
33S
37Cl
79Br
81Br
83Kr
127I
131 Xe
139La
141Pr
143 Nd
145 Nd
231Pa
229Th
235U
147 Sm
149 Sm
151Eu
153Eu
157 Gd
155 Gd
139Tb
163Dy
161Dy
165Ho
167Er
173Yb

MR Spectroscopic Imaging

- MRI- Basics and k-Space Encoding
- Single Voxel Spectroscopy
- Multi-voxel Spectroscopy/Spectroscopic Imaging
- *Acceleration Techniques*: Phase-encoding, parallel Imaging, Echo-planar Imaging, Concentric Rings, Radial Imaging and more
- Multi-dimensional MR Spectroscopic Imaging (2D spectral+3D spatial)
- Conclusions

David Geffen School of Medicine

MRI Uses Three Magnetic Fields

Static High Field (B_0)
Creates or polarizes signal
1000 Gauss to 110,000 Gauss
(Earth's field is 0.5 G)

Gradient Fields
1-4 G/cm
Used to image: determine spatial position of MR signal

Radiofrequency Field (B_1)
Excites or perturbs signal into a measurable form
On the order of 0.1 G but in resonance with MR signal
RF coils also measure MR signal
Excited or perturbed signal returns to equilibrium
Important contrast mechanism

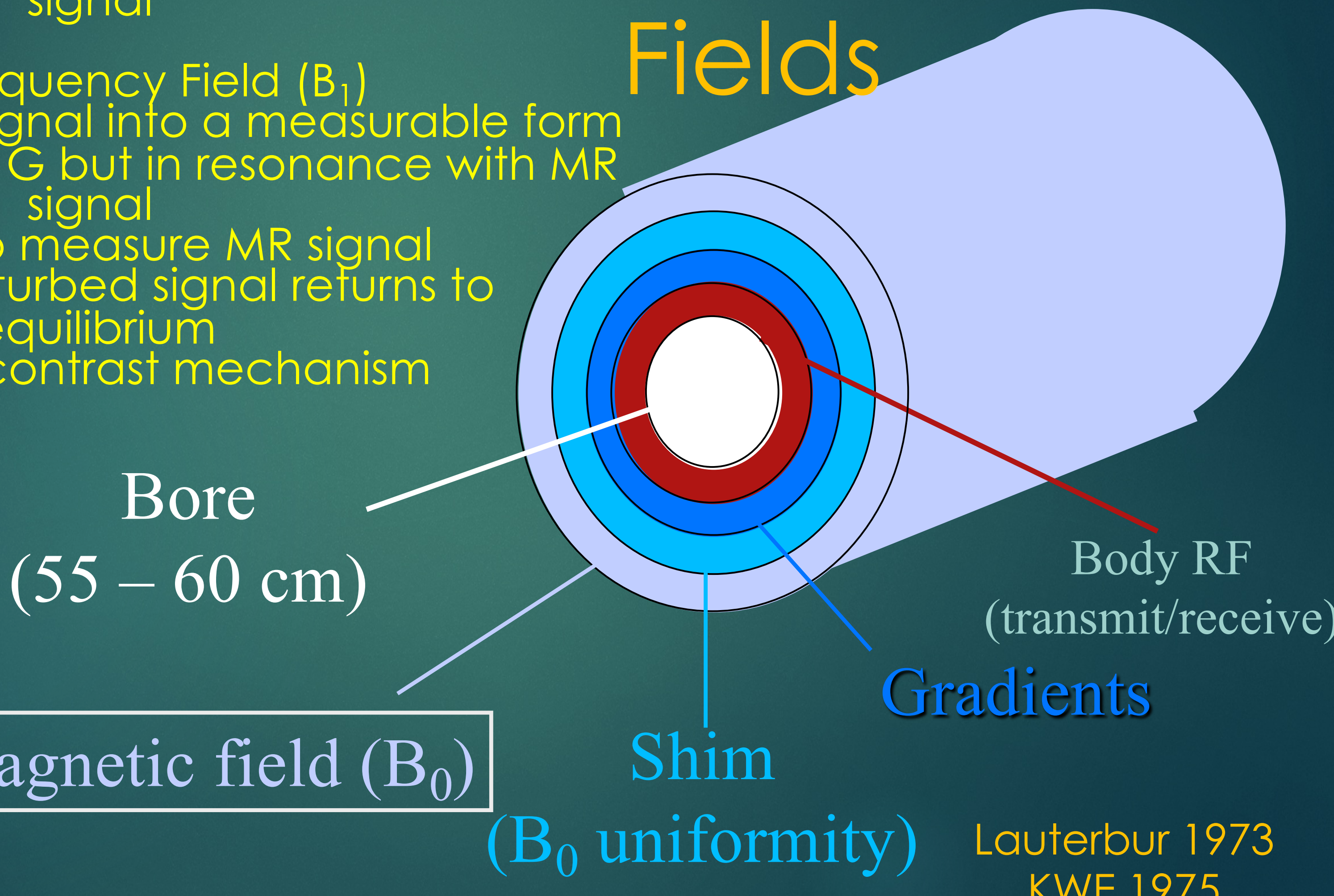

Lauterbur 1973
KWE 1975

David Geffen
School of Medicine

Effect of pulsed field gradients (X, Y, Z)- Spatial Localization

Every imaging system will have three gradient coils that can modify the static field strength (Bo) in X, Y,Z directions. Thus you have the control over changing the Larmor frequencies of nuclear spins in X,Y,Z directions

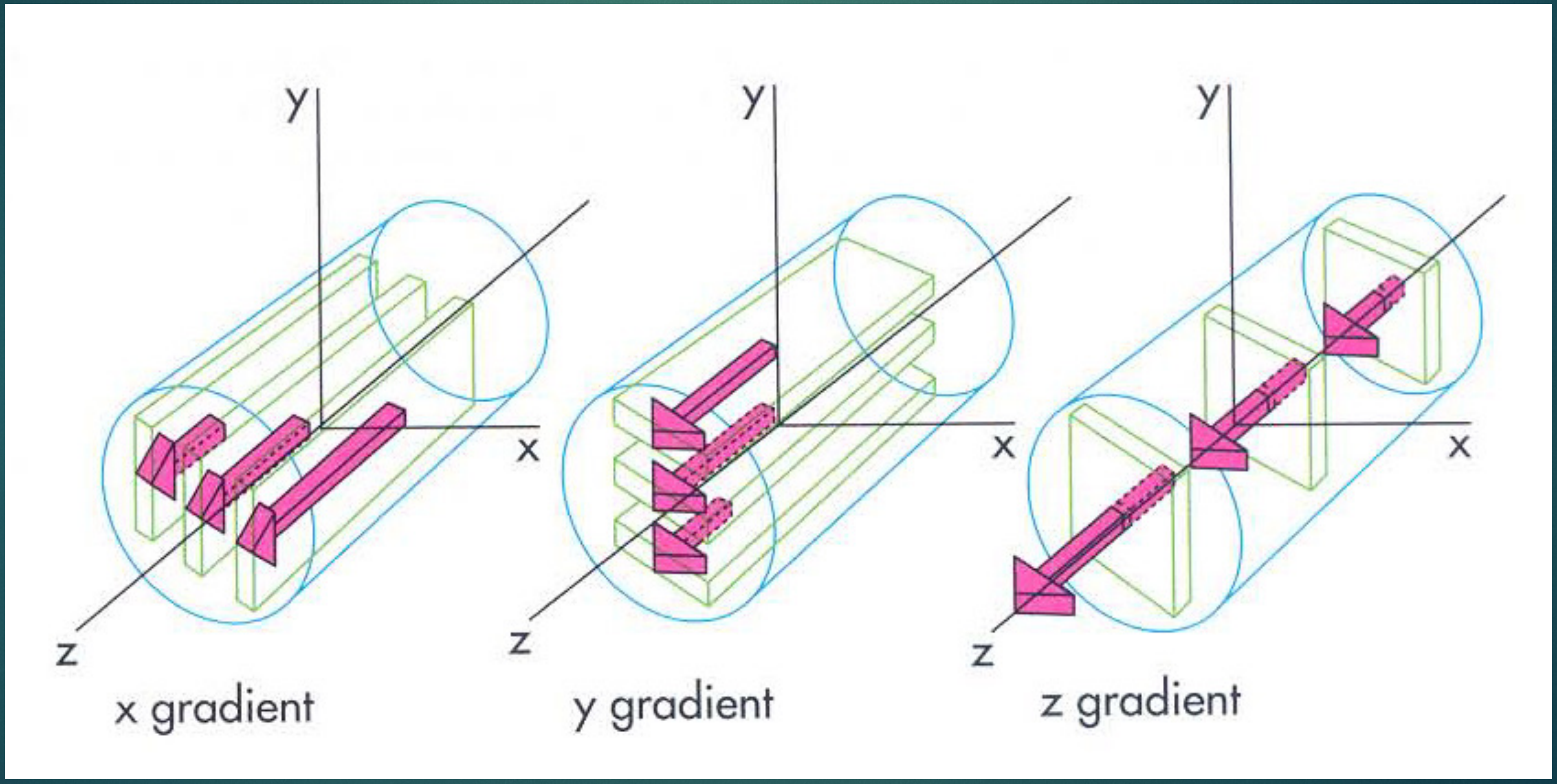

David Geffen
School of Medicine

Gradient Coils

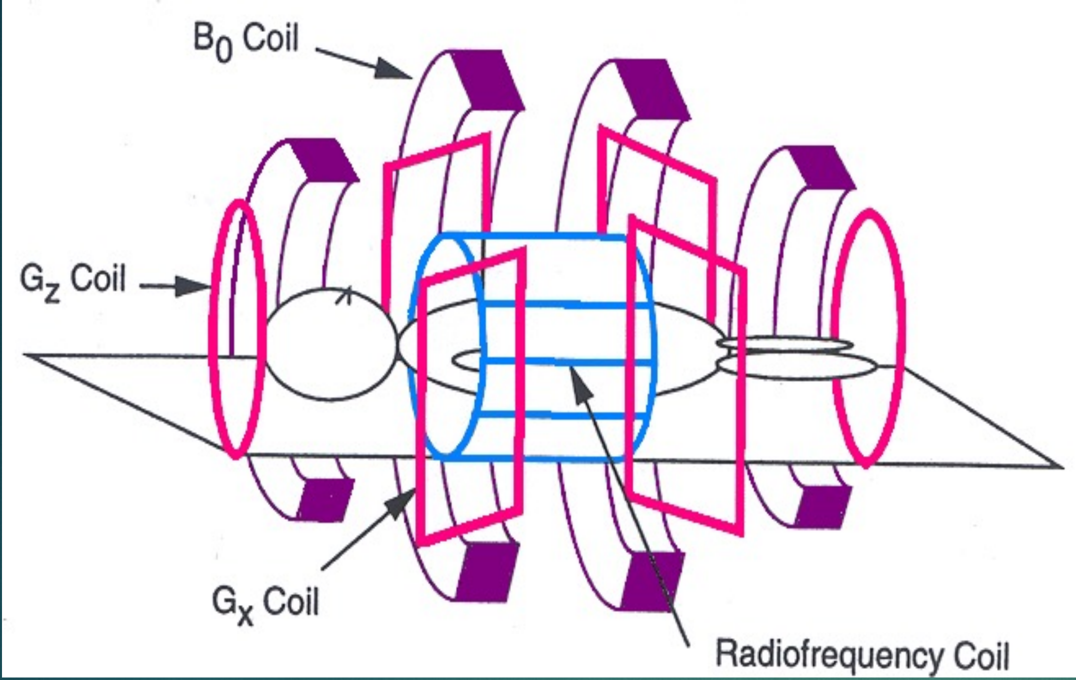

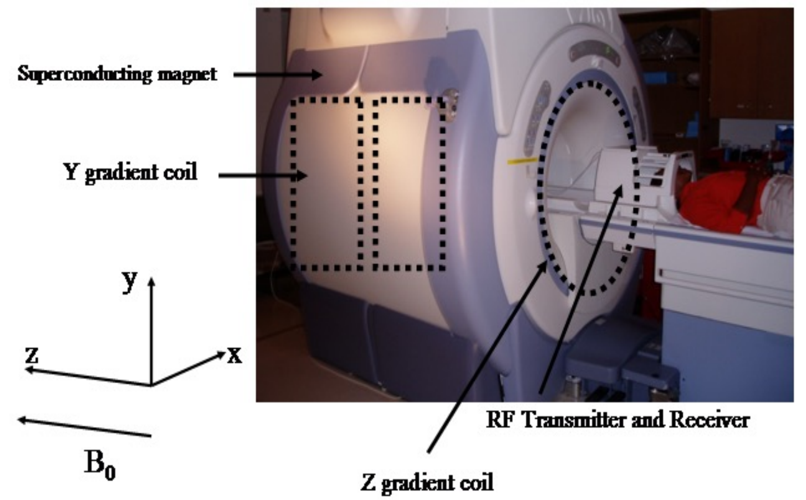

Nishimura, MRI Principles

David Geffen School of Medicine

Spatial Encoding/Slice Selection

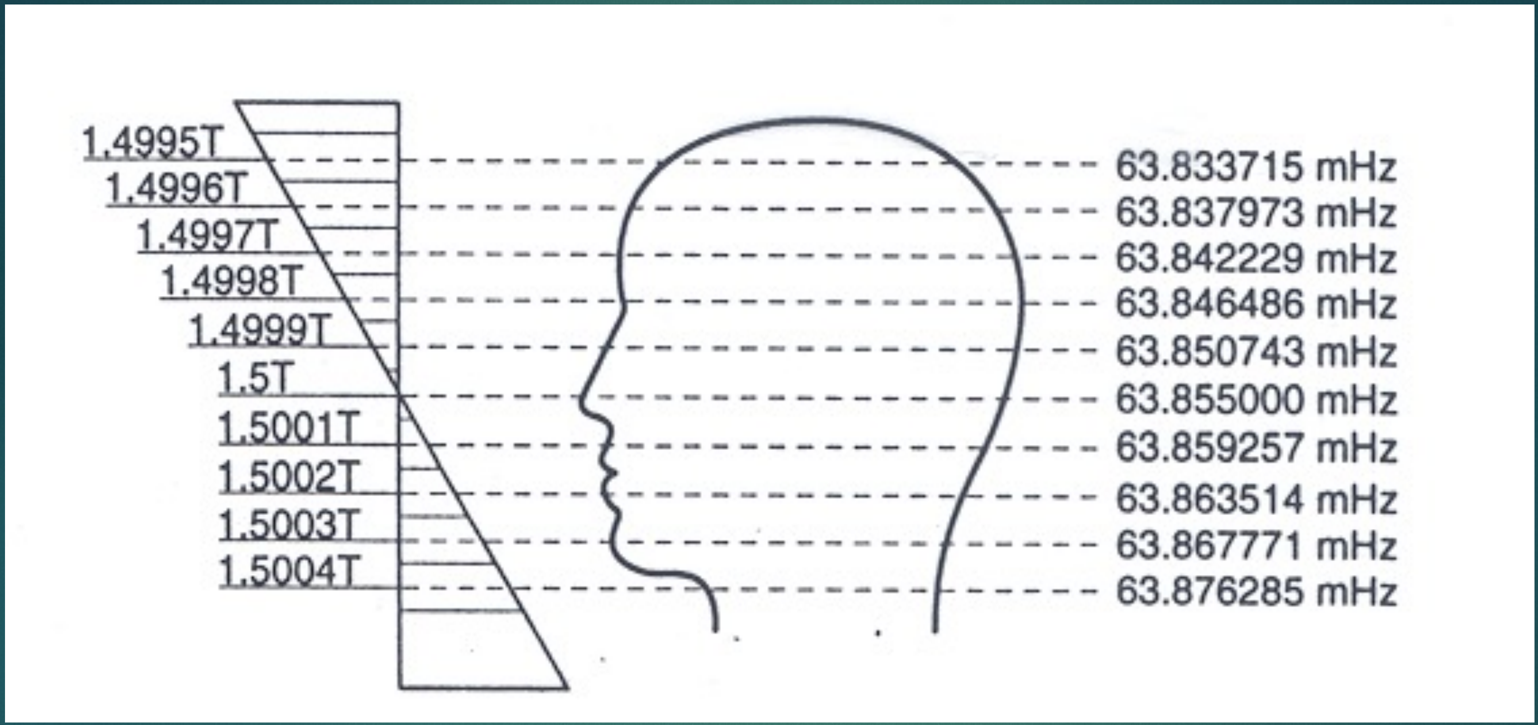

- The effects of the main magnetic field and the applied slice gradient. In this example, the local magnetic field changes in one-Gauss increments accompanied by a change in the precessional frequency from chin to the top of the head.

k-Space Acquisition

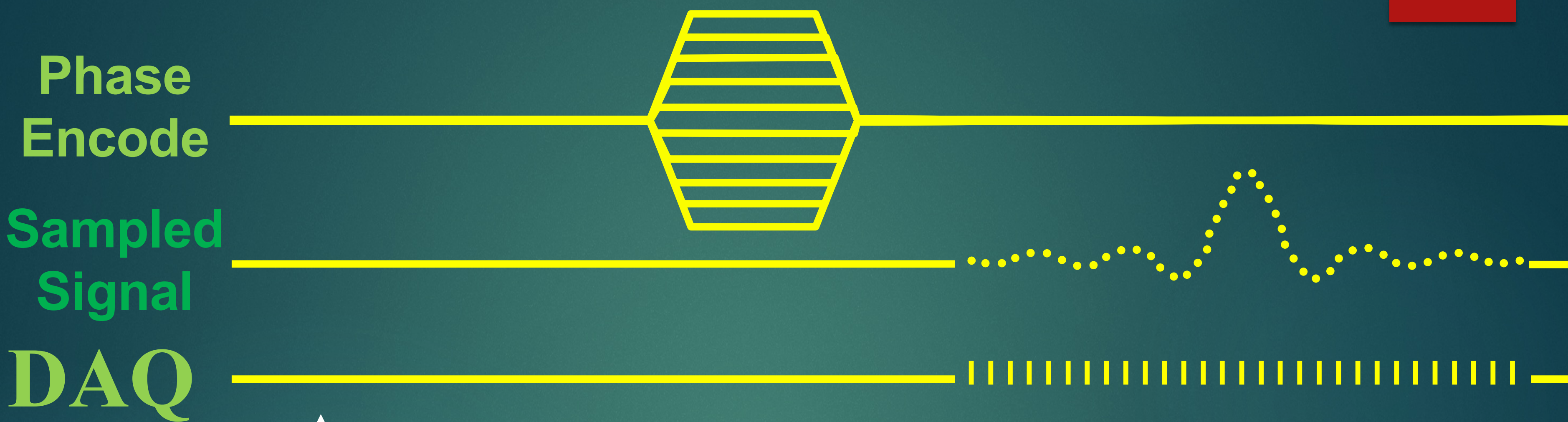

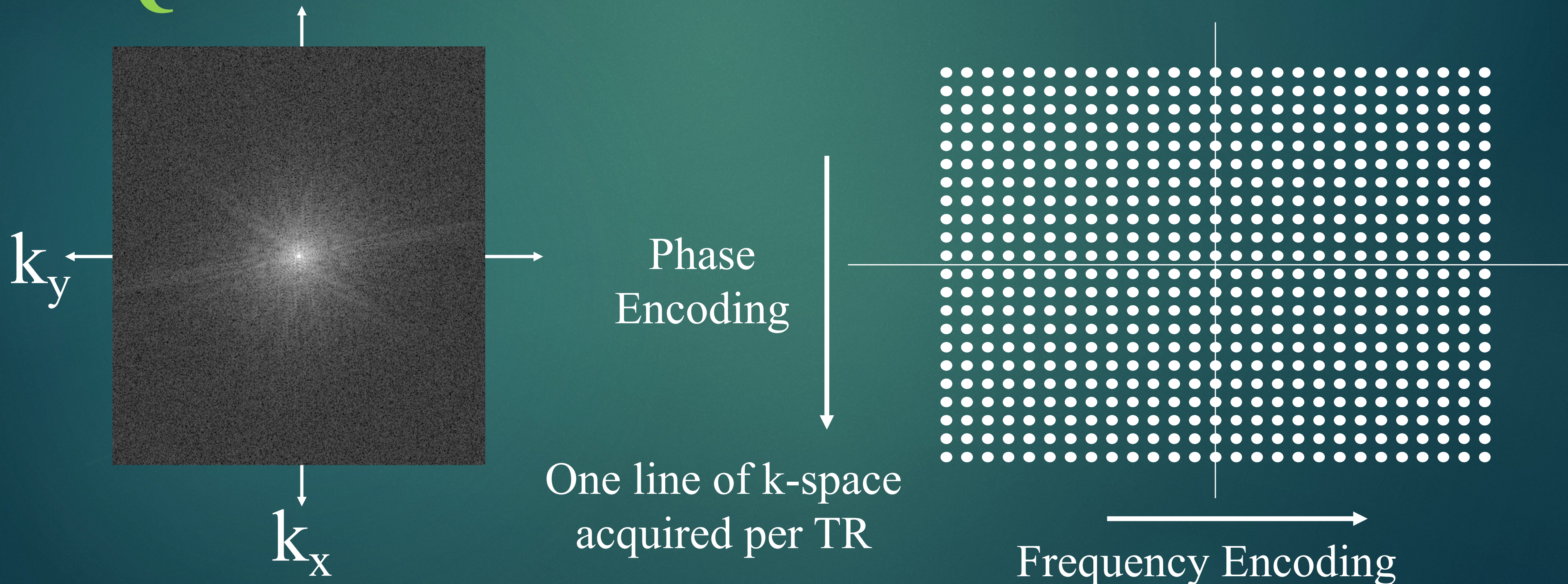

One line of k-space acquired per TR

Kumar Welti Ernst JMR 18;69-83 1975; Edelstein et al. Spin Warp Imaging. PBM 1980

Fourier Zeugmatography/Spin-Warp Imaging

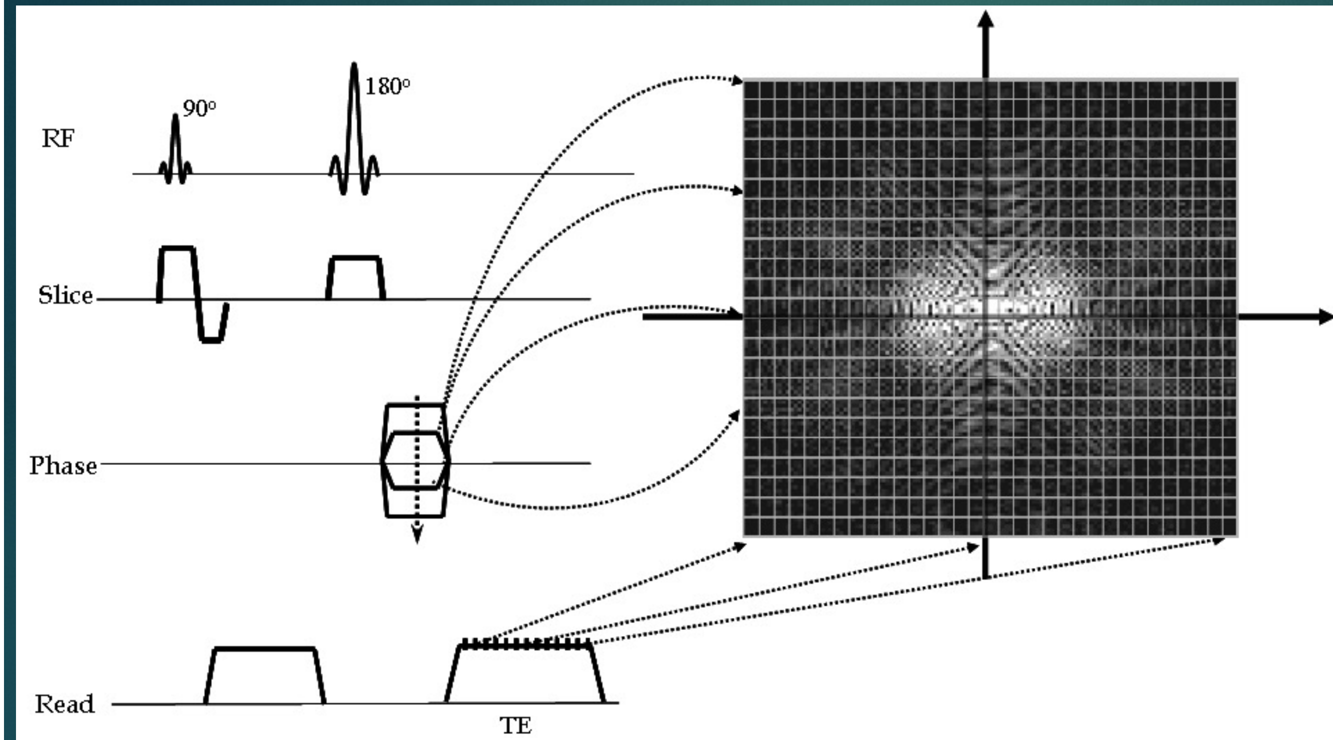

Gradient applied along the y-axis will cause the spins to precess at a frequency determined by their y position, and is called phase encoding. Next a gradient is applied along the x-axis and the spin-echo is collected. The frequency components of the echo gives information of the x-position and the phase values give information of the y-position.

$$S(t_x,t_y) = \iint \rho(x,y)\exp\left[i\gamma(G_x x t_x + G_y y t_y)\right] dx\, dy$$

$k_x = \gamma G_x t_x$ and $k_y = \gamma G_y t_y$

$$S(k_x,k_y) = \iint \rho(x,y)\exp\left[i(k_x x + k_y y)\right] dx\, dy$$

$$\rho(x,y) = \iint S(k_x,k_y)\exp\left[-i(k_x x + k_y y)\right] dx\, dy$$

Kumar Welti Ernst JMR 18;69-83 1975; Edelstein et al. Spin Warp Imaging. PBM 1980

David Geffen School of Medicine

K-Space

David Geffen School of Medicine

For a given data point in k-space, say (kx, ky), its signal S(kx, ky) is the sum of all the little signal from each voxel I(x,y) in the physical space, under the gradient field at that particular moment

$$S(k_x, k_y) = \int \int I(x, y) e^{-i2\pi(k_x x + k_y y)} dxdy$$

From this equation, it can be seen that the acquired MR signal, which is also in a 2-D space (with kx, ky coordinates), is the Fourier Transform of the imaged object.

$$Kx = \gamma/2\pi \int_0^t Gx(t)\, dt$$

$$Ky = \gamma/2\pi \int_0^t Gy(t)\, dt$$

The frequency and phase encoding gradients control the imaging trajectory in k-space

MRI, Brown et al. 1999; Principles of MRI Liang and Lauterbur 2000; MRI Pulse Sequences, Zhoe et al. 2004; EPI Theory, Technique and Application, Stehling et al. 1998

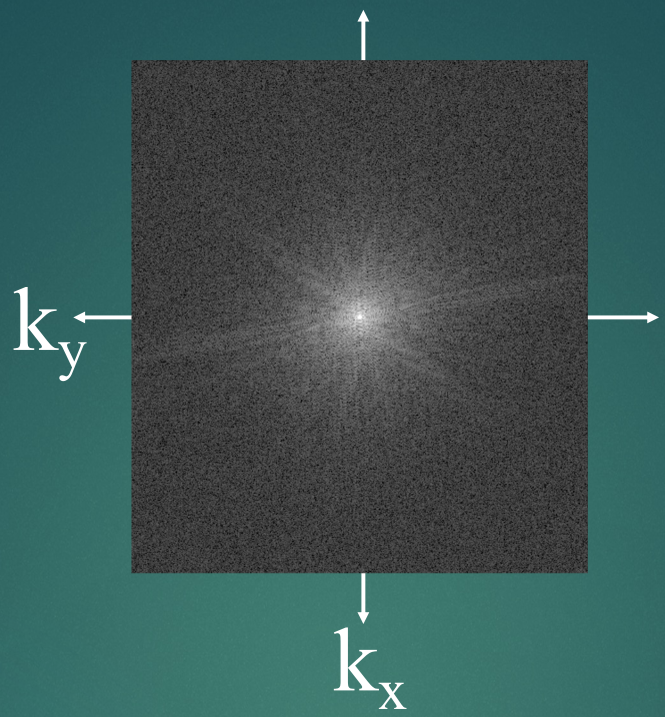

k_y
k_x

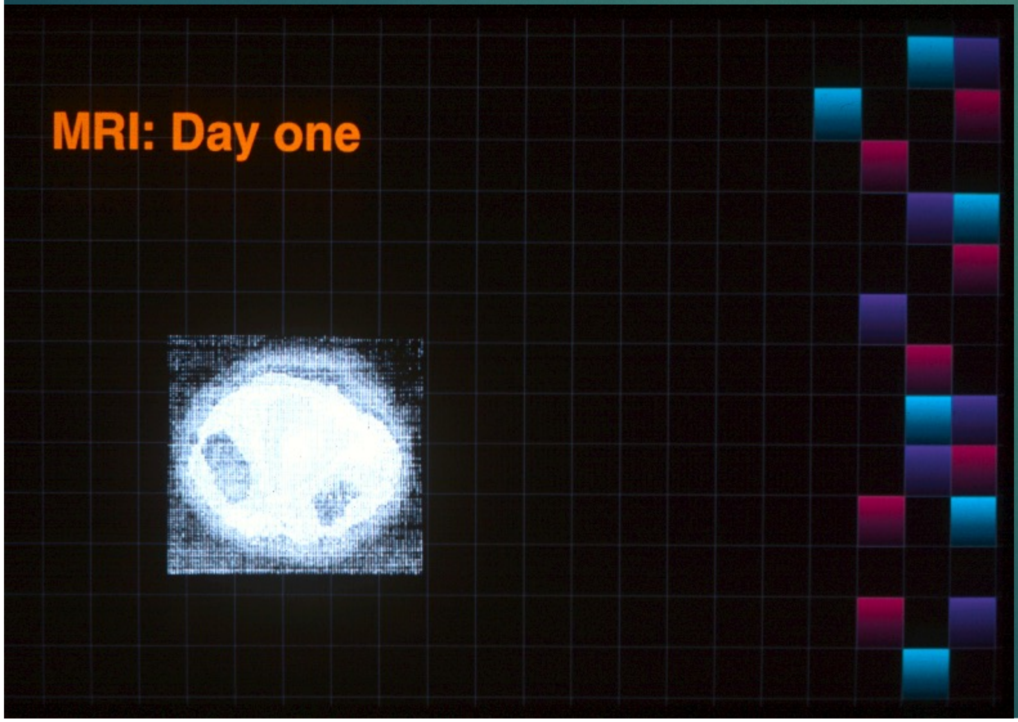

MRI: Day one

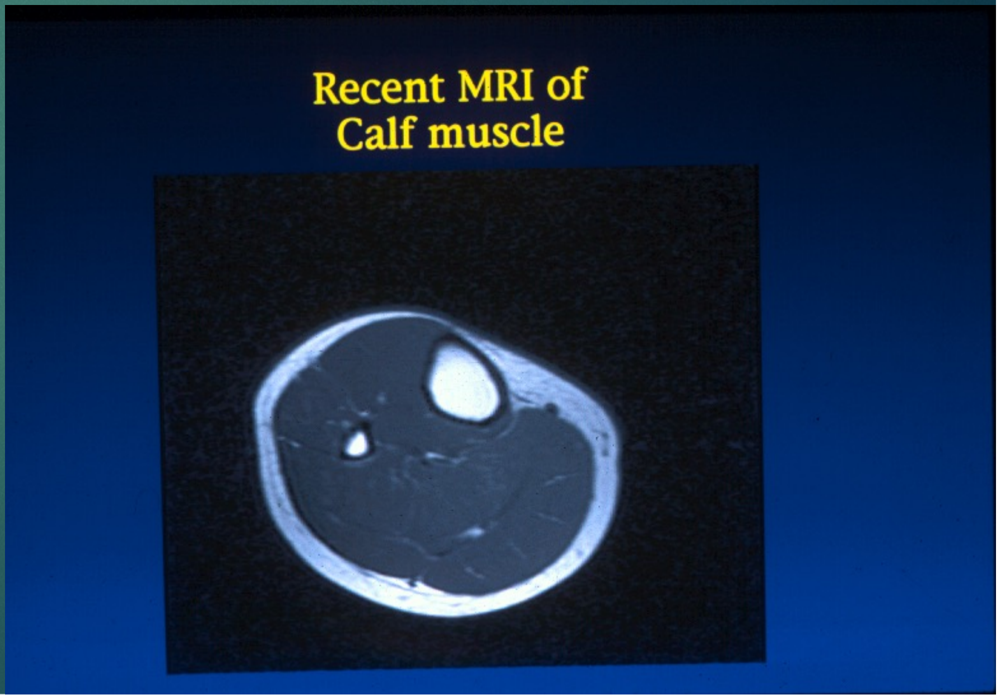

Recent MRI of
Calf muscle

Magnetic Resonance Imaging (MRI)

- MRI exploits Nuclear Magnetic Resonance (NMR) to produce water-based images
  - Signal from ^{1}H in water
  - Gray scale caused by T1/T2 relaxation and ^{1}H density within a voxel
- MRI resolution
  - 512x512 voxels in a slice
  - Sub-millimeter voxel volume
- Structural differences cause T1/T2 relaxation variation among voxels

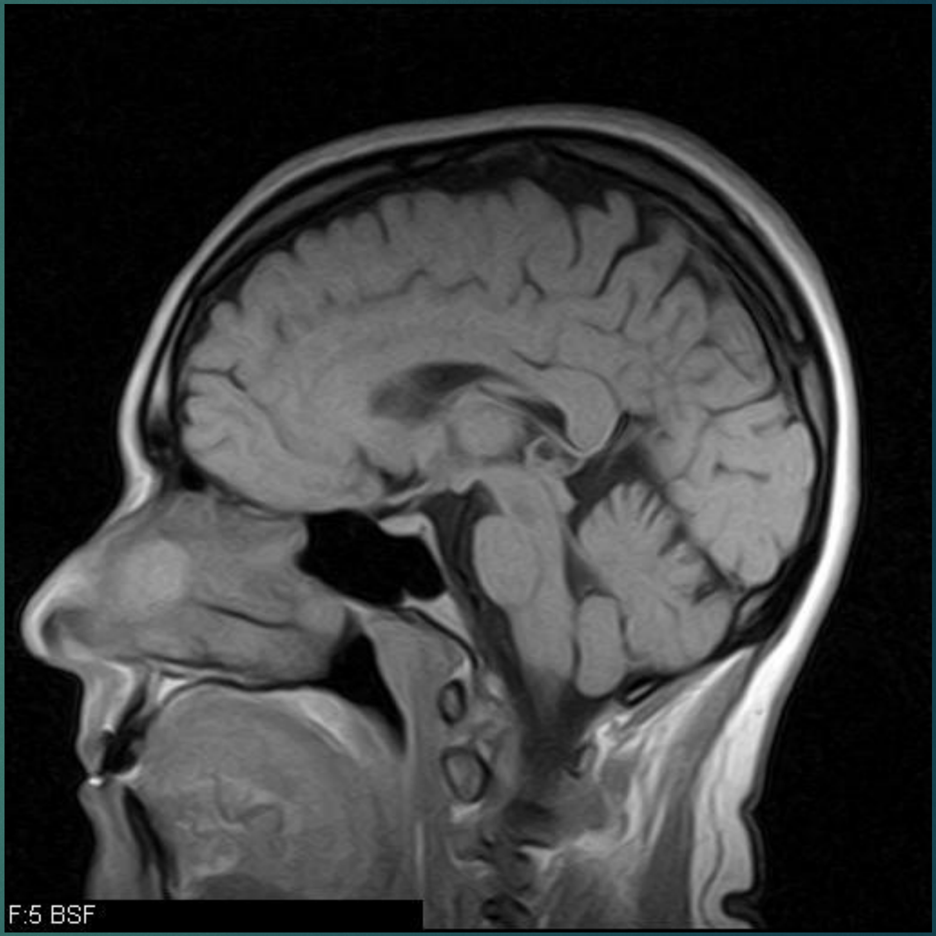

Problems with Anatomical Imaging

- Despite its superb soft tissue contrast and multiplanar capability, anatomical MRI is largely limited to depicting morphological abnormality.
- Anatomical MRI suffers from nonspecificity. Different disease processes can appear similar upon anatomic imaging, and in turn a single disease entity may have varied imaging findings.
- The underlying metabolic or functional integrity of brain cannot be adequately evaluated based on anatomical MRI alone.

- To that end, several physiology-based MRI methods have been developed to improve tumor characterization.

- Diffusion Weighted (DW) MRI/Diffusion Tensor Imaging (DTI): In addition to early diagnosis of cerebral ischemia, DW MRI is extremely sensitive in detecting other intracranial disease processes, including cerebral abscess, traumatic shearing injury, etc.
- Perfusion Imaging: Dynamic susceptibility-weighted contrast-enhanced (DSC) perfusion MRI of the brain provides hemodynamic information.
- MR Spectroscopy for biochemical characterization, Improving Specificity of cancer and more

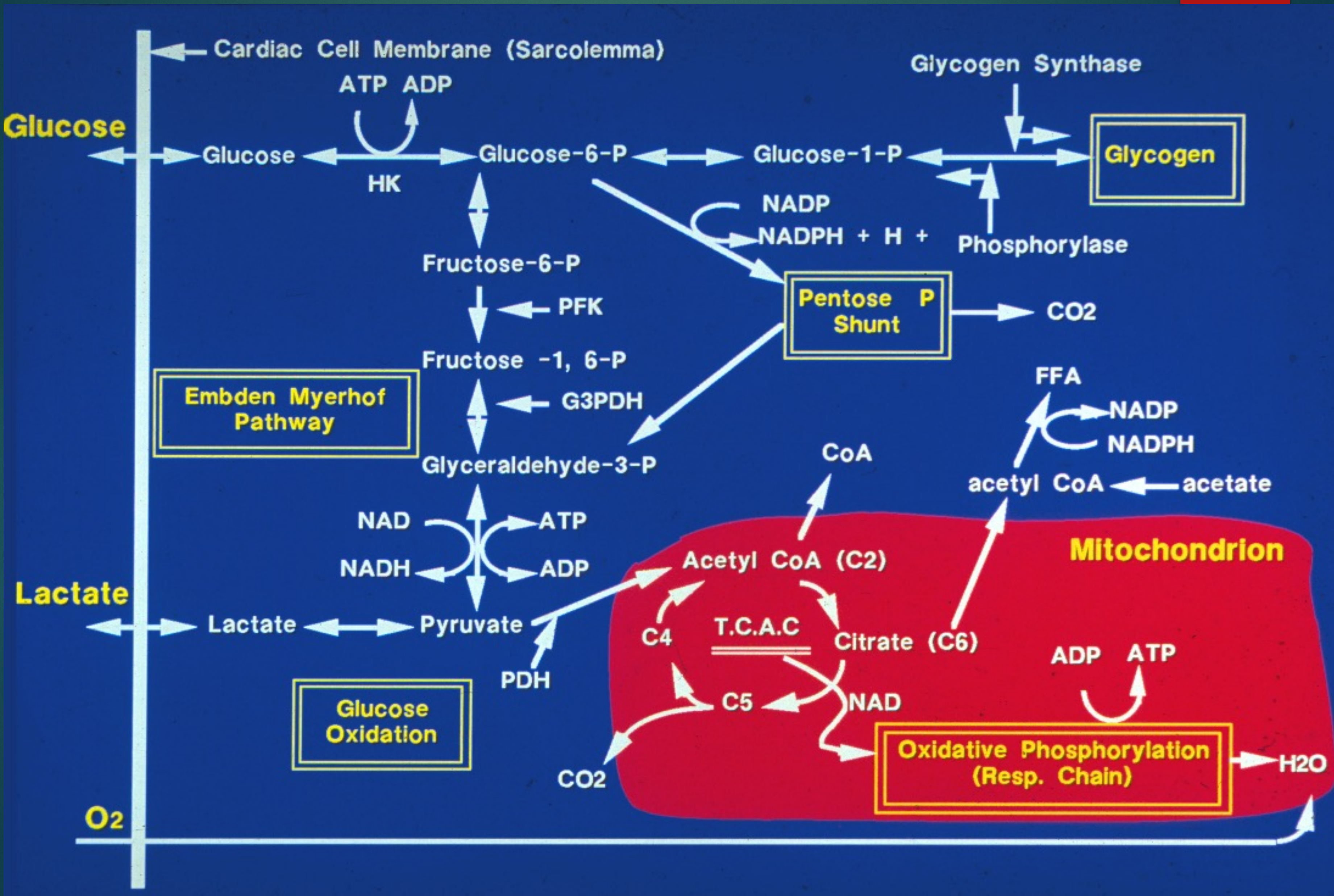
Cardiac Cell Membrane (Sarcolemma)
ATP ADP
Glucose
Glucose
HK
Glucose-6-P
Glucose-1-P
Glycogen Synthase
Glycogen
NADP
NADPH + H +
Phosphorylase
Fructose-6-P
PFK
Pentose P Shunt
CO2
Fructose -1, 6-P
G3PDH
Embden Myerhof Pathway
FFA
NADP
NADPH
Glyceraldehyde-3-P
CoA
acetyl CoA
acetate
NAD
NADH
ATP
ADP
Mitochondrion
Acetyl CoA (C2)
Lactate
Lactate
Pyruvate
C4
T.C.A.C
Citrate (C6)
PDH
ADP ATP
C5
NAD
Glucose Oxidation
CO2
Oxidative Phosphorylation (Resp. Chain)
H2O
O2

Point Resolved Spectroscopy, PRESS

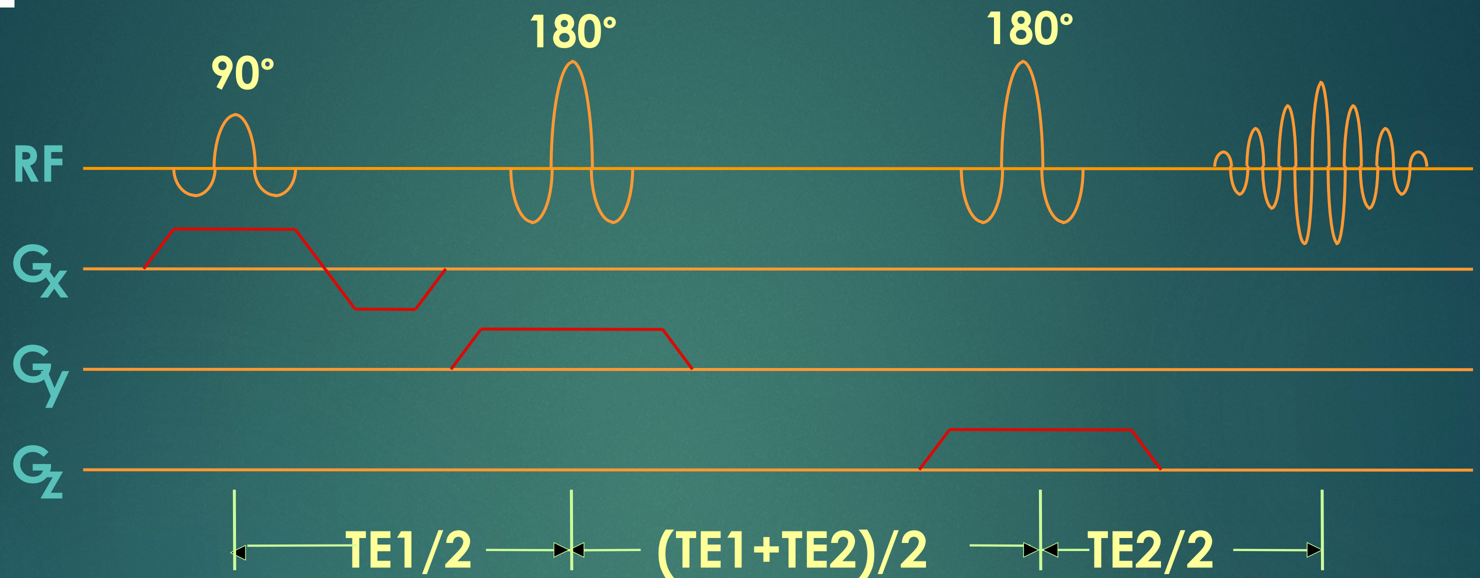

- A slice-selective 90° pulse is followed by two slice-selective 180° refocusing pulses
- Achieves localization within a single acquisition
- Suitable for signals with long T_2 – ^1H MRS

Bottomley PA. Annal NY Acad Sci 1987; 508: 333-348.

STEAM: Frahm MRM 1989

Localization

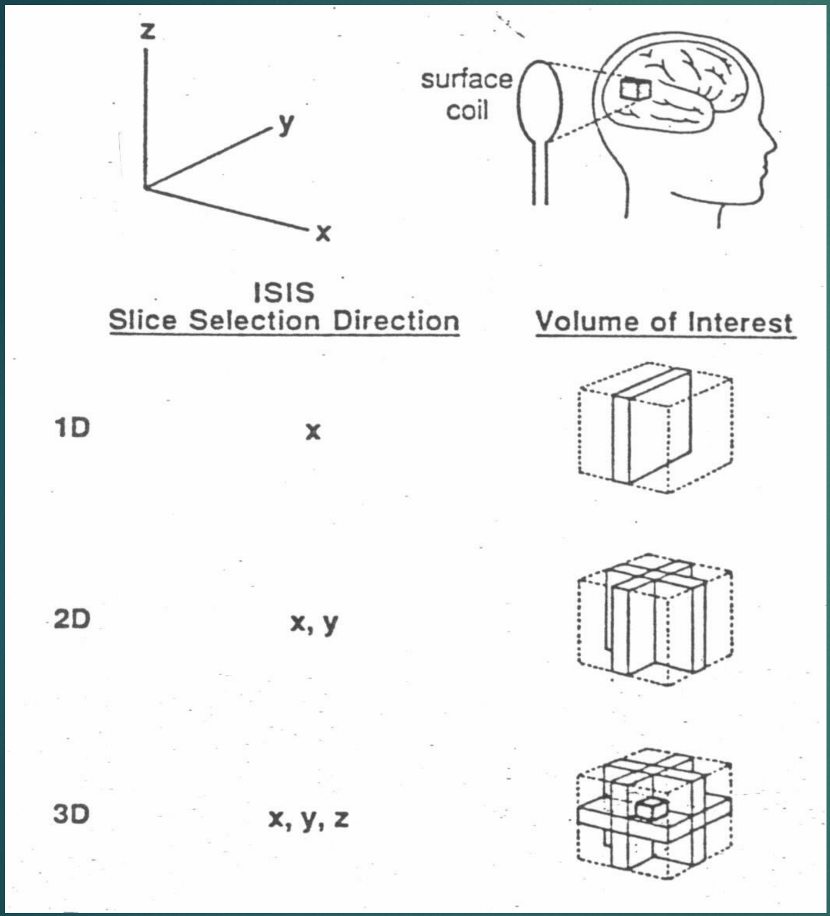

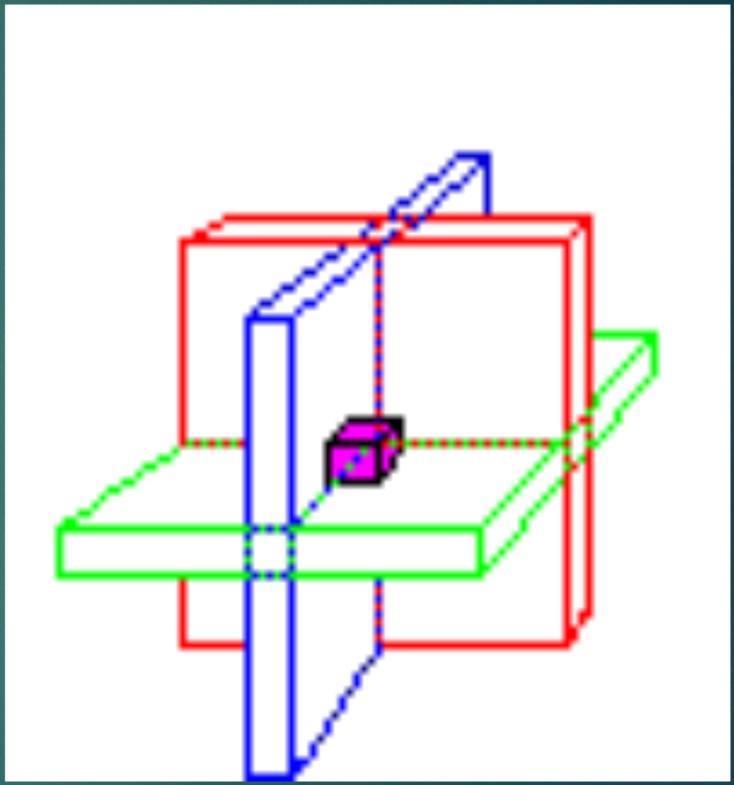

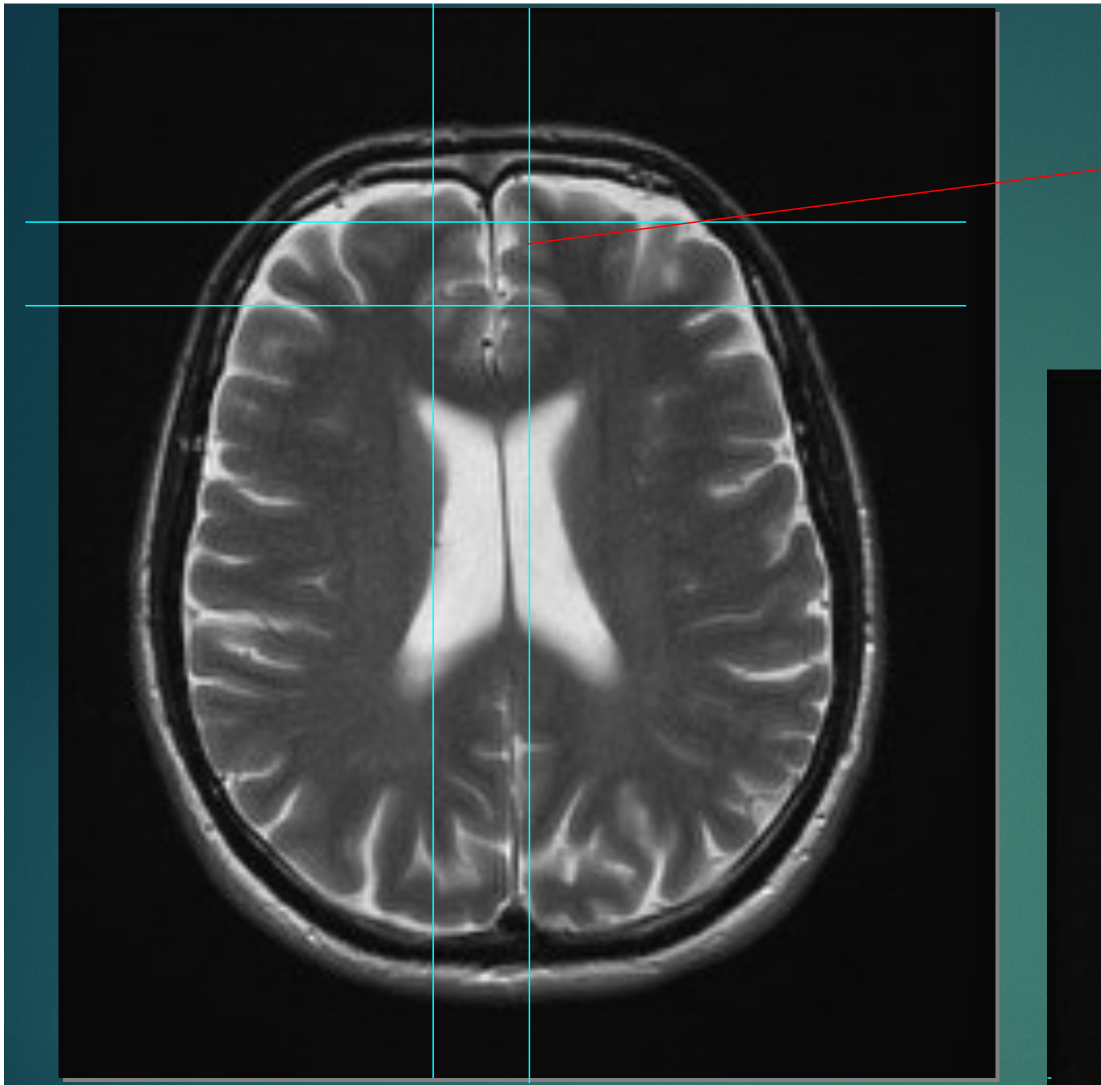

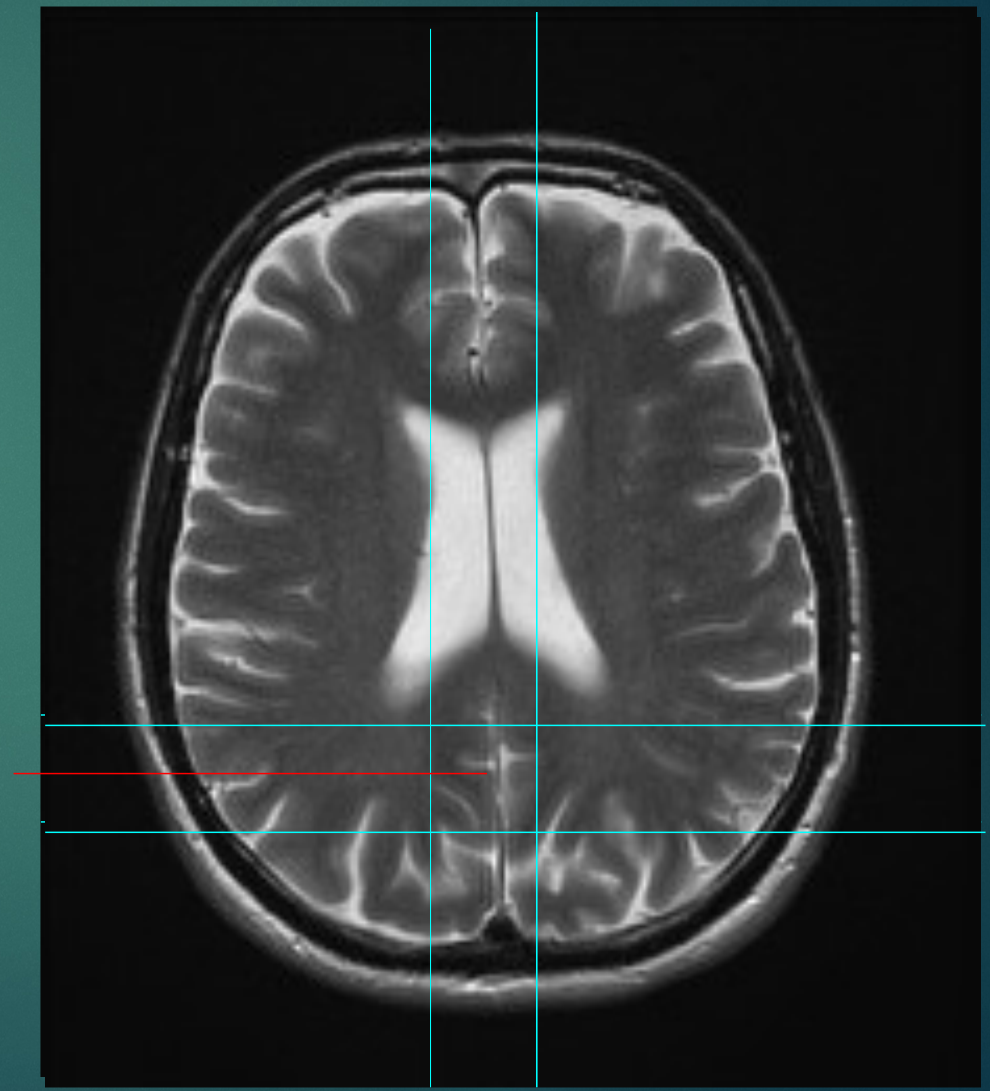

5-10 minutes for each voxel MRS
Total duration = Nx10 minutes for N voxels???

Single Voxel Spectroscopy

David Geffen School of Medicine

disadvantages

- requires large sample volume ($2x2x2$ cm^3 or more)
- requires many averages for adequate SNR
- limited coverage
- can only cover a small region in one experiment

Multi-Voxel Spectroscopy

David Geffen School of Medicine

the problem of limited coverage can be fixed by taking conducting multiple experiments from different locations

this is problematic as the total experimental time will scale with the number of different voxels you wish to measure

Spectral Characteristics from different zones in Healthy (<40 years) Volunteer

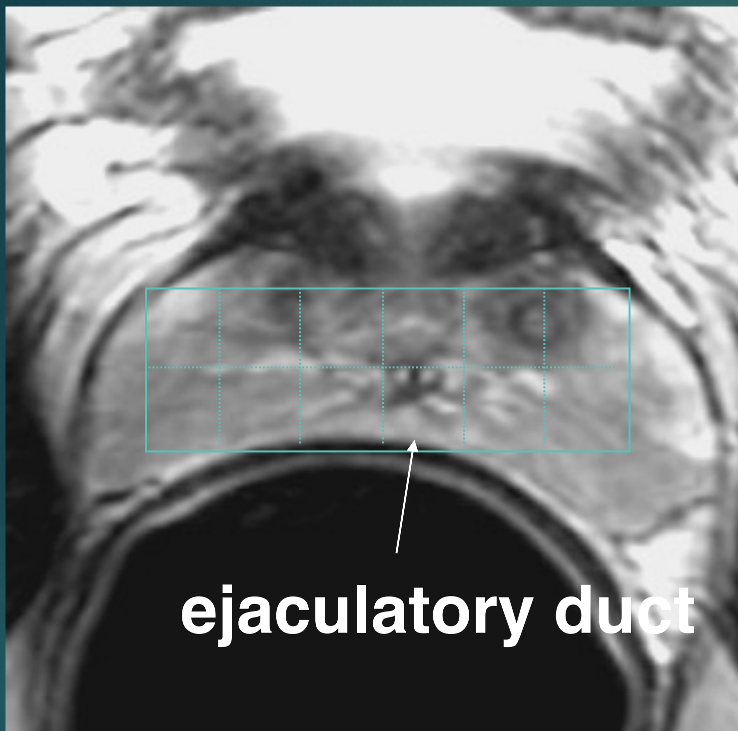

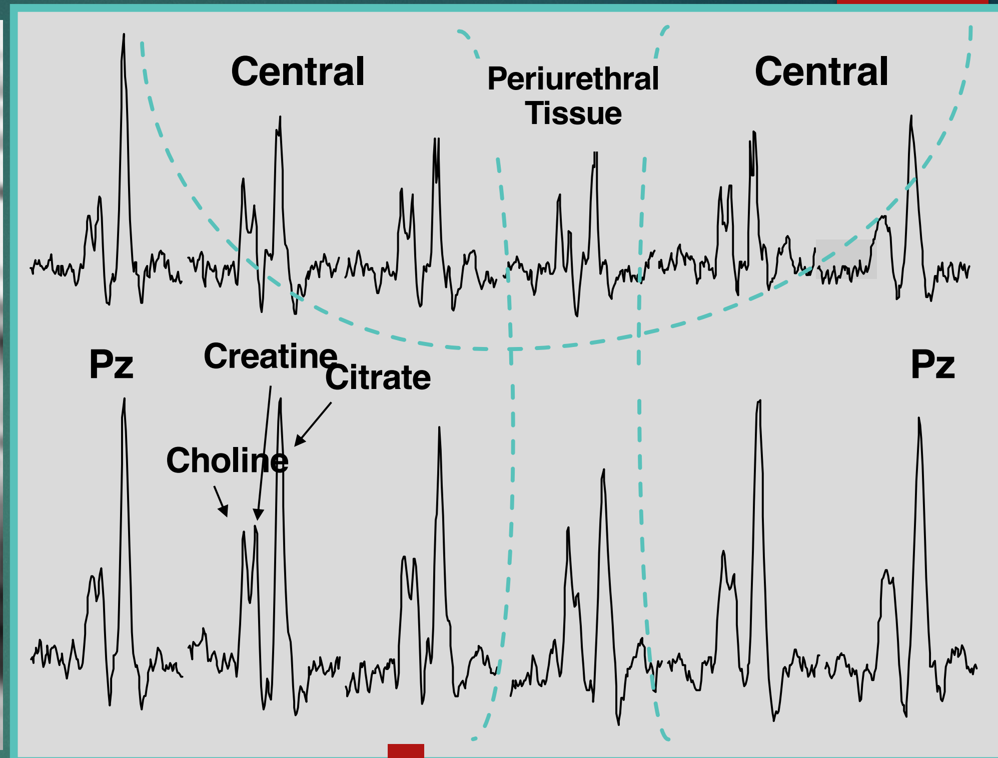

Three Distinctive Metabolic Patterns

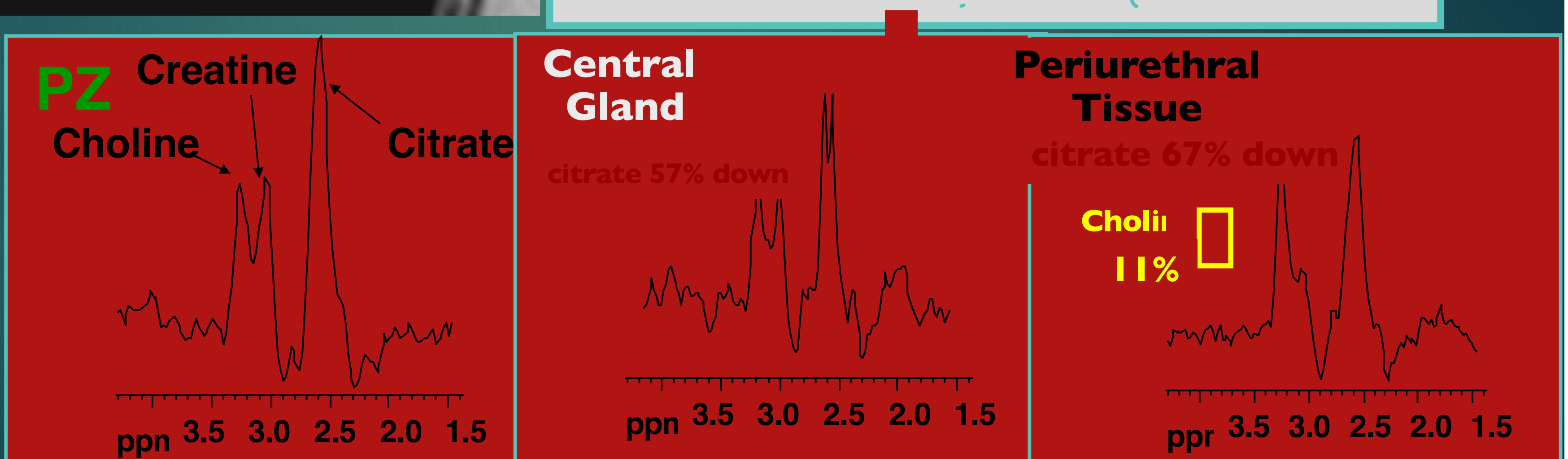

Courtesy: Prof. John Kurhanewicz

David Geffen School of Medicine

Proc. Natl. Acad. Sci. USA
Vol. 79, pp. 3523–3526, June 1982
Biophysics

NMR chemical shift imaging in three dimensions

(*in vivo* biochemistry/^{31}P imaging/metabolite mapping)

T. R. BROWN*, B. M. KINCAID*, AND K. UGURBIL†

*Bell Laboratories, Murray Hill, New Jersey 07974; and †Department of Biochemistry, Columbia University, New York, New York 10032

Communicated by John J. Hopfield, March 10, 1982

ABSTRACT A method for obtaining the three-dimensional distribution of chemical shifts in a spatially inhomogeneous sample using Fourier transform NMR is presented. The method uses a sequence of pulsed field gradients to measure the Fourier transform of the desired distribution on a rectangular grid in $(\mathbf{k},t)$ space. Simple Fourier inversion then recovers the original distribution. An estimated signal/noise ratio of 20 in 10 min is obtained for an "image" of the distribution of a 10 mM phosphorylated metabolite in the human head at a field of 20 kG with 2-cm resolution.

the resonant frequency of the spins) varying linear gradient, $[\mathbf{G}(t)\cdot\mathbf{x}]\hat{z}$, as shown in Fig. 1, how will this affect the FID? Under these conditions, the phase of each spin at time t after a rf pulse will depend on both $\mathbf{x}$ and δ as its instantaneous frequency is now given by $\frac{d\phi}{dt} = \gamma H_T(t)$, where γ is the gyromagnetic ratio for the species under observation and $H_T(t) = [H_o + \mathbf{G}(t)\cdot\mathbf{x}](1 + \varepsilon)$. Here we have just augmented the externally applied field, $H_o + \mathbf{G}(t)\cdot\mathbf{x}$, by $(1 + \varepsilon)$ to take into account the electronic shield-

MRSI/CSI

greater coverage can be obtained by spatially encoding time signals with phase-encoding gradients

phase-encoded data is encoded in k-space

this allows for more voxels to be collected in a single experiment as well as smaller voxels

1D Spatial Encoding

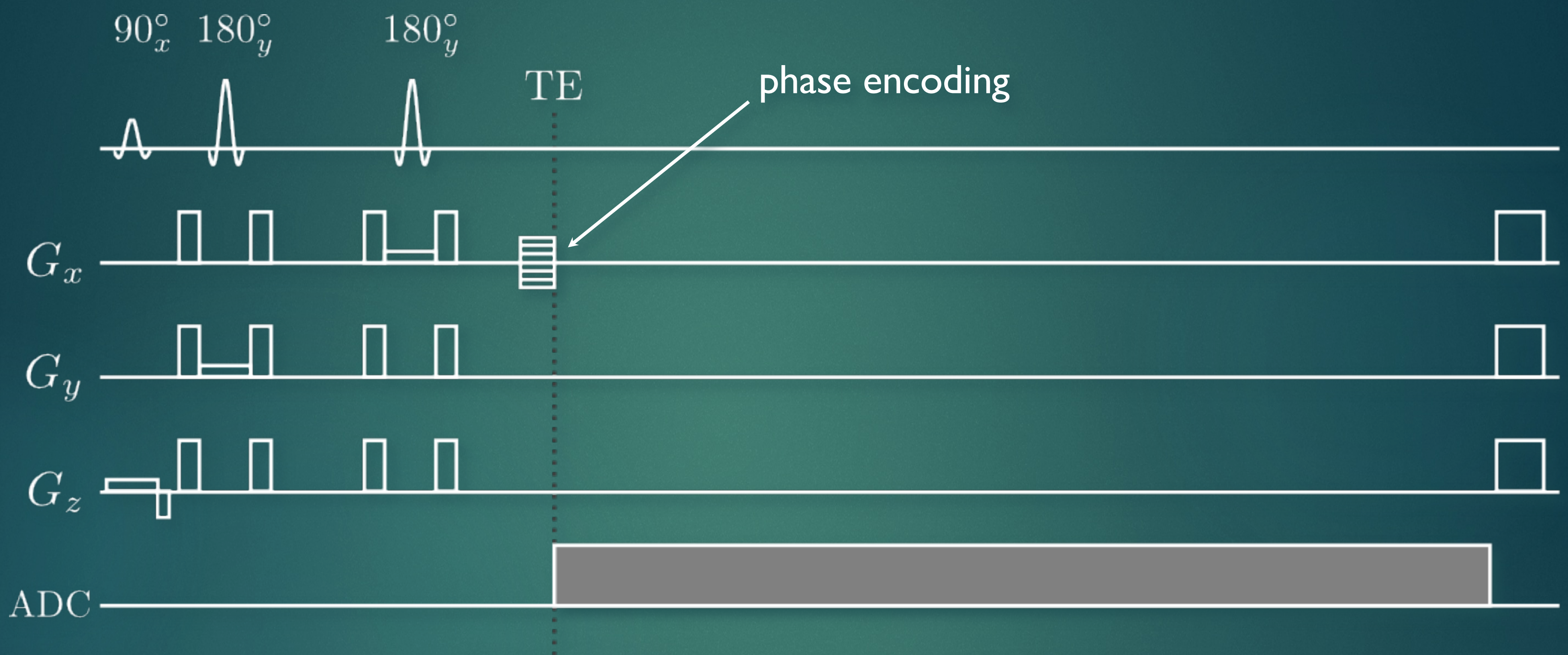

sample 1D spectroscopic imaging pulse sequence

each FID is phase encoded along one dimension

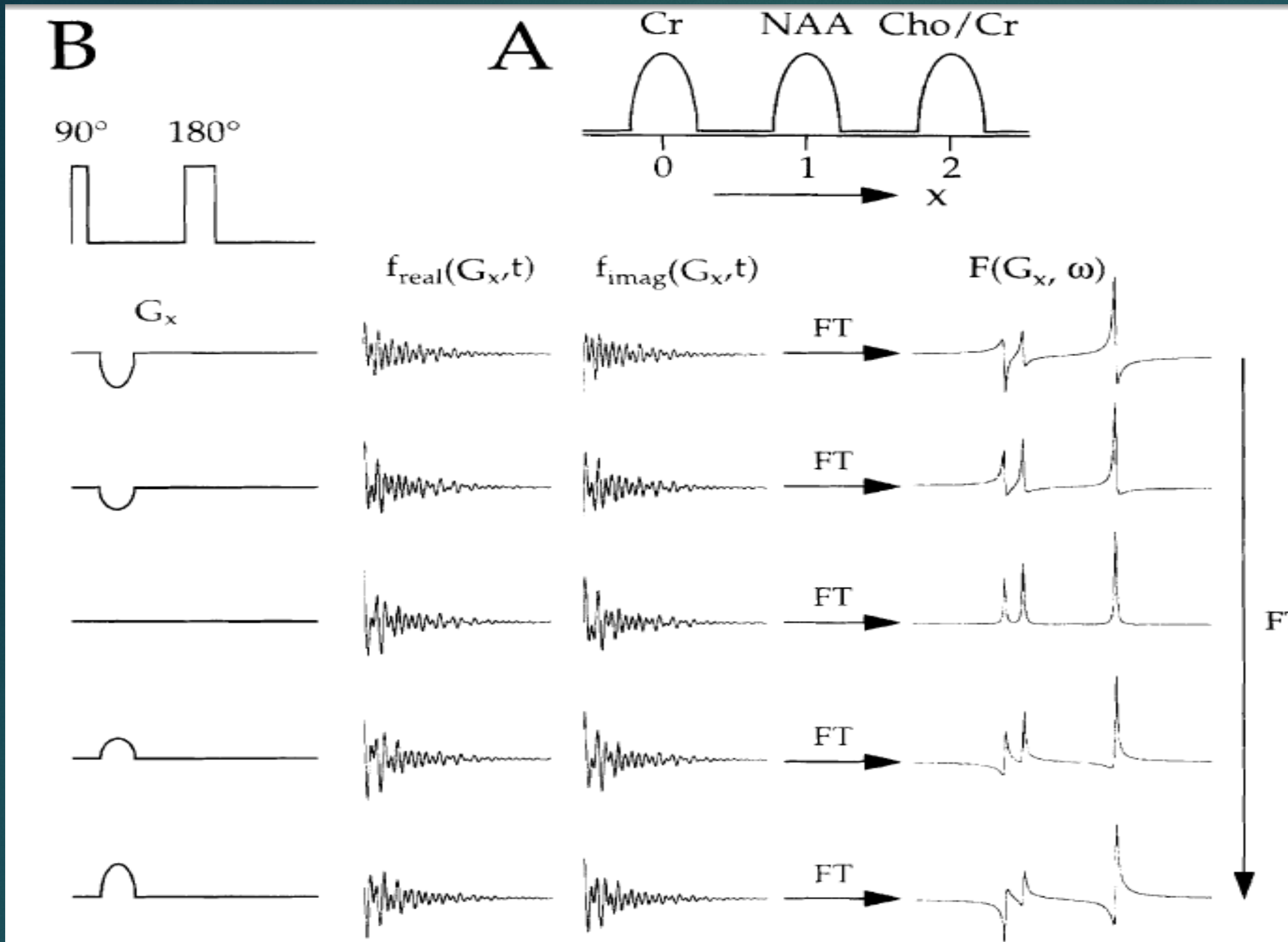

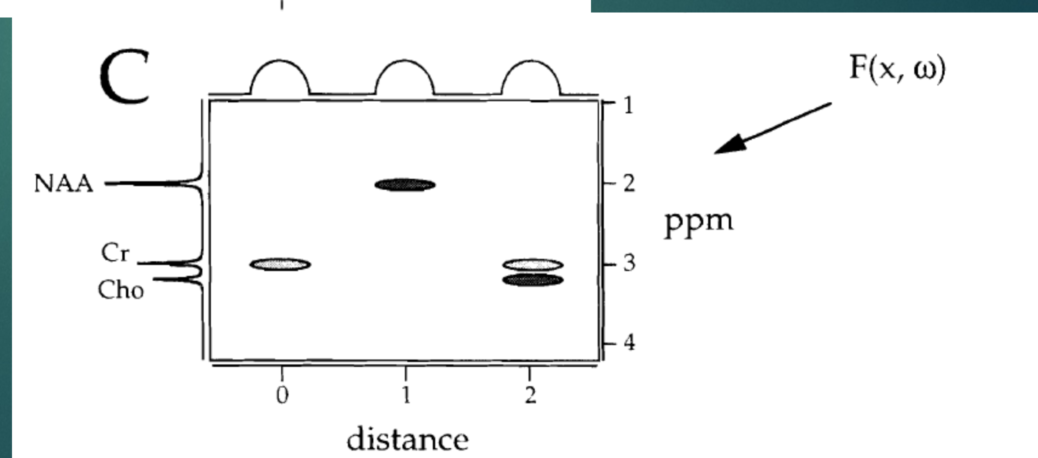

Resulting SI data set
After FFT along x and t
we get

2D Spectroscopic Imaging

how do we fill out 2D k-t-space?

same as before except phase encoding happens in two different dimensions now

Spatial Encoding

how do we use gradients to move around k-space?

$$\vec{k}(t) = \frac{\gamma}{2\pi}\int_0^t \vec{\mathrm{G}}(\tau)\mathrm{d}\tau$$

we can move anywhere in k-space so long as we program our gradients correctly

2D Spatial Encoding

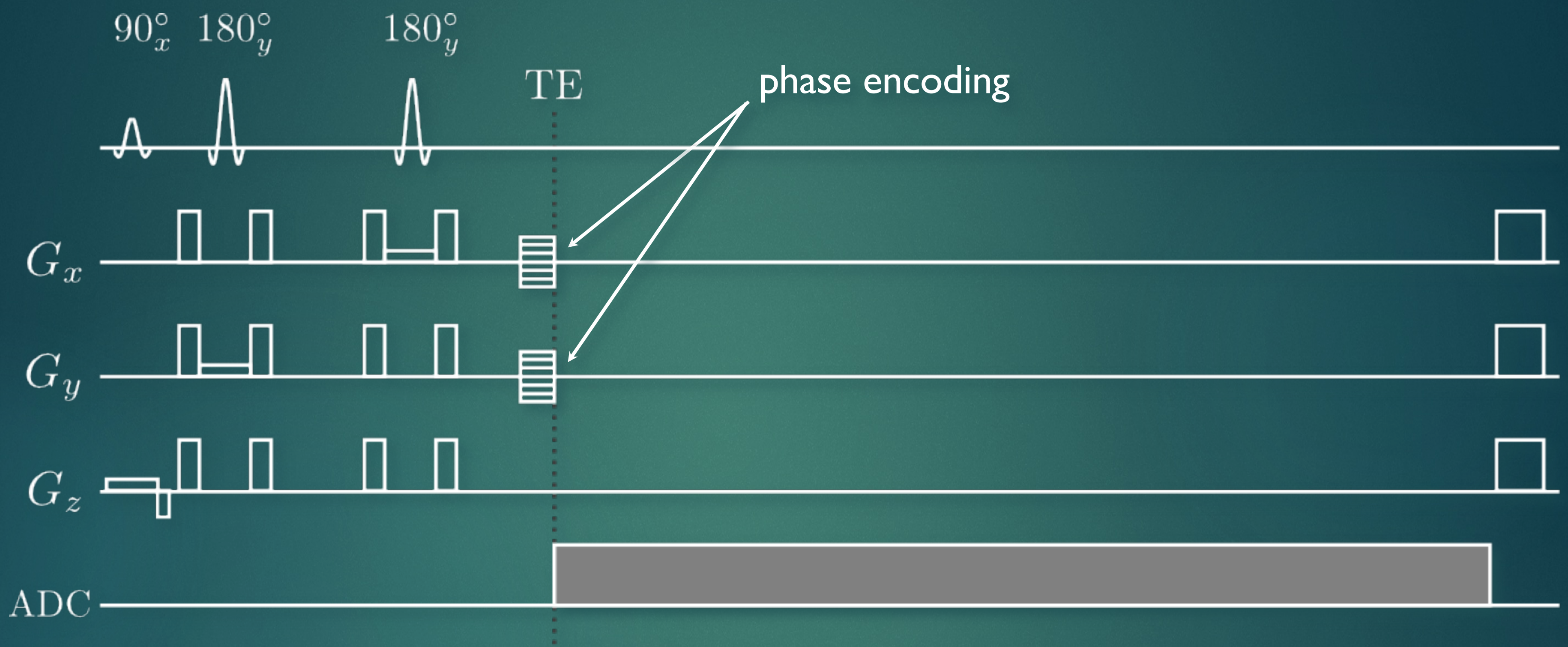

sample 2D spectroscopic imaging pulse sequence

each FID is phase encoded along one dimension

3D Spatial Encoding

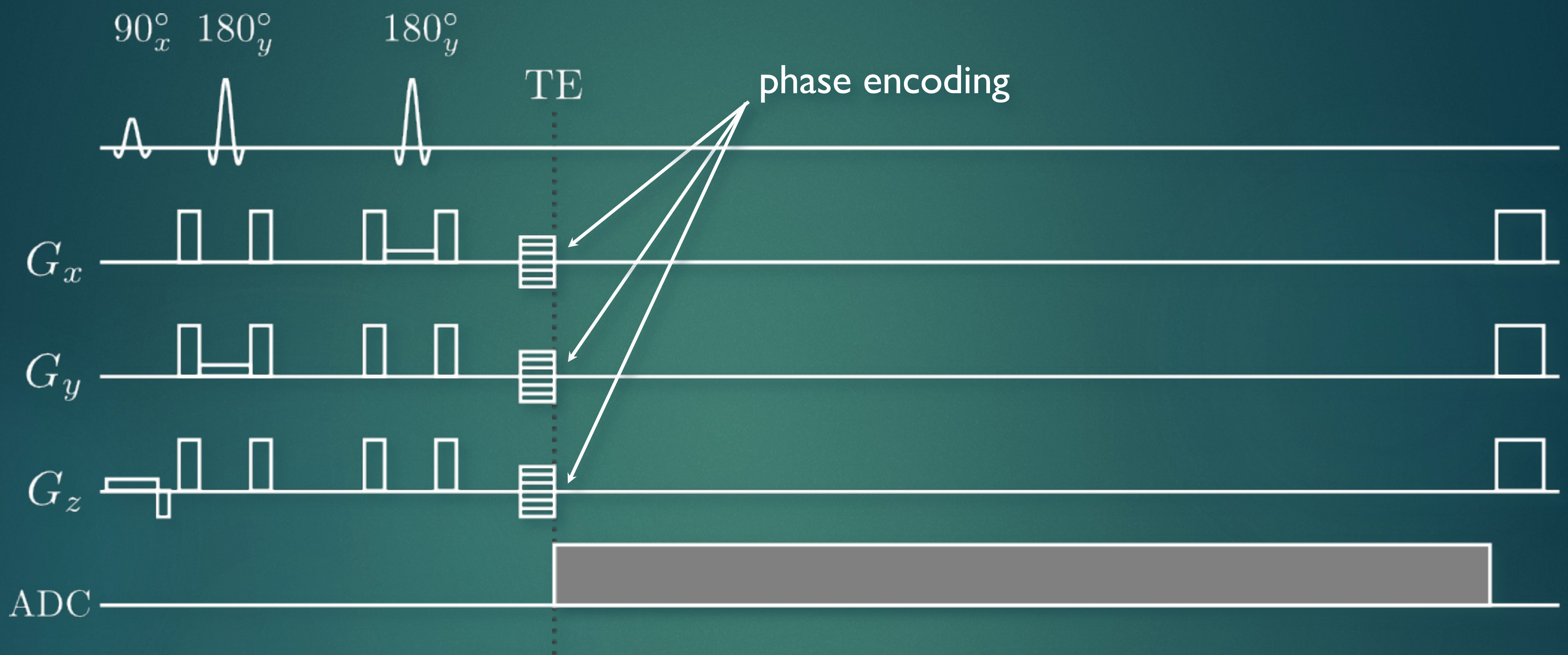

sample 3D spectroscopic imaging pulse sequence

each FID is phase encoded along one dimension

Brown 1982
Maudsley 1984

Sampling Considerations

constant time, vary amplitude

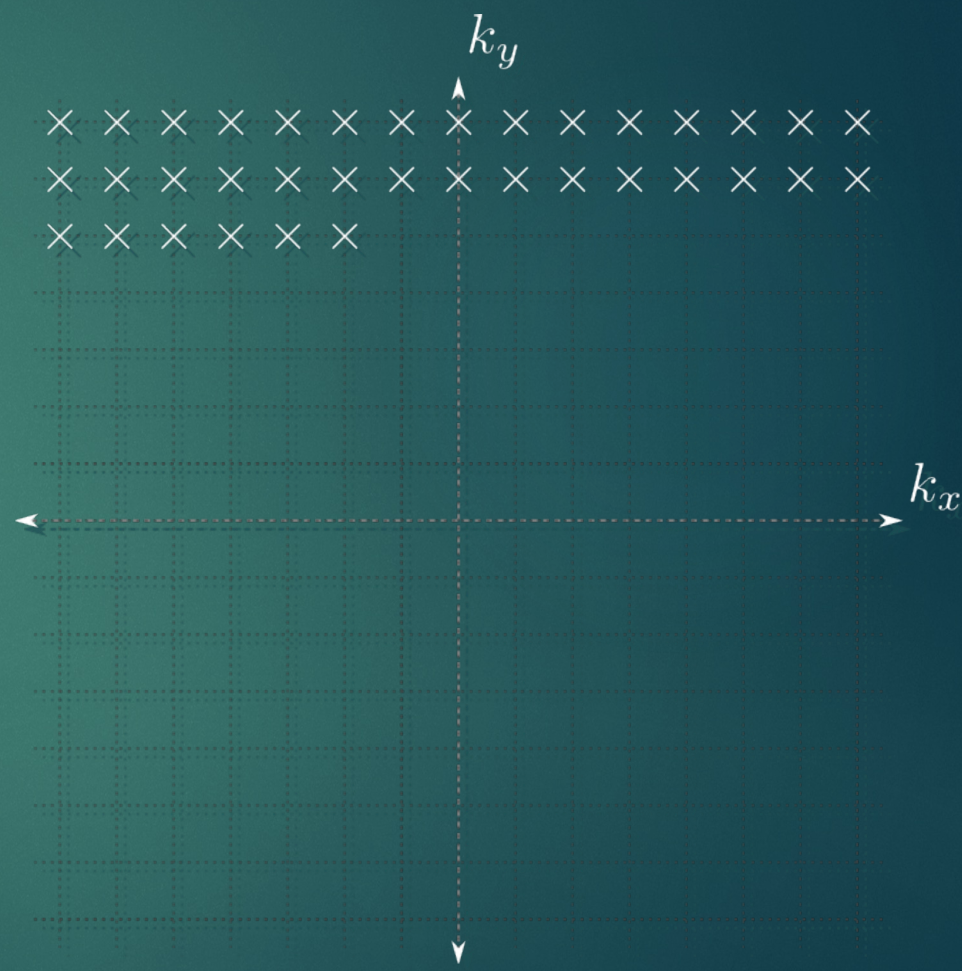

$$\Delta k_x = \frac{1}{\mathrm{FOV}_x} \quad \Delta k_y = \frac{1}{\mathrm{FOV}_y}$$

$$k_x = n\Delta k_x = \frac{n_x}{\mathrm{FOV}_x} = \gamma \mathrm{G}_x t$$

$$k_y = n\Delta k_y = \frac{n_x}{\mathrm{FOV}_y} = \gamma \mathrm{G}_y t$$

$$\mathrm{G}_x = \frac{n_x}{\gamma \mathrm{FOV}_x t} \quad \mathrm{G}_t = \frac{n_t}{\gamma \mathrm{FOV}_y t}$$

MRSI

Each k-space point is individually collected on a cartesian grid

Image data is obtained by applying 2D FFT along spatial dimensions

Total acquisition time is thus

$N_x \times N_y \times \mathrm{TR} \times \mathrm{NEX}$

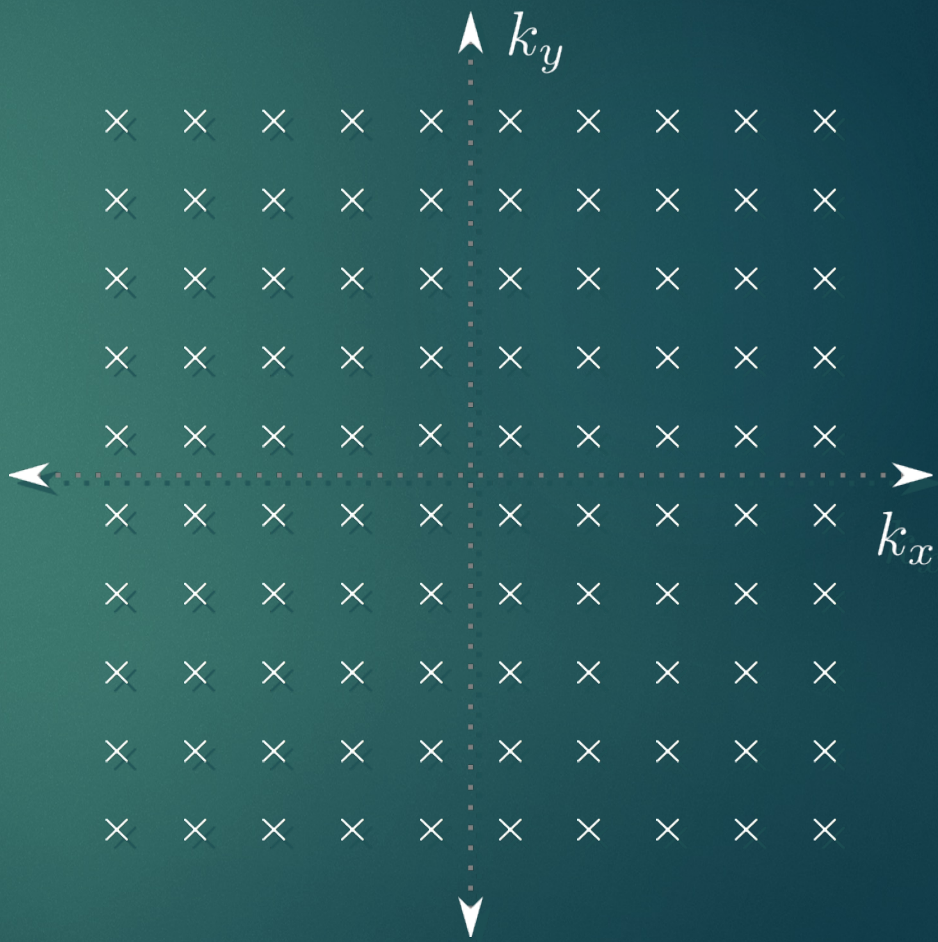

3D Spatial Encoding

the amount of time for a CSI scan is thus

$$N_x \times N_y \times N_z \times \mathrm{TR} \times \mathrm{NEX}$$

for a 32x32x1 scan (2D) with a TR = 1s and 1 average, the scan time is 17 minutes

for a 32x32x16x1 scan (3D) with a TR = 1s and 1 average, the scan time is 4.5 hours

without acceleration techniques, CSI is very slow and inefficient (and low res)

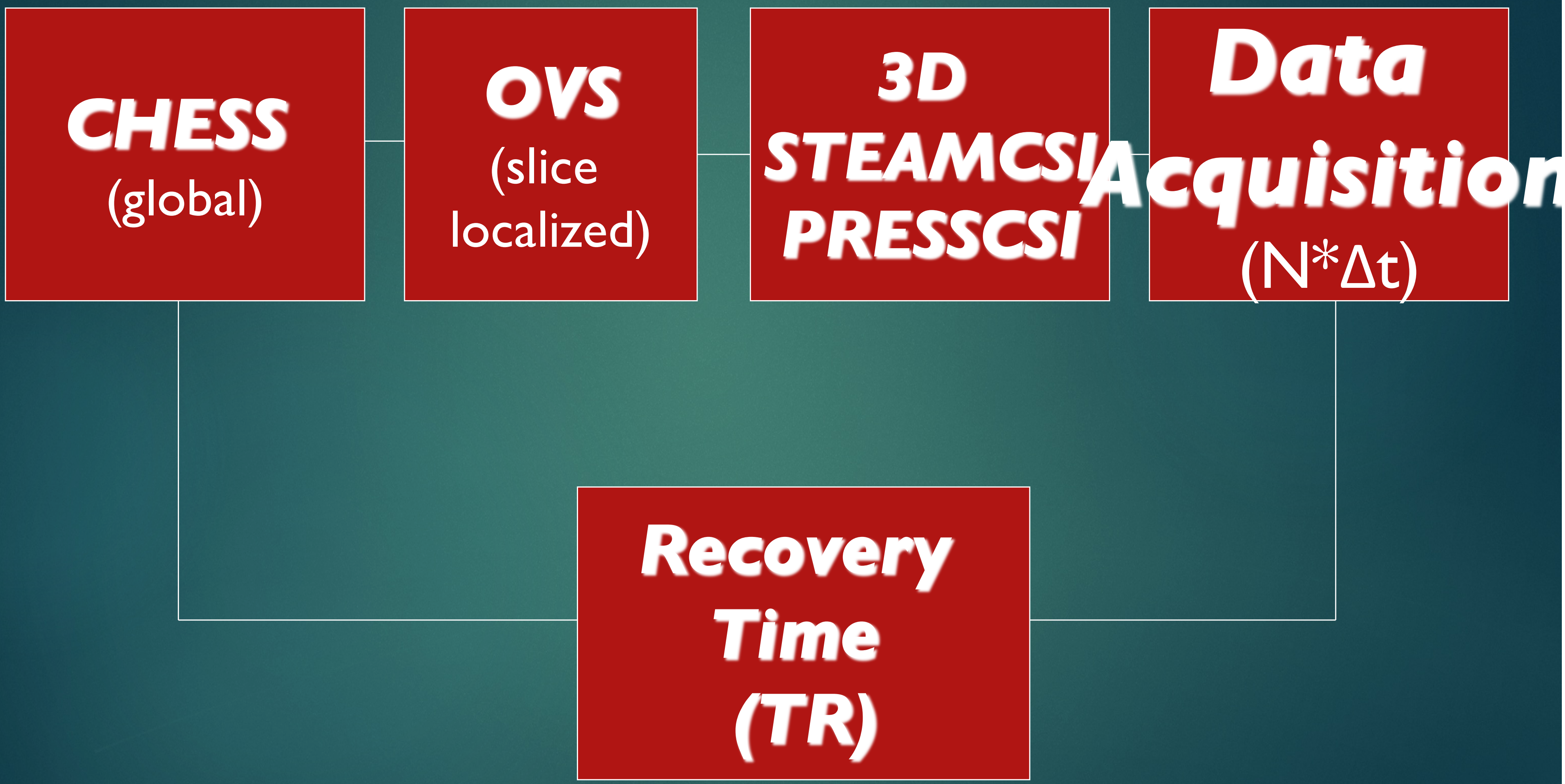
CHESS
(global)
OVS
(slice
localized)
3D
STEAMCSI
PRESSCSI
Data
Acquisition
(N*Δt)
Recovery
Time
(TR)

MR Spectroscopic Imaging (2-3 Phase Encoded)

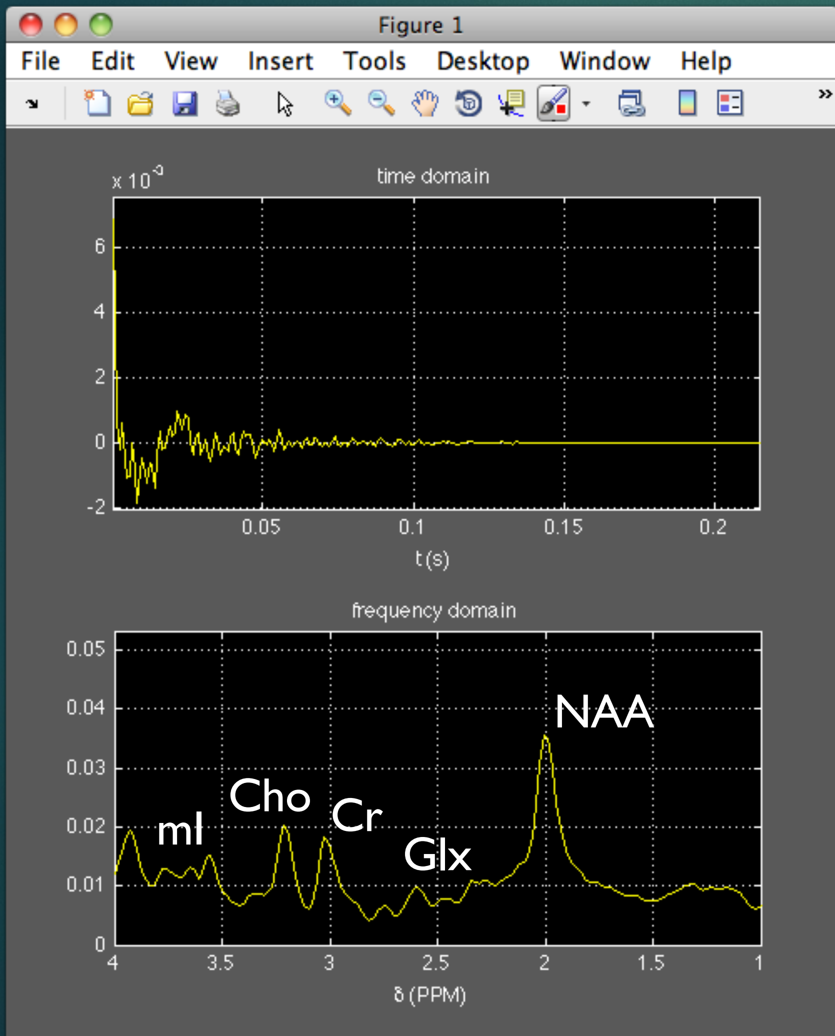

localized spectra

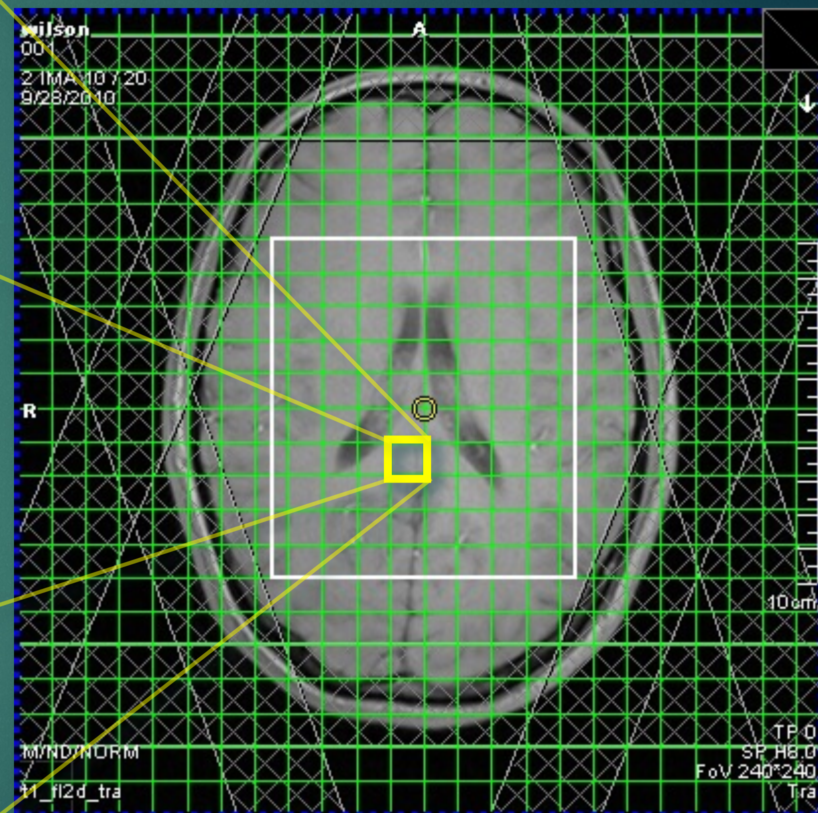

David Geffen School of Medicine

MR Spectroscopic Imaging (Contd.)

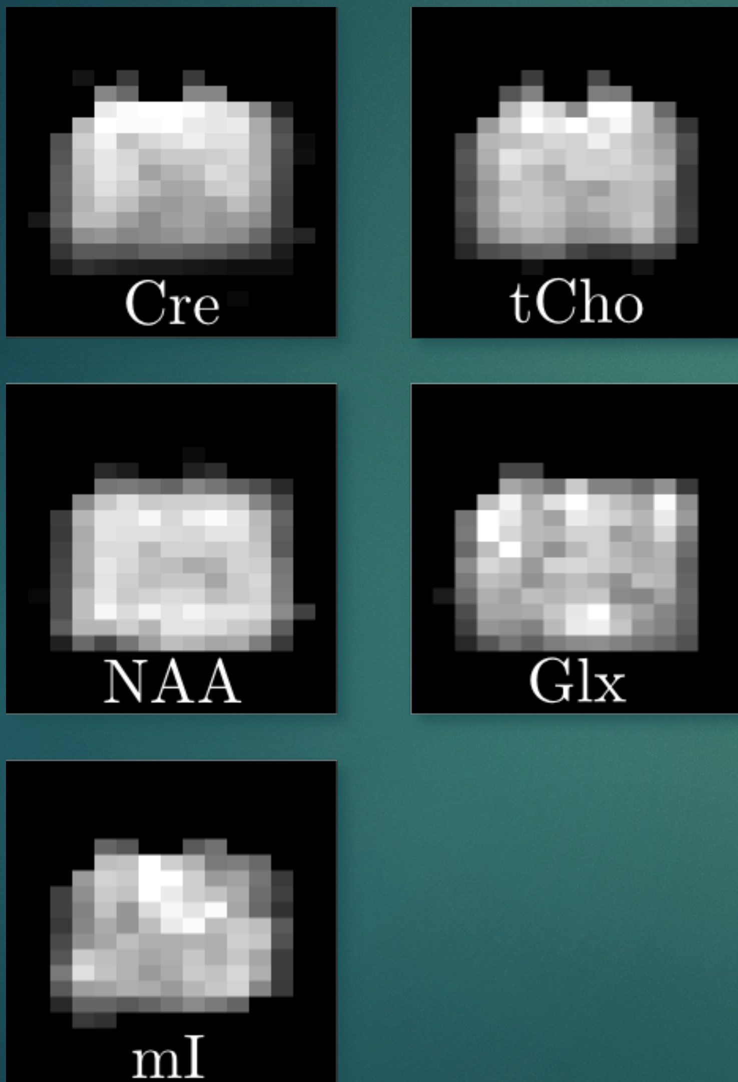

metabolite maps

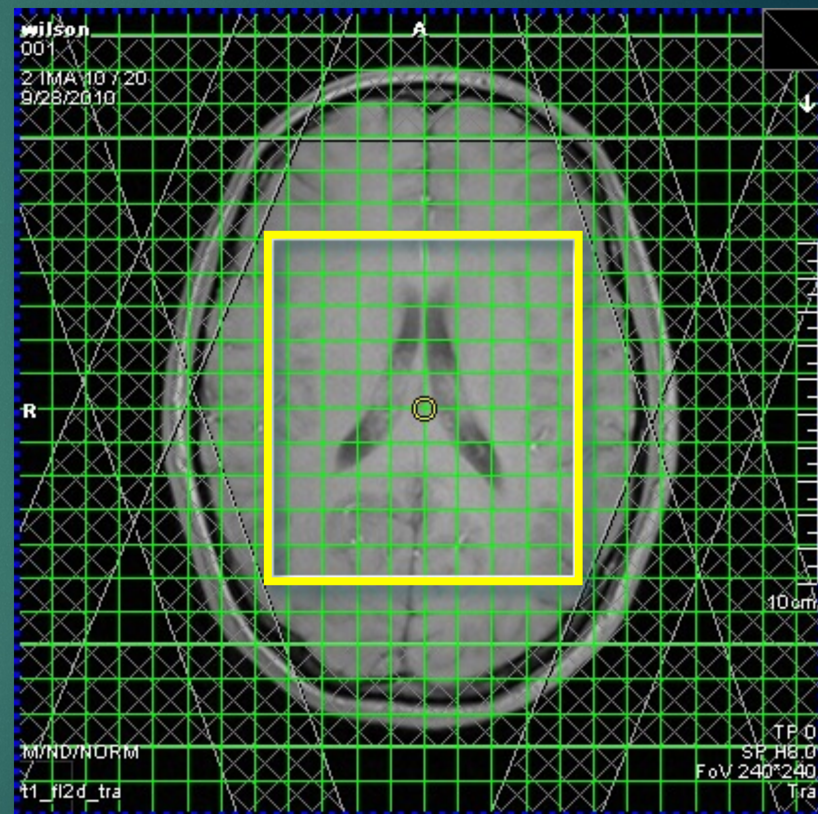

High resolution metabolite maps

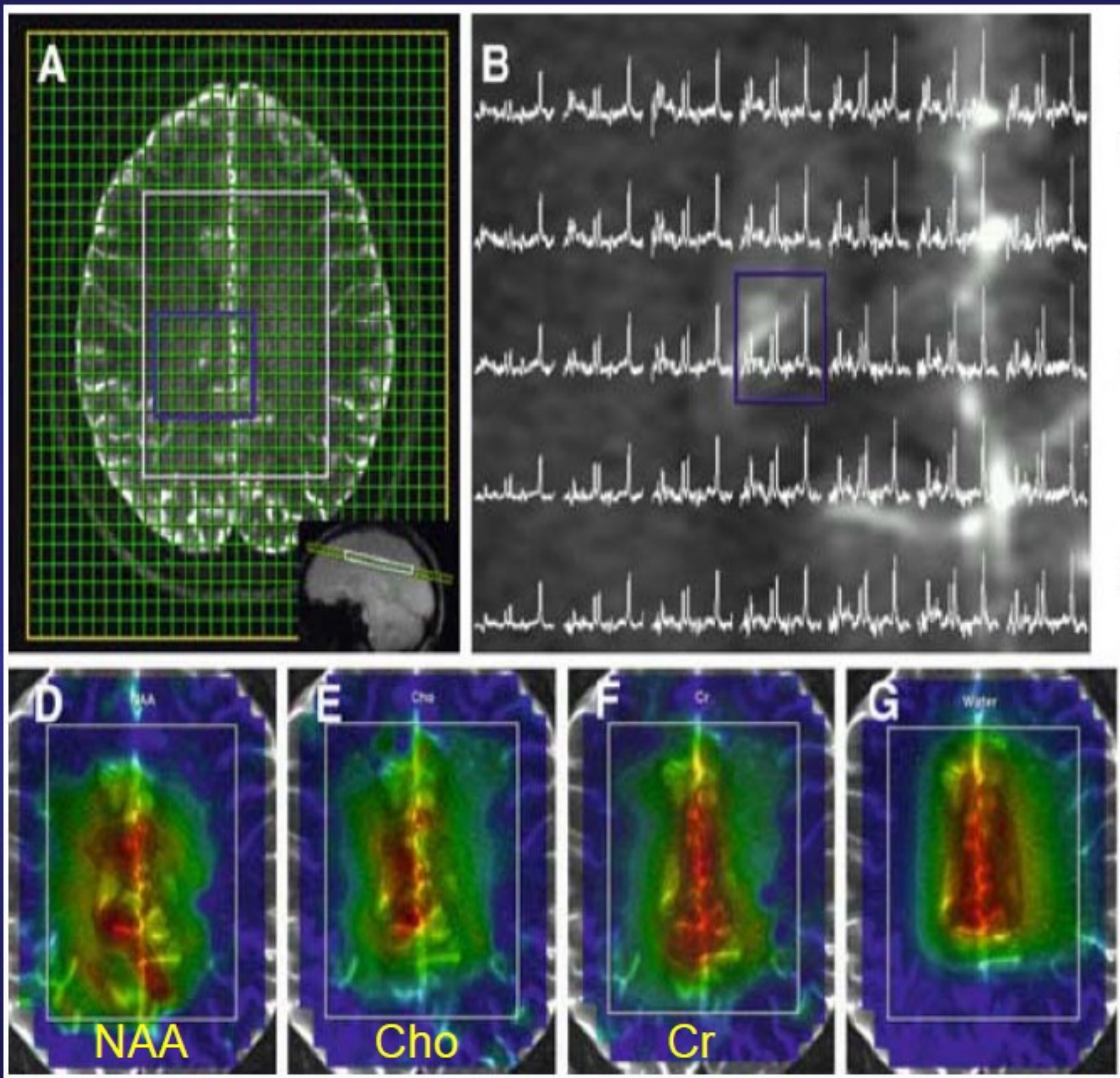

3D MRSI, TE 50, 0.14 cc voxel, 10mins
LASER seq, CP head coil

Scheenen TWJ et al. Magn Reson Mat Phy Biol Med 21:95-101, 2008

Metabolic mapping quality – 3T vs 7T

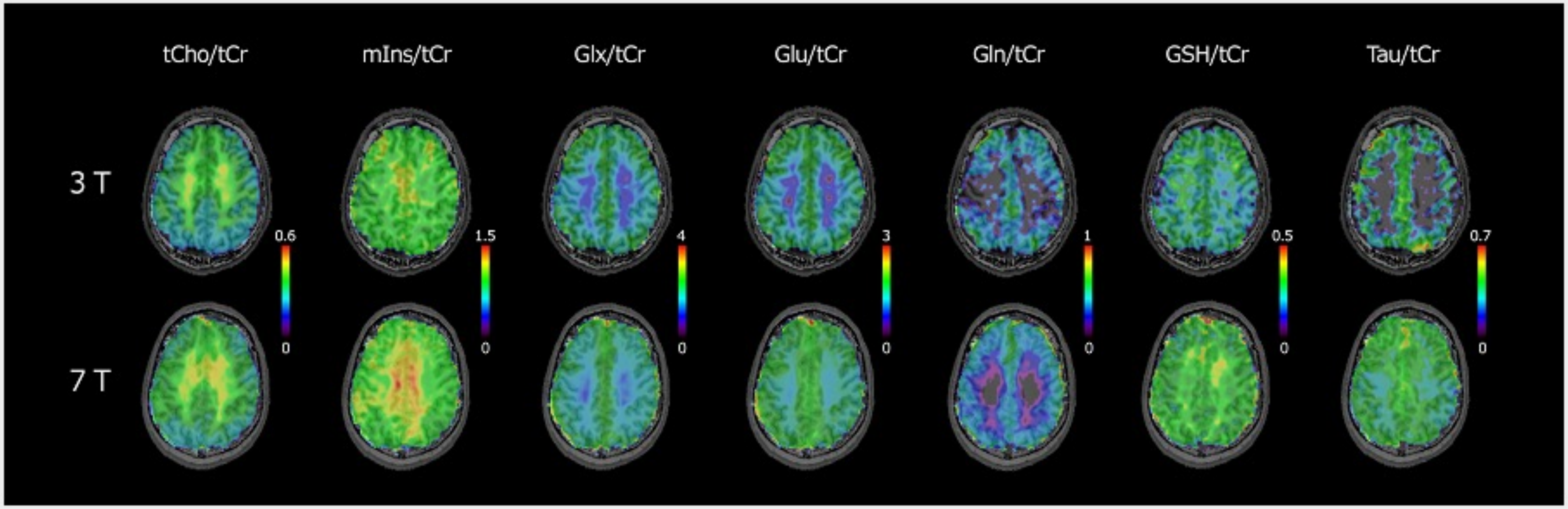

Figure 4. Metabolic maps acquired with FID-MRSI at 3T and 7T. Reliable quantification over the whole slice was possible for Glu/tCr, Gln/tCr, GSH/tCr and Tau/tCr at 7T but not at 3T. Values are displayed in a.u.

Heckova et al. ISMRM 2016

How long does it take to perform a multi- voxel 2D/3D MRSI?

2D MRSI (2 spatial+1spectral):
Total duration = TR*NEX*Nx*Ny
=1s*1*32*32= 17 minutes

3D MRSI (3 spatial+1spectral):
Total duration = TR*NEX*Nx*Ny*Nz
=1s*1*32*32*16= 4.53 hours
=1s*1*16*16*8= 34 minutes

Acceleration Techniques

The goal

- to reduce the number of excitations in order to reduce the total scan time (1-10 minutes)

The strategies

- Selective Averaging
- Parallel Imaging
- Turbo Spin Echo (TSE) techniques
- Echo-Planar (EP) techniques
- Concentric Ring Trajectories (SI-CONCEPT)
- Radial (Golden Angle View Ordering) and TV regularizer

Fast MRSI

- Elliptical weighting
  - Reduced spatial sampling of k-space with only the central ellipsoid being acquired (reduction factor typically = 2)
- Parallel Imaging Reconstruction
  - Reduced acquisitions of k-space by increasing the spacing between k-space samples. Additional spatial information from multiple receiver coils is then used to increase the spatial FOV to the original size.

Selective Averaging

Average the parts of k-space with greater intensity

Significantly reduces total scan time

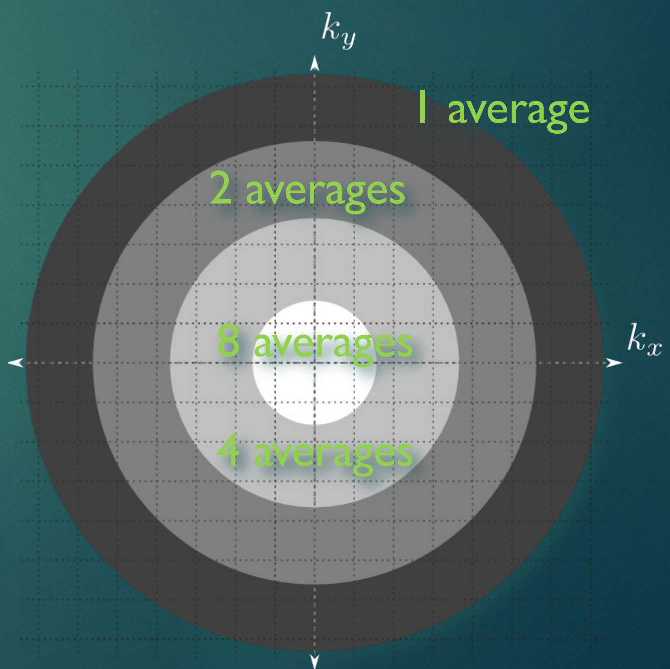

MRI/MRSI Data Display

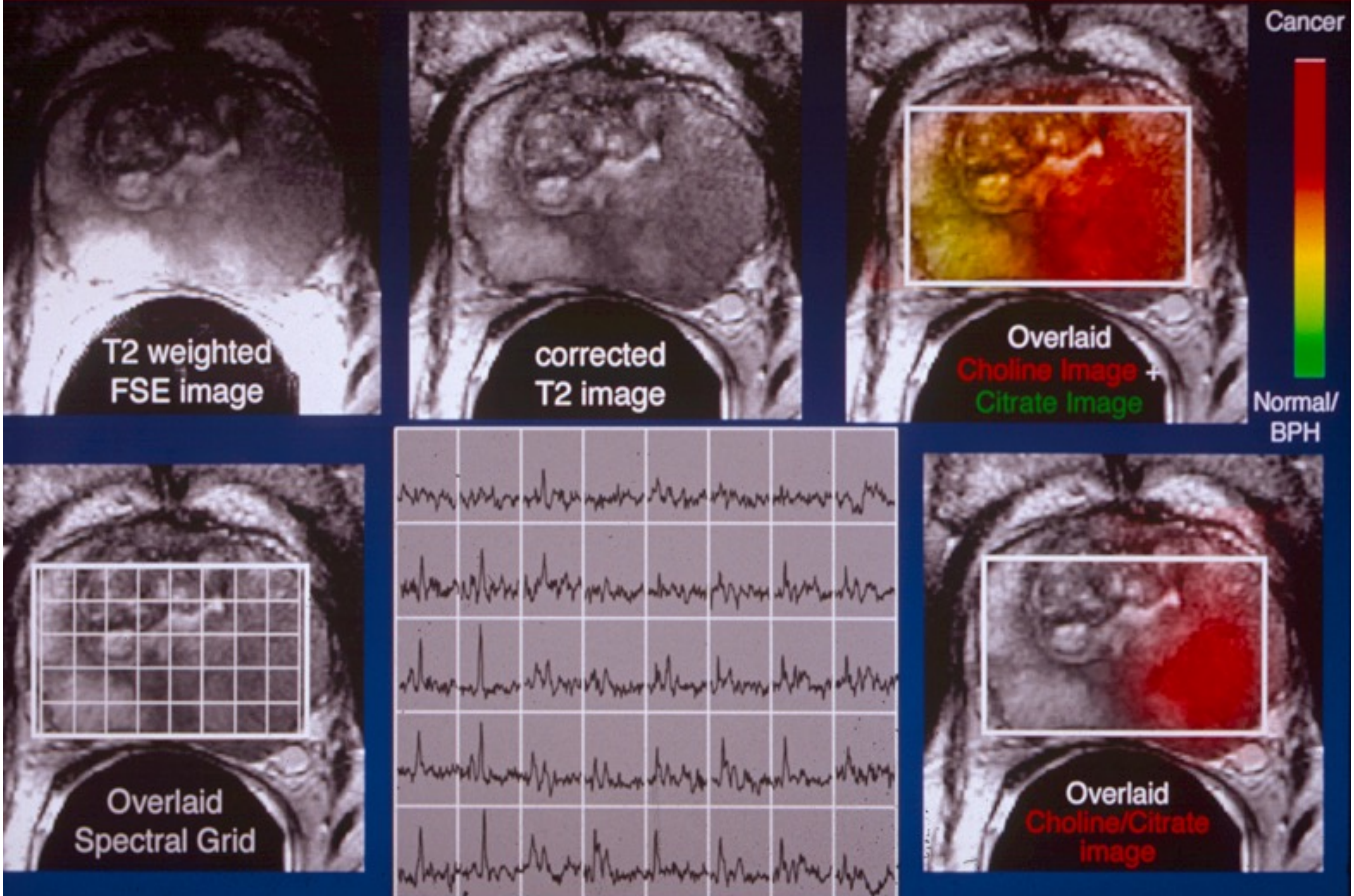

Parallel Imaging

Multi-coil reconstruction (SENSE/GRAPPA)

advantages

- reduced scan time

disadvantages

- reduced SNR from reduced number of excitations

Larkman and Nunes PBM 2007; Preussmann 1999; Sodickson 1999

Echo-Planar Spectroscopic Imaging (EPSI)

echo-planar spectroscopic imaging uses a repeated time-varying readout gradient to collect the same spatially encoded information as a function of time

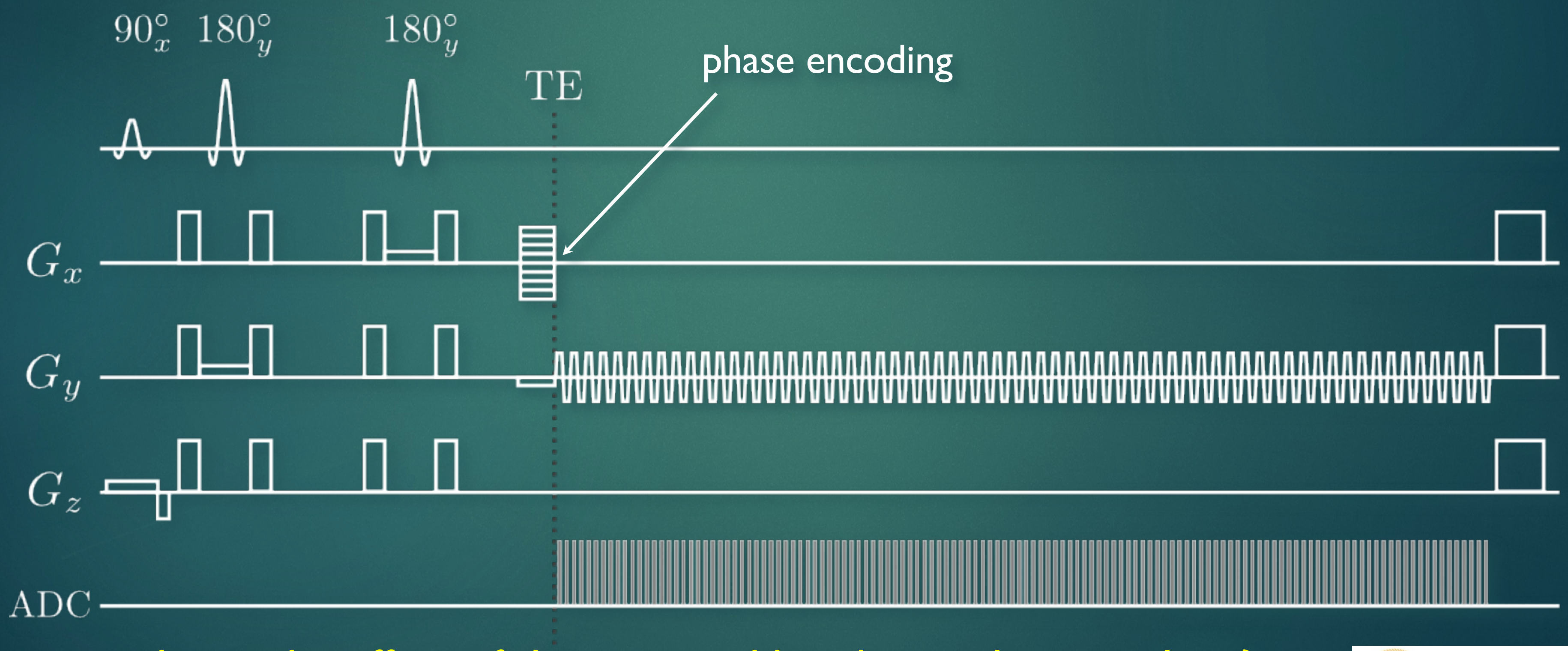

what is the effect of the repeated bipolar gradient readout?

Mansfield 1984, Posse 1994, Lipnick 2008

David Geffen School of Medicine

Echo-Planar SI

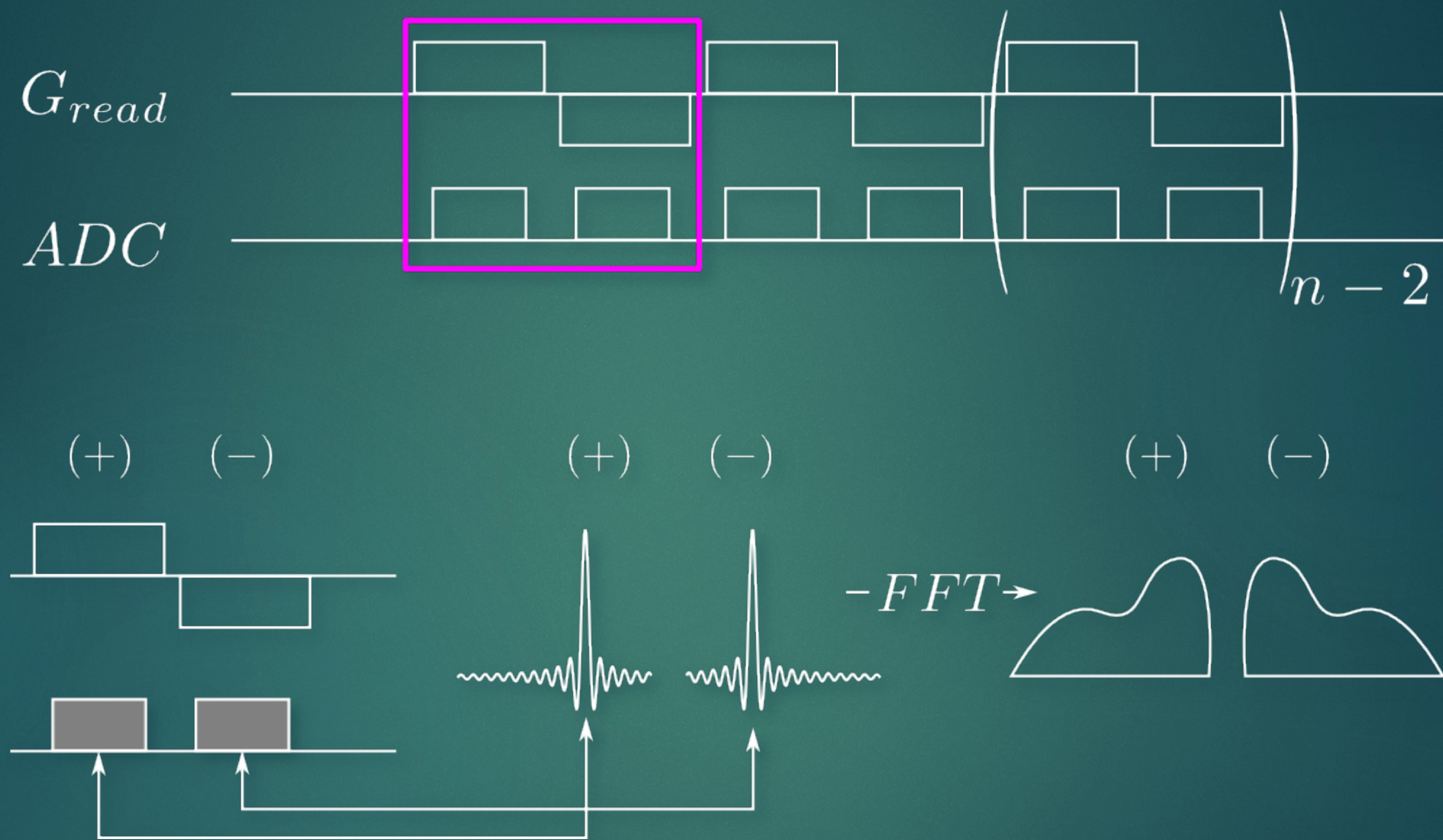

two sets of echoes (odd and even) form which are mirror images of each other

Mansfield 1984, Posse 1994, Lipnick 2008

Echo-Planar SI

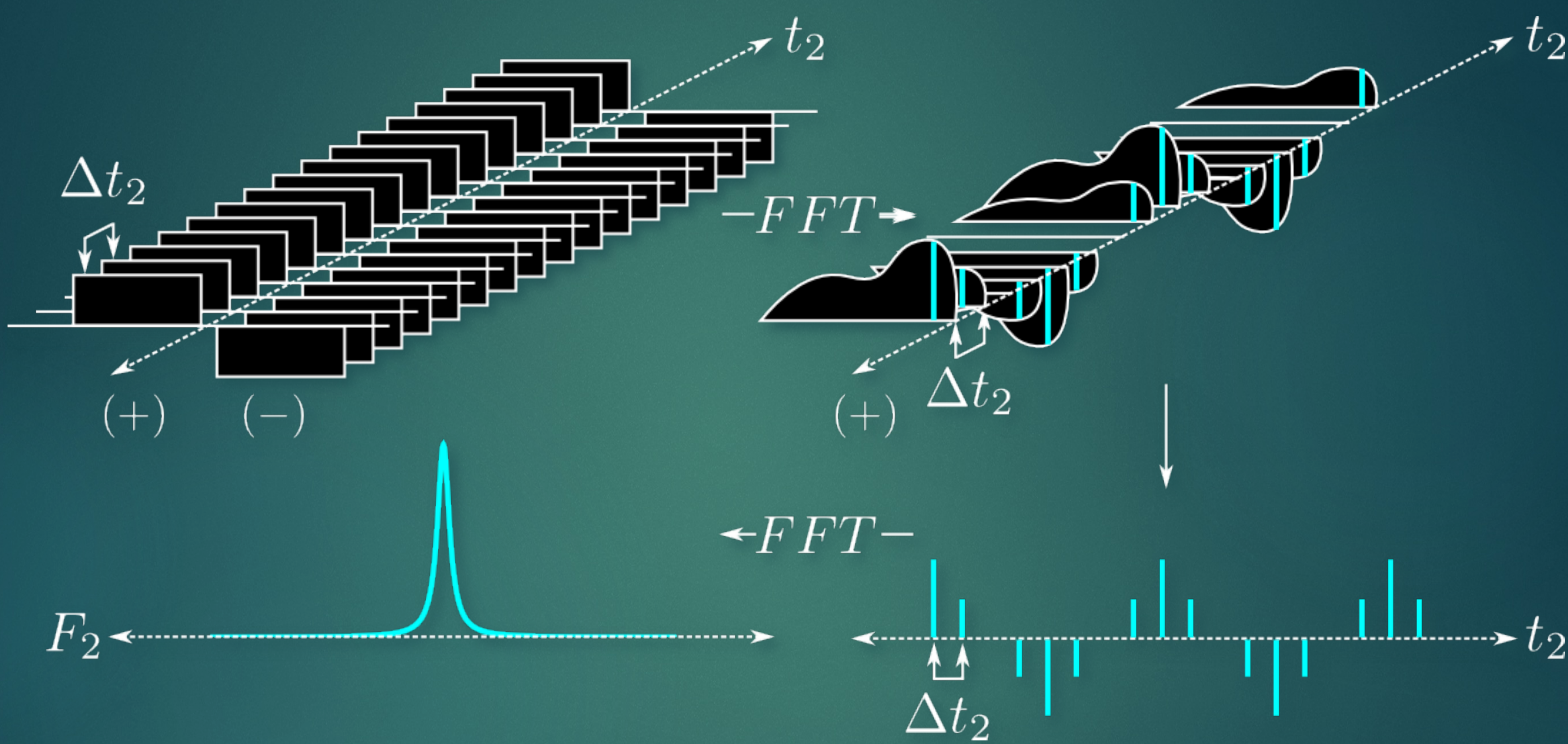

the repeated nature of the readout gradients spatially encodes as a function of time

Mansfield 1984, Posse 1994, Lipnick 2008

EPSI

A single line in k-space is collected in a single excitation

Image data is obtained by applying 2D FFT along spatial dimensions

Total acquisition time is thus $N_x \times \mathrm{TR} \times \mathrm{NEX}$

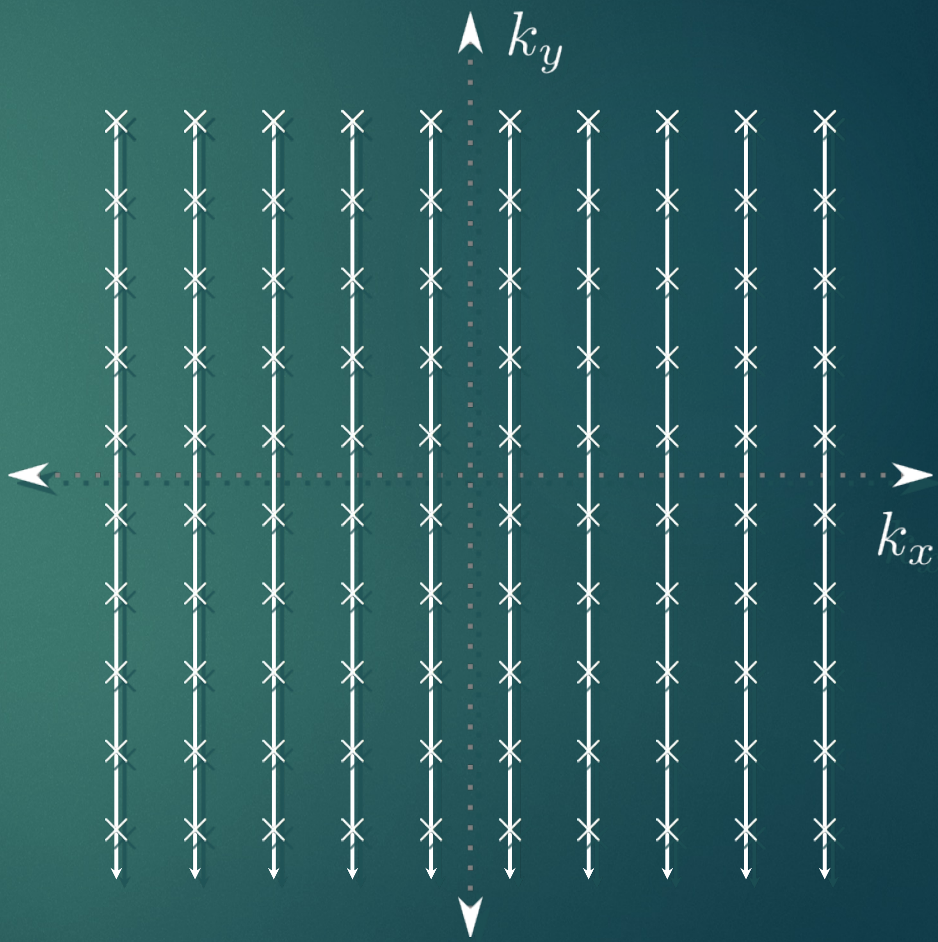

Mansfield 1984, Posse 1994, Mulkern 2000, Lipnick 2008

Echo-Planar SI

the amount of time for a MRSI scan is thus

$$N_x \times N_z \times \mathrm{TR} \times \mathrm{NEX}$$

for a 32x32x16 scan (3D) with a TR = 1s and 1 average, the scan time is 8.5 minutes

Using all 3 phase-encoding,
3D MRSI (3 spatial+1spectral):
Total duration = TR*NEX*Nx*Ny*Nz
=1s*32*32*16= 4.5 hours

significant reduction in scan time!

Echo-Planar SI

advantages

- significantly reduced scan time

disadvantages

- echo-planar readout creates undesired eddy currents which can distort spectra
- reduced SNR from reduced number of excitations
- very demanding on the hardware (reduced spectral bandwidth)

Why Concentric Circular sampling?

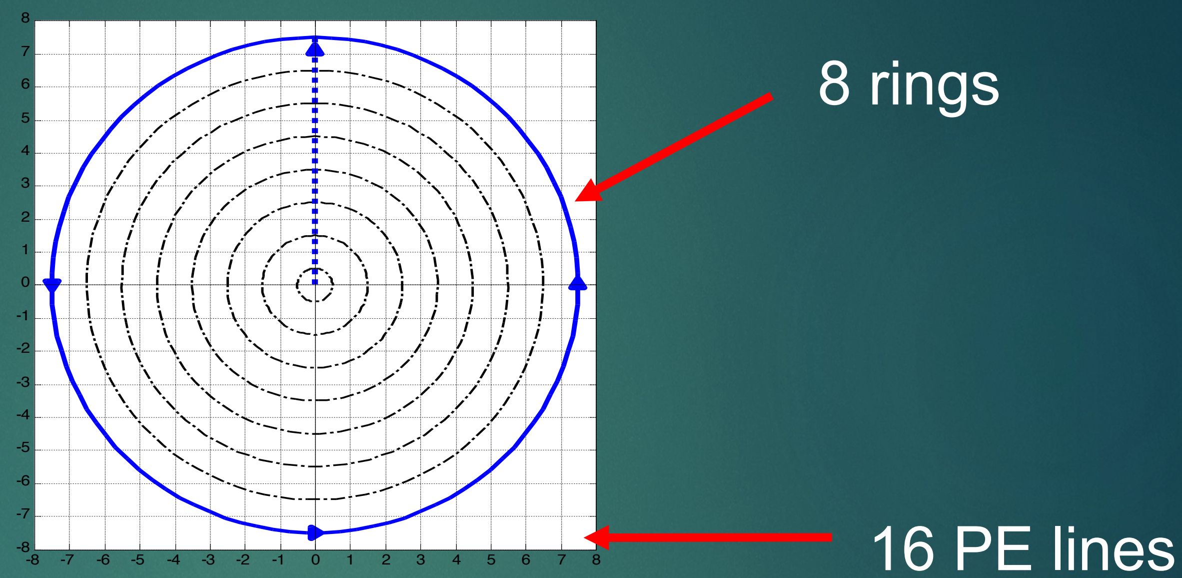

- More efficient k-space sampling due to symmetry of concentric circles → half the number of excitations required for similar k-space coverage
- Outer corners of k-space contain little signal and are usually filtered away anyway

Matsui 1986, Zhou 998, Wu 2009; Furuyama 2012

Concentric Circles (SI-CONCEPT)

A single ring in k-space is collected in a single excitation

Image data **cannot** be processed by 2D FFT since it is not cartesian

Total acquisition time is thus

$$\frac{1}{2}N_x \times \mathrm{TR} \times \mathrm{NEX}$$

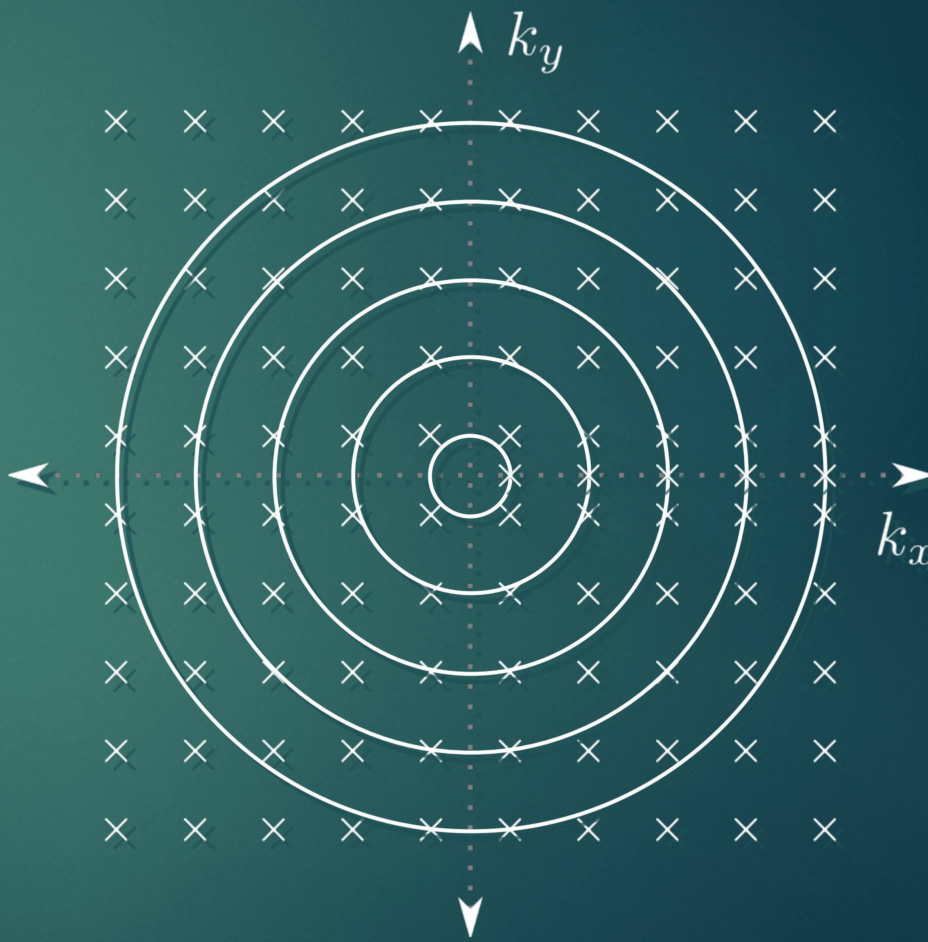

JK Furuyama, NE Wislon, MA Thomas MRM 2012

What is Concentric Circular ?

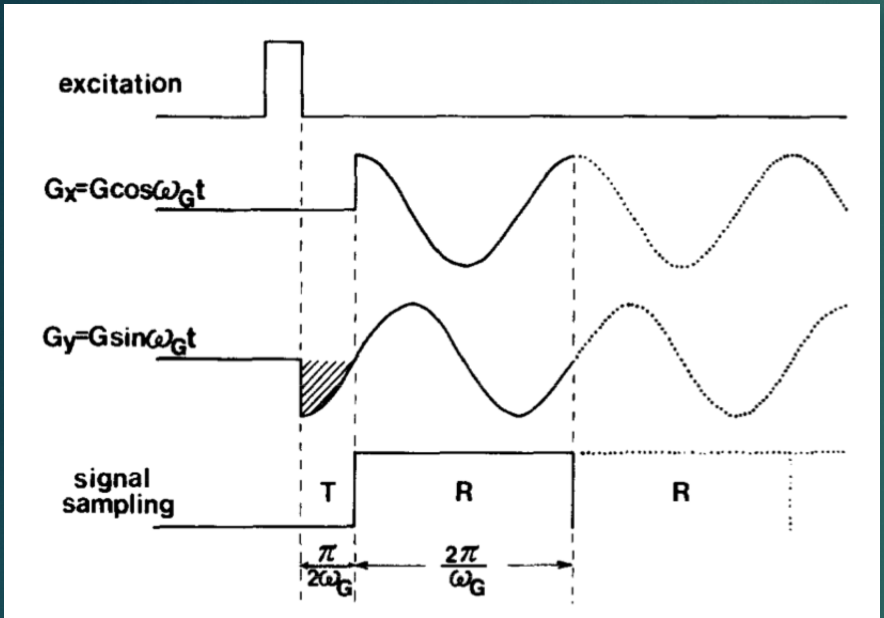

Circular k-space trajectory defined by

$$k_x(t) = -k_n \sin\left(\frac{2\pi}{T}(t - TE)\right)$$

$$k_y(t) = +k_n \cos\left(\frac{2\pi}{T}(t - TE)\right)$$

where k_n is the radius of the *n*th ring and T is the spectral dwell time in the direct dimension

Gradient waveforms are thus given by

$$G_x(t) = -\frac{4\pi^2 k_n}{\gamma T}\cos\left(\frac{2\pi}{T}(t - TE)\right)$$

$$G_y(t) = -\frac{4\pi^2 k_n}{\gamma T}\sin\left(\frac{2\pi}{T}(t - TE)\right)$$

Matsui S, Kohno H, *J. Magn. Reson.* **70**, 157-162 (1986)

JK Furuyama, NE Wislon, MA Thomas MRM 2012

SI-CONCEPT Pulse Sequence

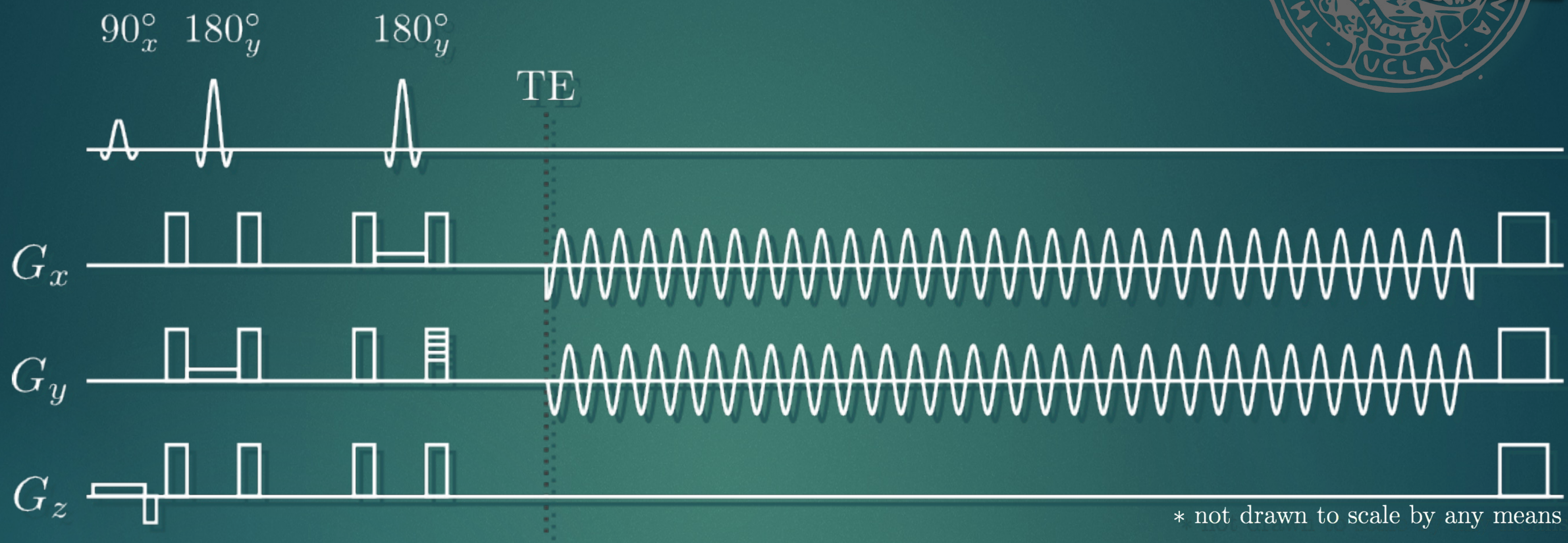

The use of a concentric k-space trajectory is readily applied to ordinary CSI sequences

Repeatedly tracing the same circle in k-space encodes both spatial and spectral information

JK Furuyama, NE Wislon, MA Thomas MRM 2012

Concentric Circles

Convert polar data to cartesian?

how?

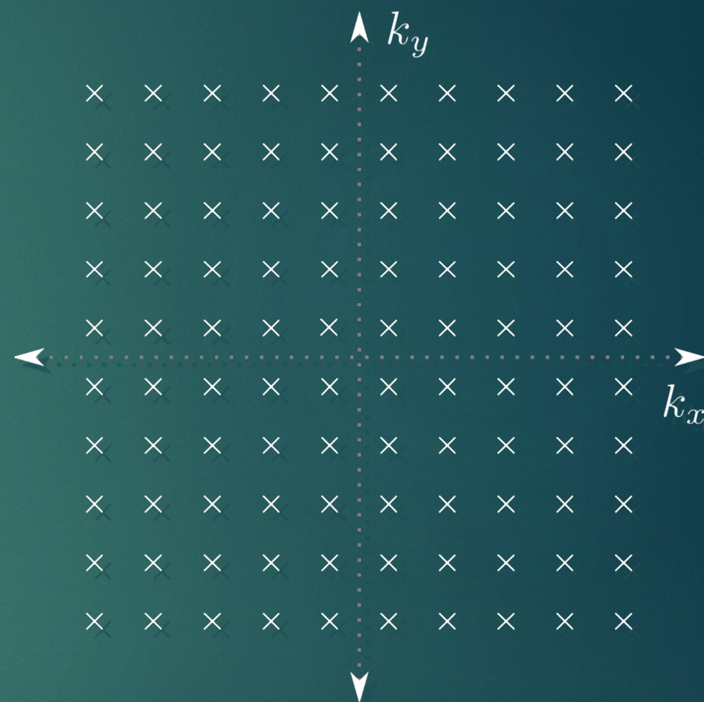

Gridding takes any arbitrary k-space trajectory and convolves it onto a cartesian grid

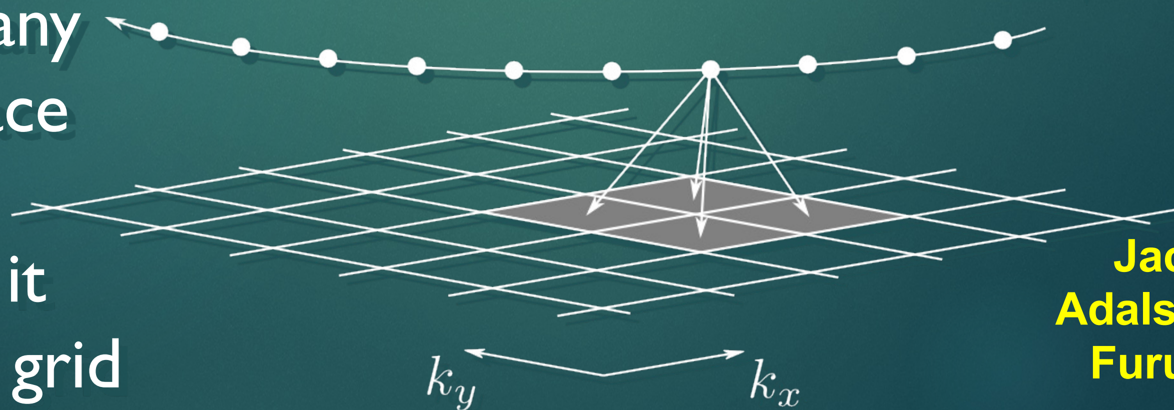

Jackson 1991
Adalsteinsson 1998
Furuyama, 2012

Concentric Circular Imaging

- Polar Data

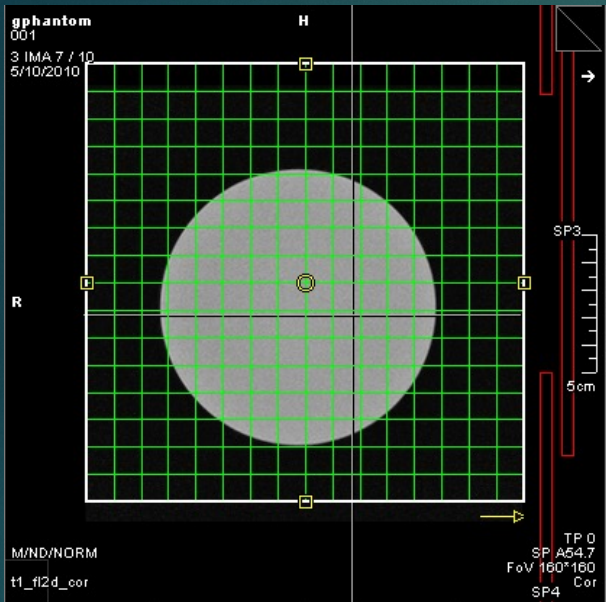

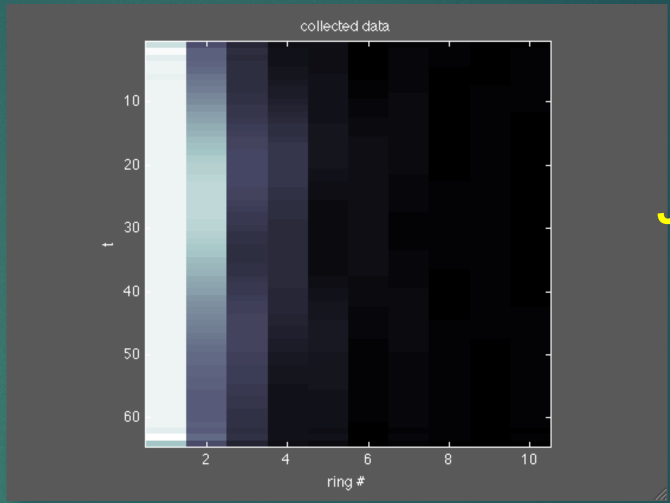

JK Furuyama, NE Wislon, MA Thomas MRM 2012

- reconstructed Human Brain Spectra

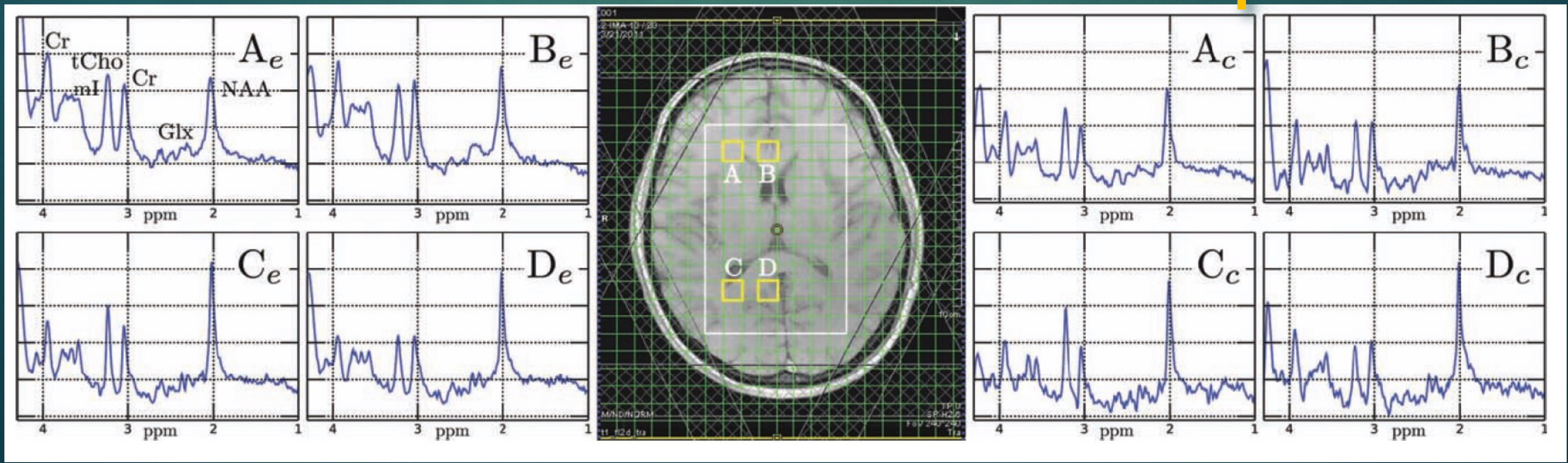

MRSI vs. EPSI vs. SI-CONCEPT

-MRSI

$$N_x \times N_y \times \mathrm{TR} \times \mathrm{NEX}$$

-EPSI

$$N_x \times \mathrm{TR} \times \mathrm{NEX}$$

-SI-CONCEPT

$$\frac{1}{2} N_x \times \mathrm{TR} \times \mathrm{NEX}$$

Faster!

Hingerl et al. Inv Rad. 2020

*…..Brain coverage among all measured matrix sizes ranging from a 32 × 32 × 31 matrix with 6.9 × 6.9 × 4.2 mm nominal voxel size acquired in ~**3 minutes** to an 80 × 80 × 47 matrix with 2.7 × 2.7 × 2.7 mm nominal voxel size in ~**15 minutes** for different brain regions.*

Emir and coworkers, MRM 2020

*"A density-weighted concentric-ring trajectory metabolite-cycling MRSI technique was implemented to collect data with a nominal resolution of 0.25 mL within **3 minutes and 16 seconds**."*

Advantages of Concentric Circular Trajectories

- Less demanding on gradient hardware → higher spectral BW achievable (required at higher field strengths to prevent spectral aliasing)
- Eddy currents not as severe especially for *inner* k-space data
- Continuous readout during acquisition (EP-COSI without ramp sampling only samples during ~75% readout)
- Inherently less sensitive to motion artifacts
- **Lower maximum slew rates for equal resolutions and spectral BW**
- (> 50% less for actual scan parameters used)

Drawbacks

- Sampling during time-varying readout gradients leads to increased noise variance[1]
  - SNR gains from averaging compensate so that sensitivity per time in both sequences is similar
- More complicated post-processing
  - Data must be regridded in order to apply FFT
  - Alternatively, projection-reconstruction (PR) algorithms can be applied using inverse radon transform

Emir 2017; Chew 2018; Steel 2018;; Kodibagkar 2019; Hingerl 2020

1) Pipe J and Duerk J, MRM 1995

Further Acceleration???
Projection Reconstruction/Radial

Original MRI Sequence

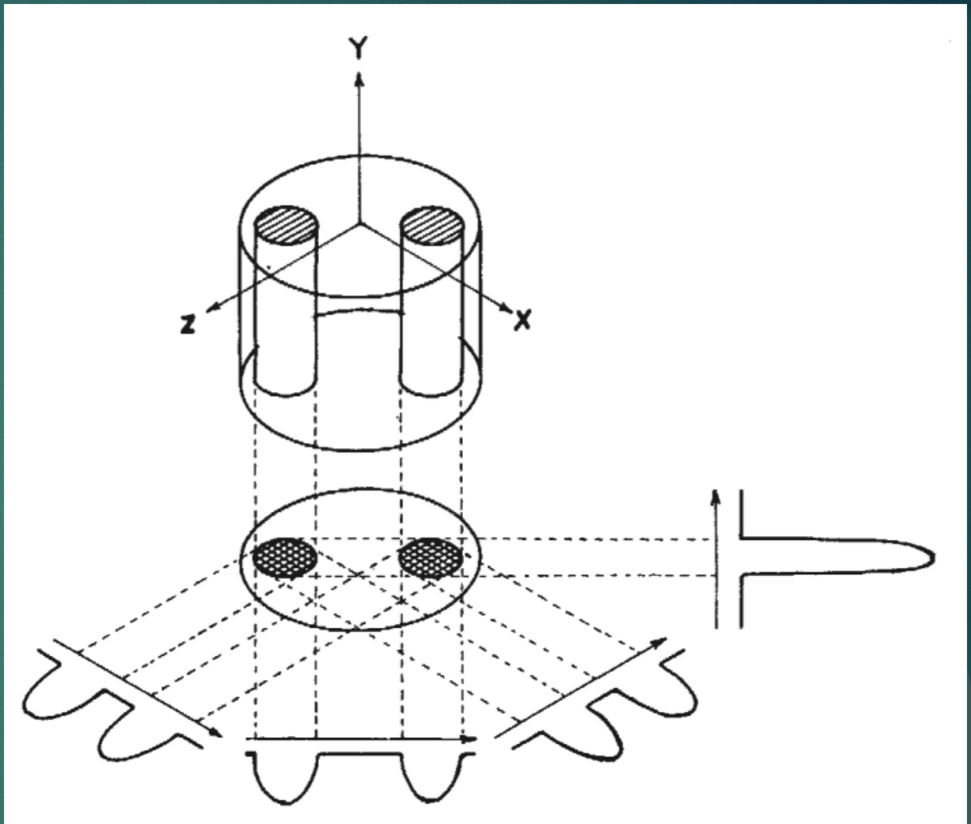

Lauterber P, *Nature* **242**, 190-191 (1973)

Series of projections taken at different angles

Radial Spectroscopic Imaging

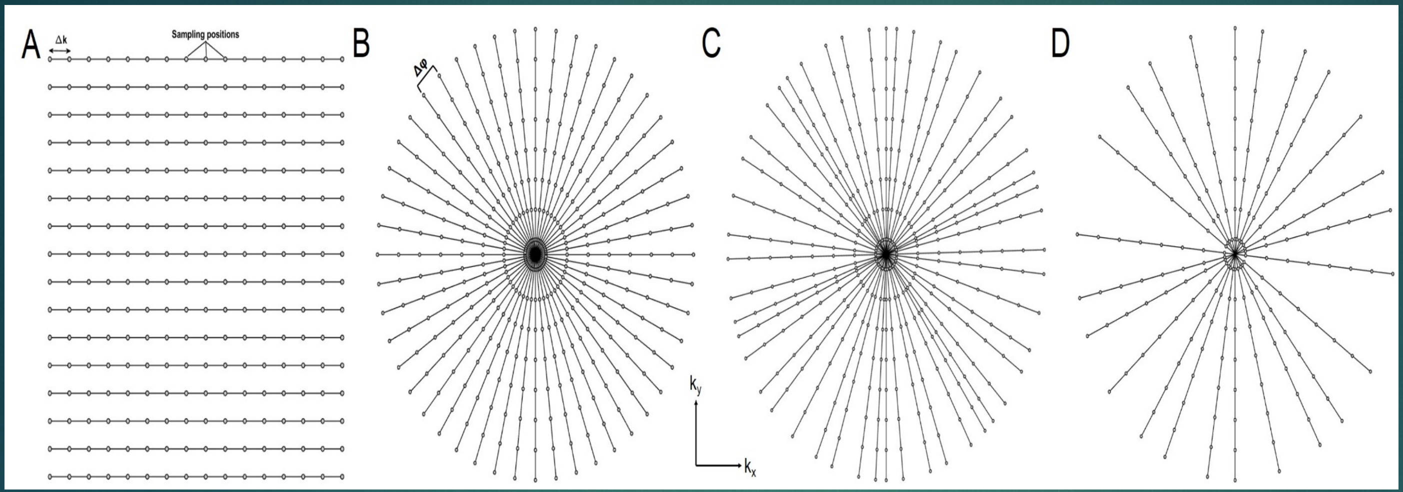

Sampling schemes using (**A**) Cartesian encoding; (**B**) radial encoding; (**C**) Golden angle radial projections successively incremented by 111.25^0, Δk=FOV. No of spokes, n_s=(π/2)*n, where n = base resolution, distance between spokes < Δk. (D) Undersampled radial acquisition (2X) compared to (C).

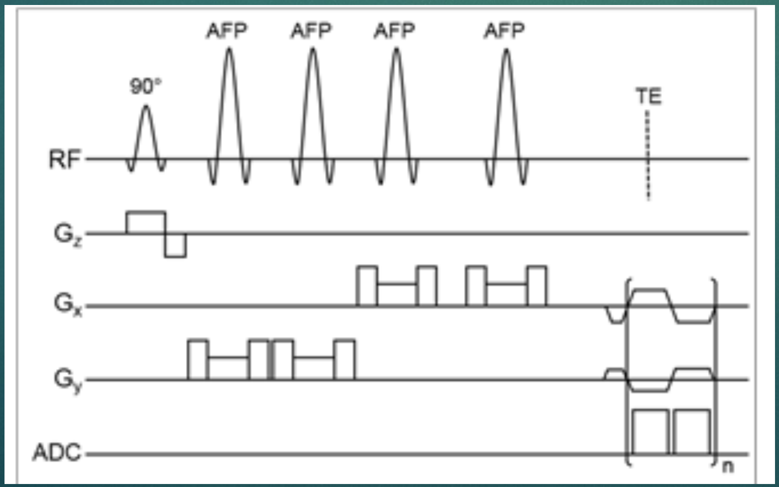

Saucedo, M. Sarma, MA Thomas
ISMRM 2020
MRM 2021

Radial Spectroscopic Imaging

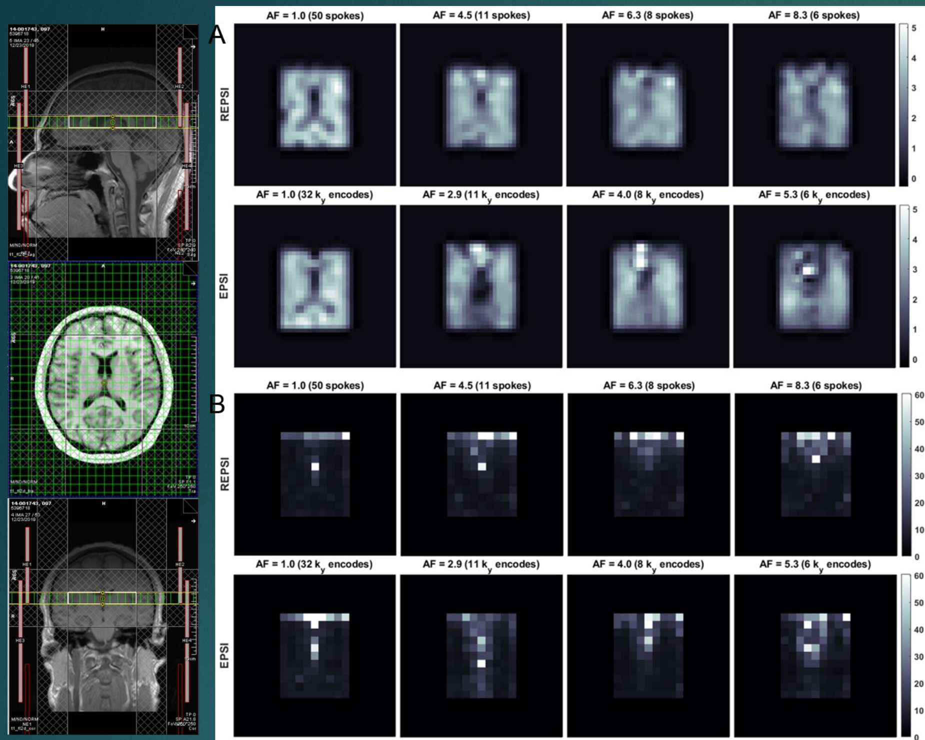

(Left) VOI localization in a 33 year-old healthy male volunteer. (A) tNAA maps from fully-sampled (AF = 1.0) REPSI and EPSI brain data (leftmost column), and tNAA maps from CS reconstructions of prospectively undersampled brain data acquired with 11, 8, and 6 radial spokes or k_y-lines. These maps are interpolated by a factor of two. (B) CRLB maps for the tNAA maps shown in (A).

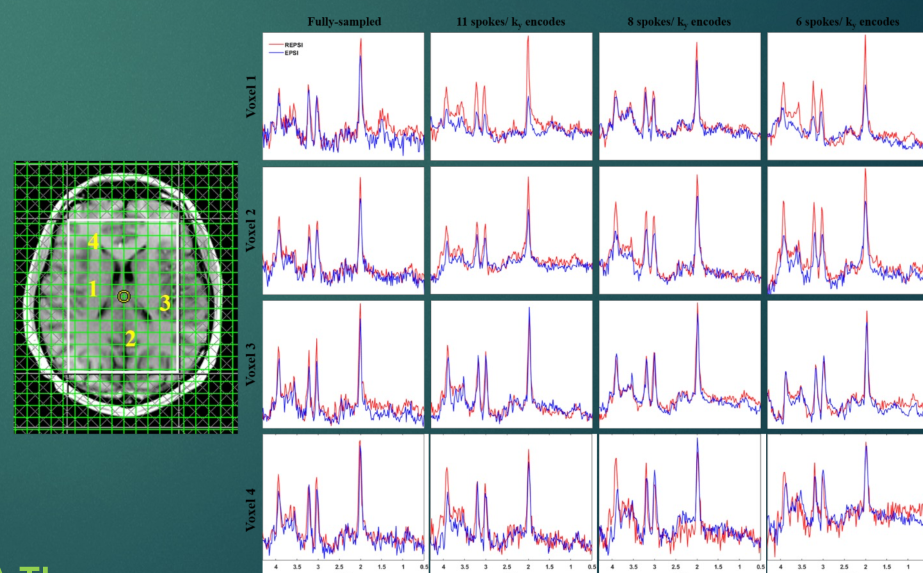

Representative and CS reconstructions of prospectively undersampled *in vivo* brain data from a 32 year-old healthy male volunteer. Spectra extracted : 1 – right putamen to corona radiata, 2 - occipital gray matter, 3 – left posterior insular cortex, and 4 – frontal white matter. Both the REPSI and EPSI data were prospectively undersampled with 11, 8, and 6 acquired radial spokes or k_y-lines, respectively.

A. Saucedo, M. Sarma, MA Thomas
MRM 2021

Rosette-Trajectories-based Spectroscopic Imaging (ROSE-SI)

David Geffen School of Medicine

A single petal in k-space is collected in a single excitation

Rosette trajectory is defined as

$$k(t) = k_{max} \sin(\omega_1 t) e^{i\omega_2 t}$$

Total acquisition time depends on the radial oscillation frequency (ω_1) and the rotational frequency (ω_2)

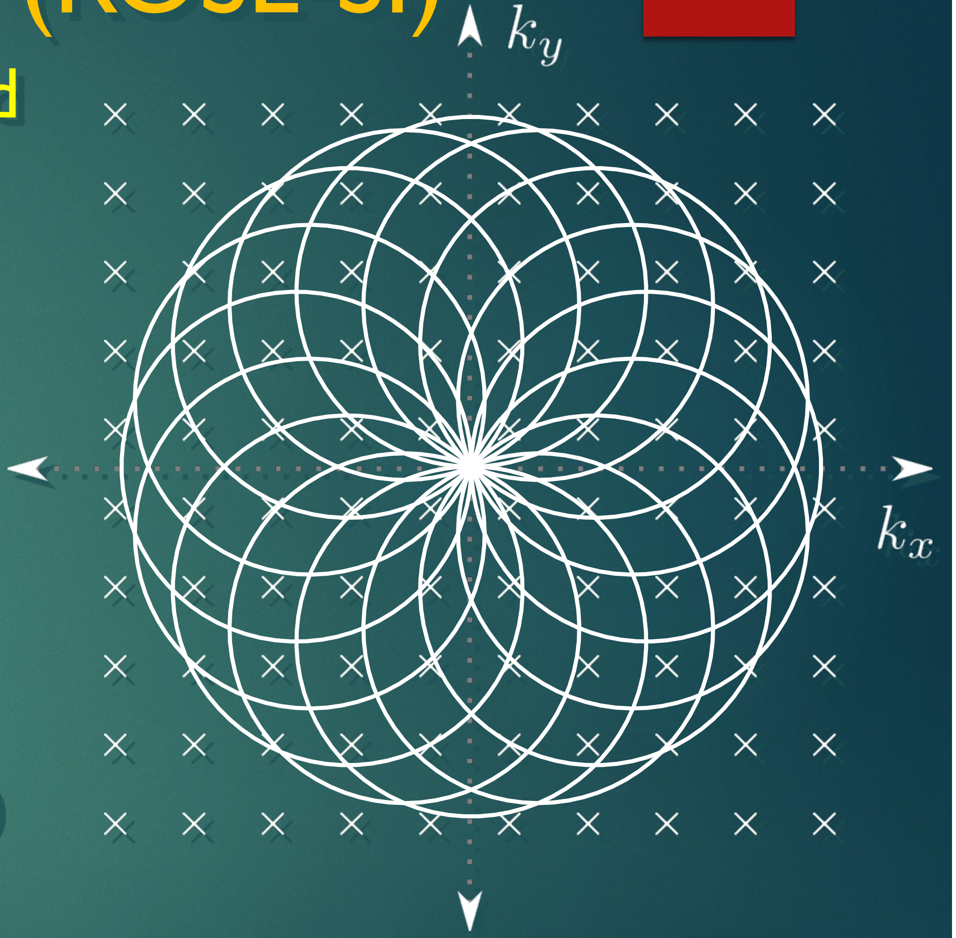

$$\frac{\omega_2}{\omega_1} \leq 1, \; N_{sh} \cong \frac{\pi \times N_x}{\sqrt{1 + 3\times(\omega_2/\omega_1)^2}}$$

$$\frac{\omega_2}{\omega_1} > 1, \; N_{sh} \cong \frac{\pi \times N_x}{\sqrt{3 + (\omega_2/\omega_1)^2}}$$

Rosette Petals (ROSE-SI)

$N_x = 16,\ \frac{\omega_2}{\omega_1} = 1,\ N_{sh} = 26$

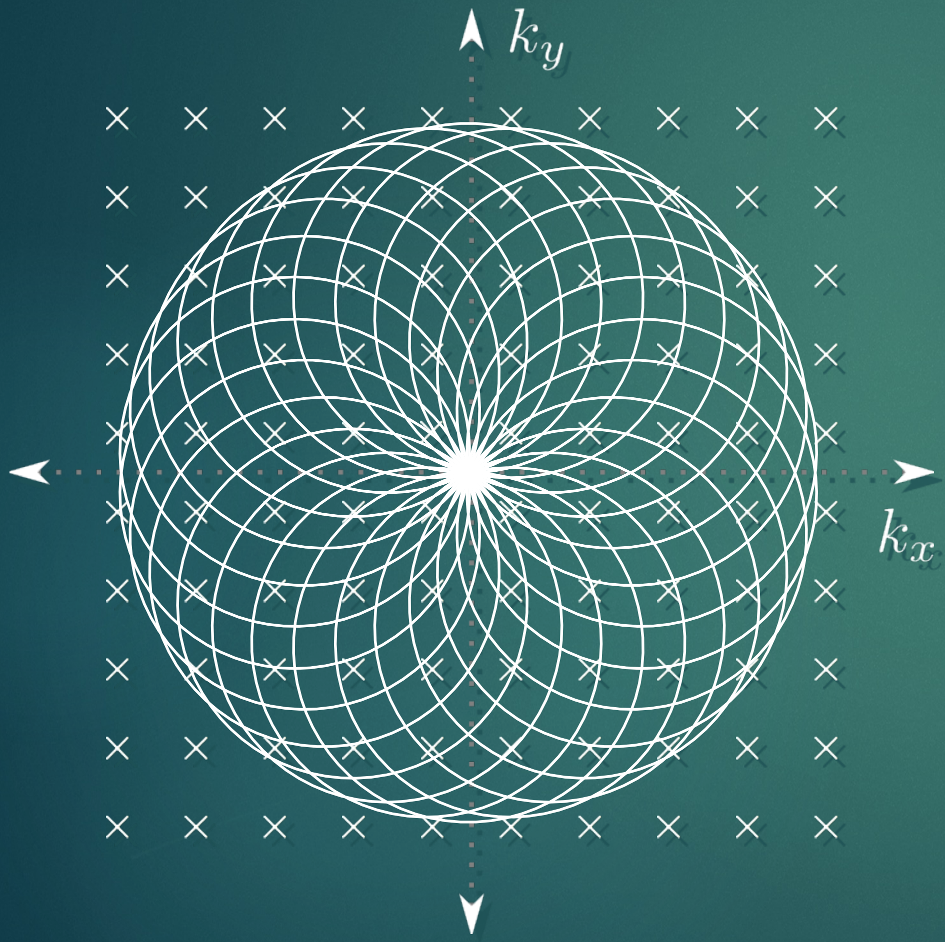

Needs 26 petals for N_x=16

$N_x = 16,\ \frac{\omega_2}{\omega_1} = 3,\ N_{sh} = 15$

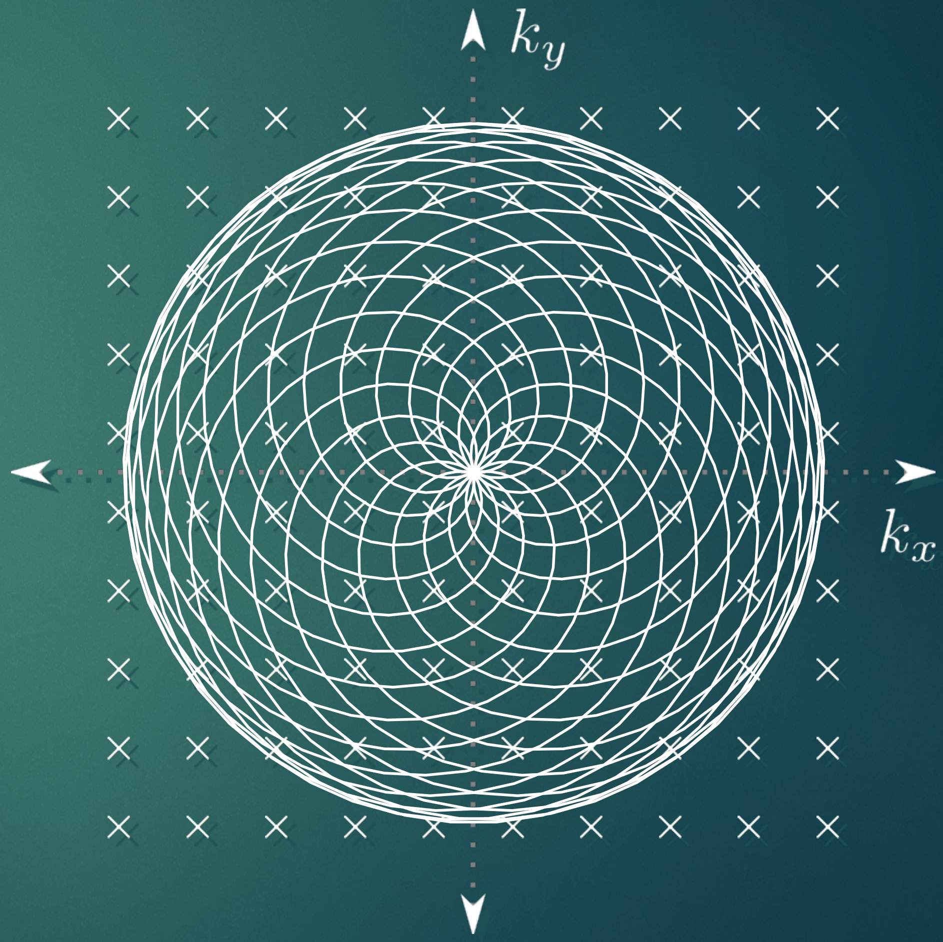

Needs only 15 petals for N_x=16

Rosette Petals (ROSE-SI)

$N_x = 32, \frac{\omega_2}{\omega_1} = 1$

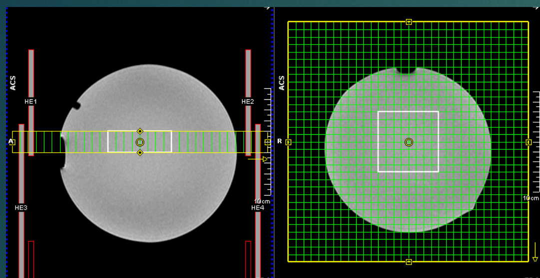

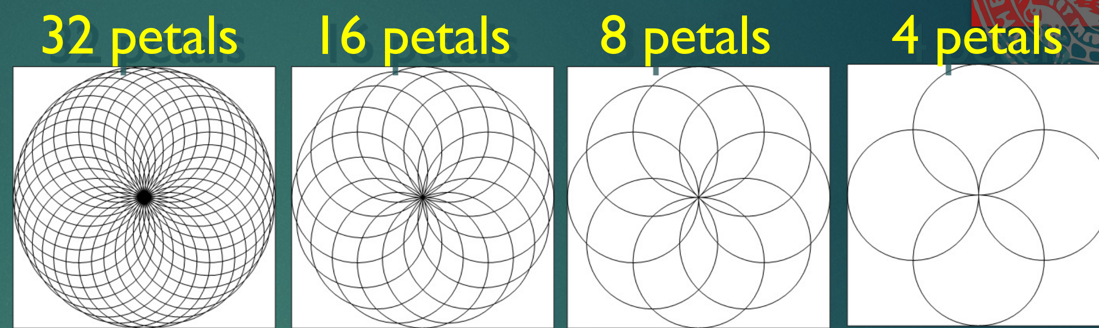

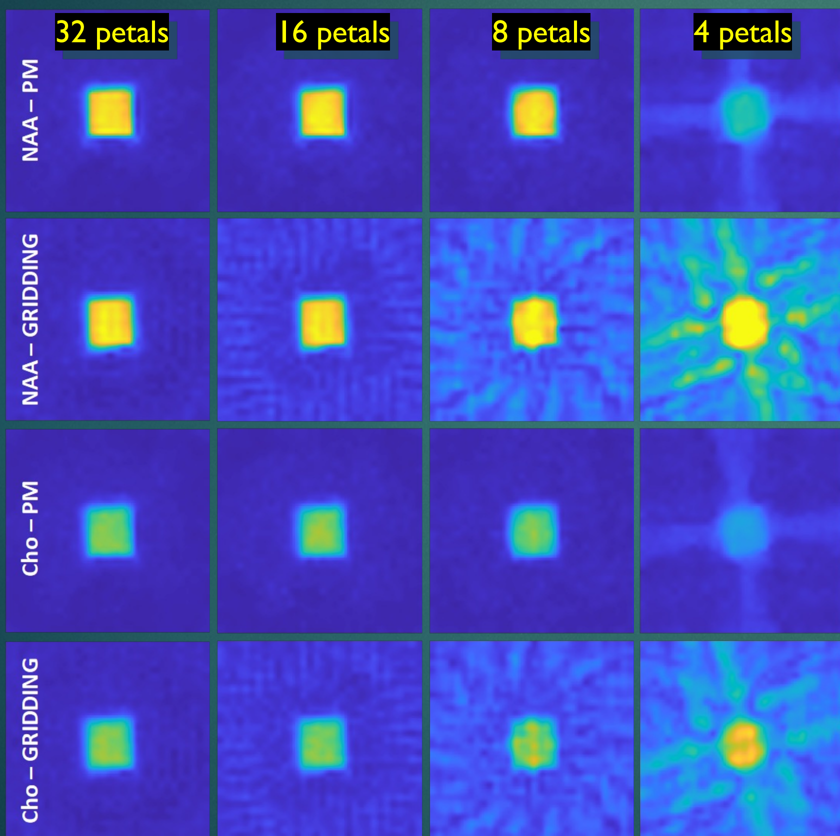

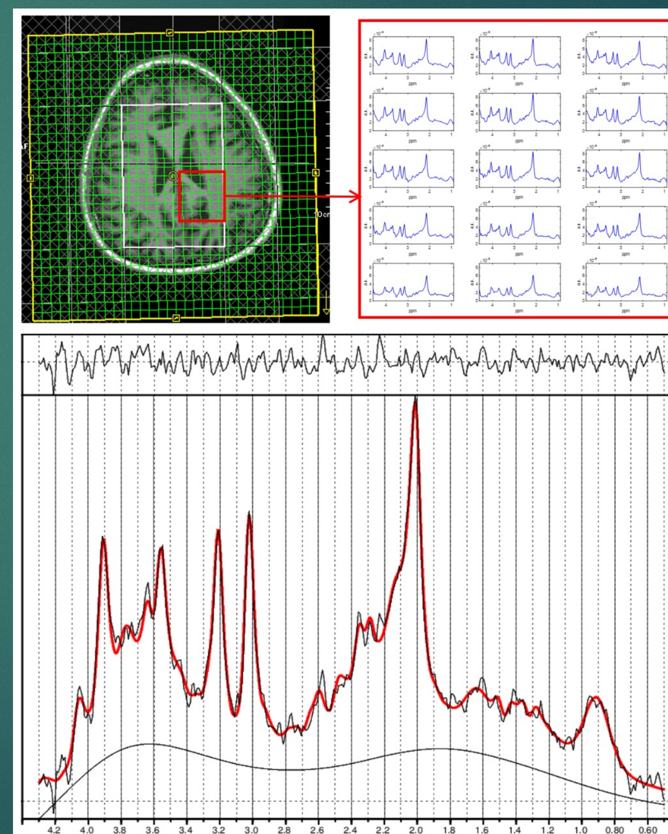

Conc.	%SD	/Cr	Metabolite
9.80E-07	40%	0.263	Ala
9.39E-07	40%	0.251	Asp
0.000	999%	0.000	Cho
3.73E-06	3%	1.000	Cr
7.25E-07	40%	0.194	GABA
1.24E-06	18%	0.331	Glc
1.47E-06	24%	0.394	Gln
4.35E-06	8%	1.164	Glu
1.01E-06	6%	0.269	GPC
9.63E-07	13%	0.258	GSH
8.94E-07	45%	0.239	Lac
3.50E-06	4%	0.938	mI
3.66E-06	5%	0.981	NAA
8.36E-07	29%	0.224	NAAG
0.000	999%	0.000	PCh
1.38E-06	26%	0.369	PE
0.000	999%	0.000	Tau
0.000	999%	0.000	-CrCH2
1.01E-06	6%	0.269	Cho+GPC+PCh
4.50E-06	4%	1.205	NAA+NAAG
5.82E-06	8%	1.558	Glu+Gln
1.51E-06	80%	0.405	Lip13a
0.000	999%	0.000	Lip13b
2.90E-07	180%	7.8E-02	Lip09
4.26E-06	16%	1.140	MM09
2.72E-07	122%	7.3E-02	Lip20
7.52E-06	18%	2.014	MM20
1.27E-06	43%	0.341	MM12
9.05E-07	110%	0.243	MM14
3.26E-06	23%	0.874	MM17
1.51E-06	80%	0.405	Lip13a+Lip13b
3.69E-06	40%	0.988	MM14+Lip13a+L
4.54E-06	14%	1.217	MM09+Lip09
7.79E-06	17%	2.087	MM20+Lip20

NO DIAGNOSTICS

MISCELLANEOUS OUTPUT

FWHM = 0.059 ppm S/N = 17
Data shift = 0.010 ppm
Ph: 13 deg 6.9 deg/ppm

A Joy, U Emir, PM Macey, MA Thomas, ISMRM 2023

Rosette Petals (ROSE-SI)

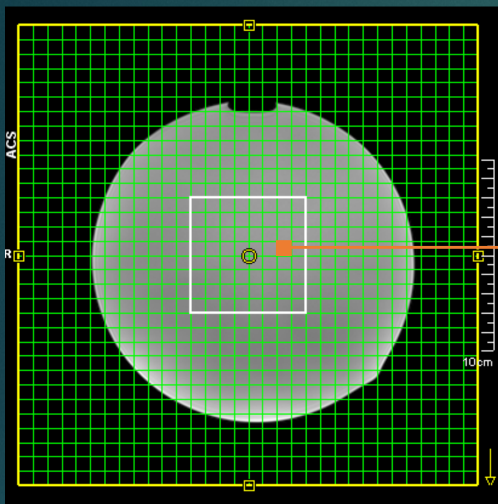

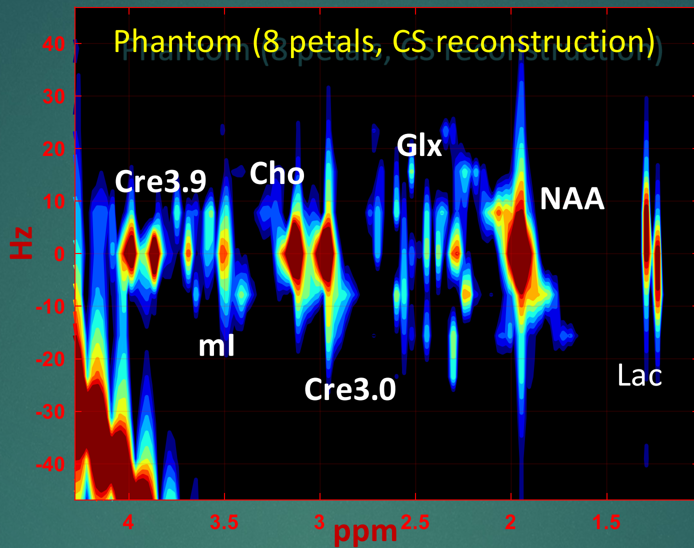

$$N_x = 32, \frac{\omega_2}{\omega_1} = 1$$

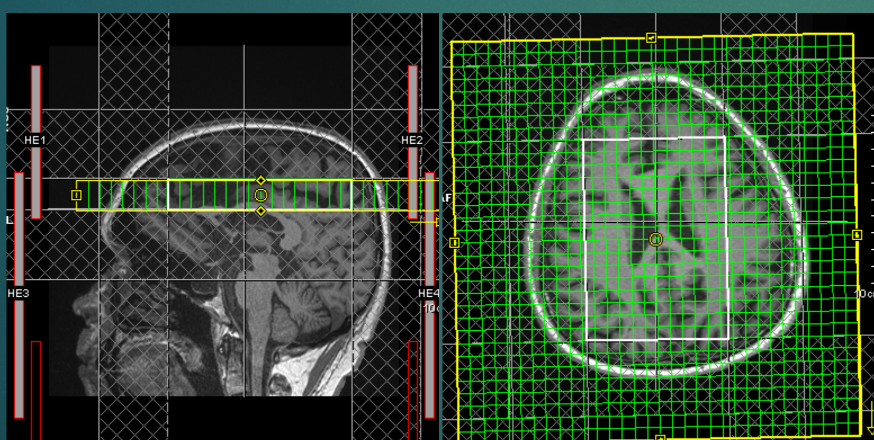

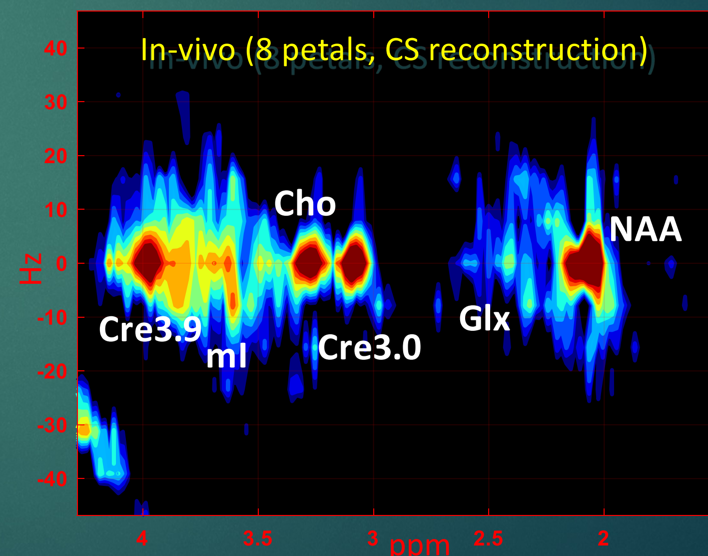

A Joy, U Emir, PM Macey, MA Thomas, ISMRM 2023

Advantages of Rosette Trajectories

- Continuous readout during acquisition (EP-COSI without ramp sampling only samples during ~75% readout)
- Inherently less sensitive to motion artifacts (due to oversampling of center of k-space)
- Less demanding on gradient hardware (especially for lower rotational frequencies)
- Higher sensitivity than the standard CSI acquisition with square k-space support.
- Freedom in trajectory design to optimize for the available hardware by adjusting ω_2/ω_1
- Encoding speed of rosette can be used to accelerate the data acquisition process.
- Higher sampling density in central and peripheral k-space allows undersampling by reduced number of petals for accelerated acquisition and CS reconstruction

Drawbacks

- Regular patterns of phase accrual in k-space can cause artifacts
- More complicated post-processing

  - Data must be regridded in order to apply FFT

  - Alternatively, non-uniform fast Fourier transform (NUFFT) can be used

Noll, TMI 1997; Schirda et al., JMRI 2009;
Shen et al., MRM 2018; Joy et al., ISMRM 2023

Single-voxel localized 2D MRS : L-COSY and JPRESS

1D MRS Quantitation

- LC-Model for 1D MRS quantitation.
- Works in frequency domain using prior knowledge

Provencher (2001)

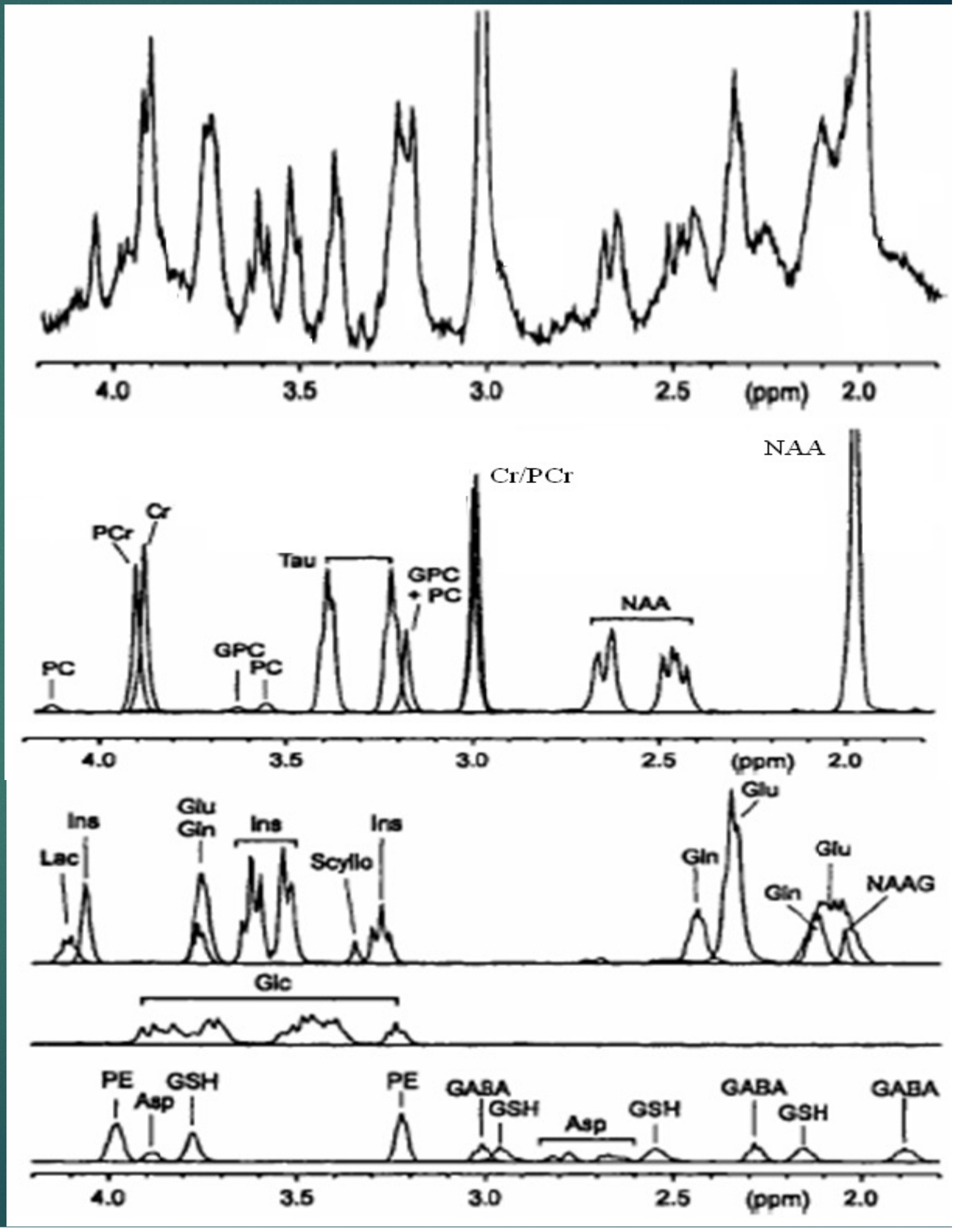

A quote from 1991 Nobel laureate Richard Ernst

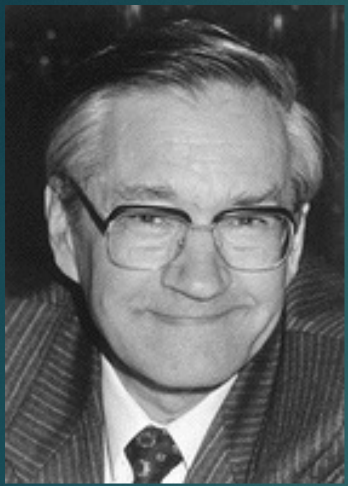

"One-dimensional spectra that are rendered inscrutable because of severe overlap may be unravelled by separating interactions of different physical origins, e.g. chemical shift and couplings, thus making it possible to spread the signals in a second frequency dimension much like opening a Venetian blind."

Why 2D Spectroscopy?

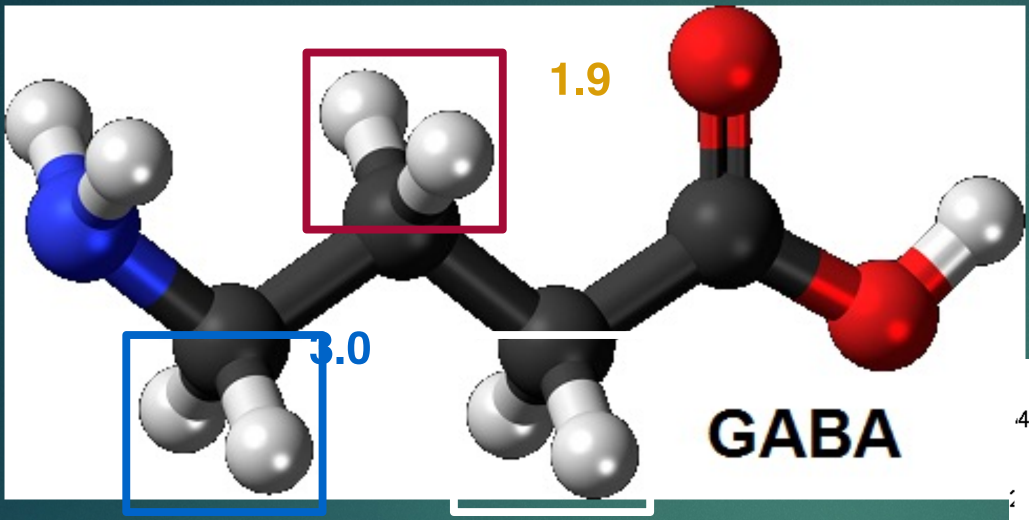

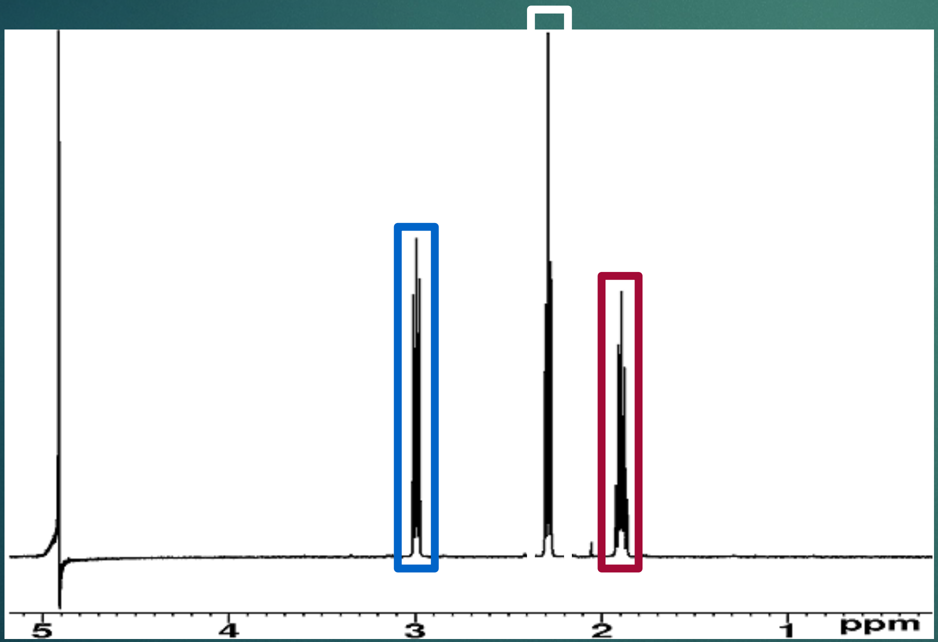

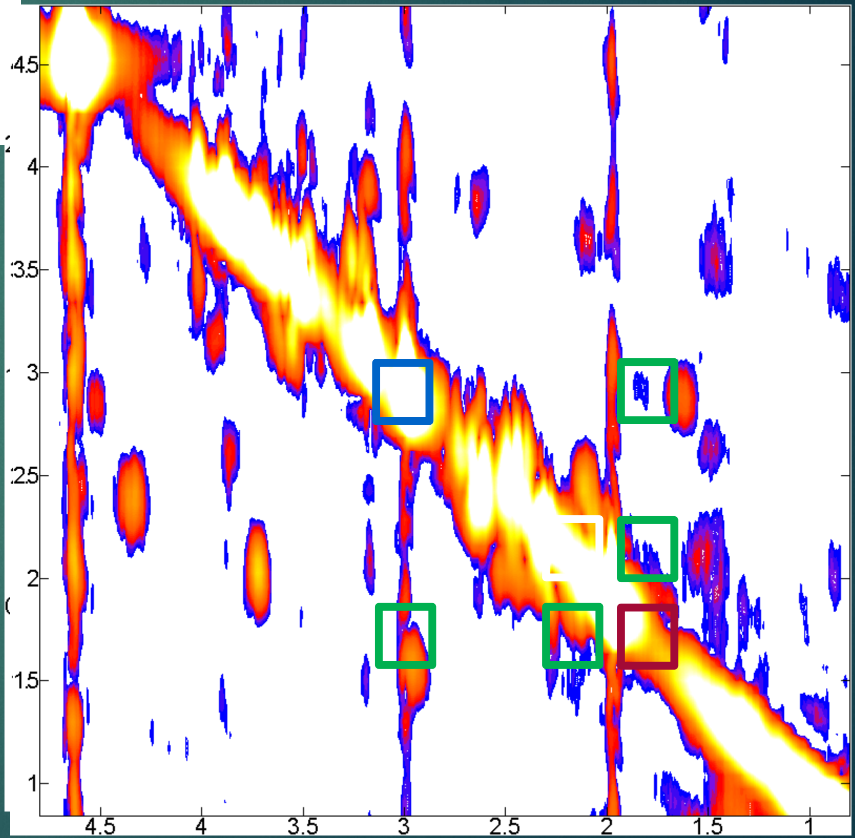

Verma et al. ISMRM 2014

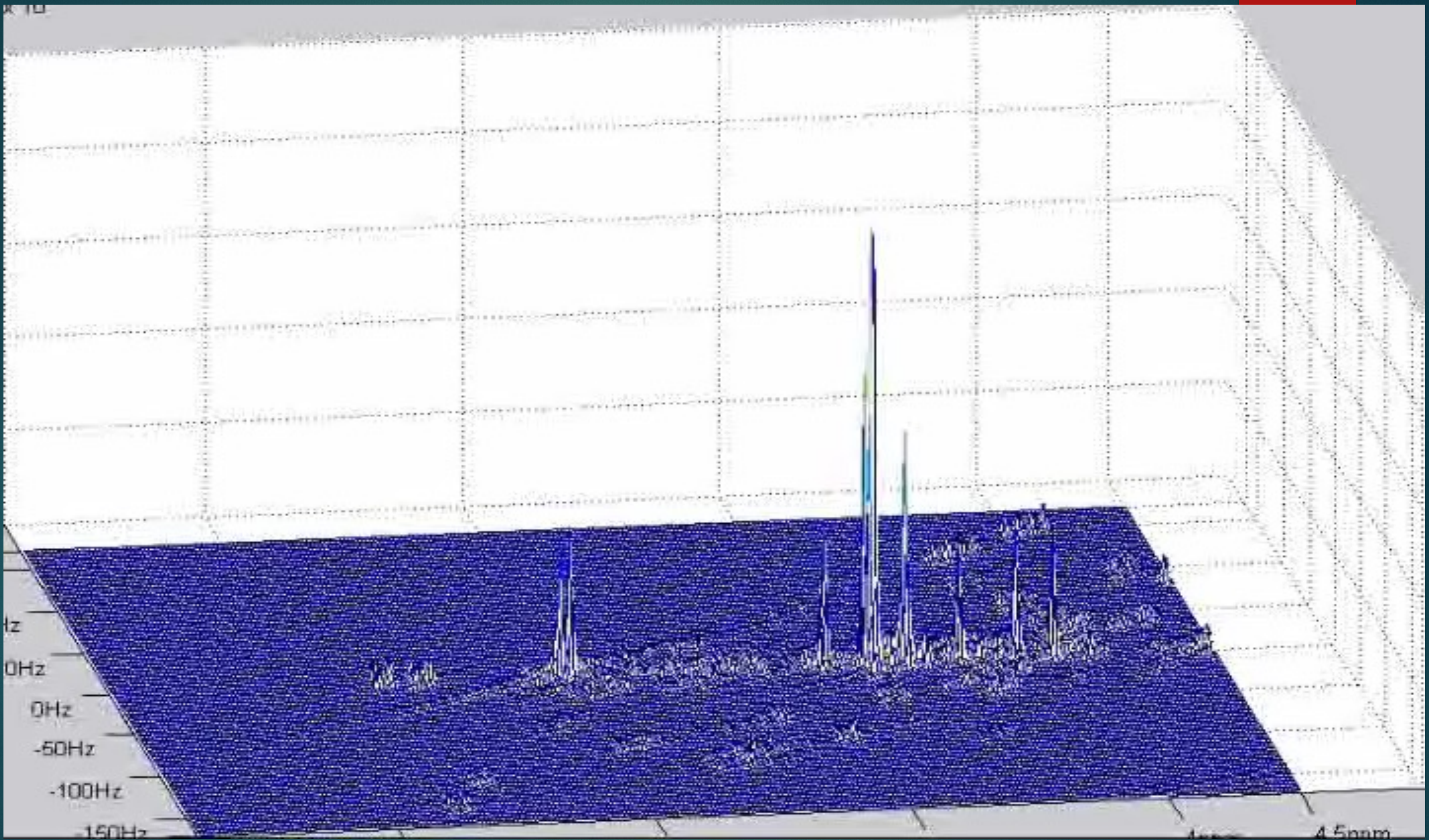
0Hz
0Hz
-50Hz
-100Hz
4.5ppm

Localized 2D Correlated Spectroscopy (L- COSY)

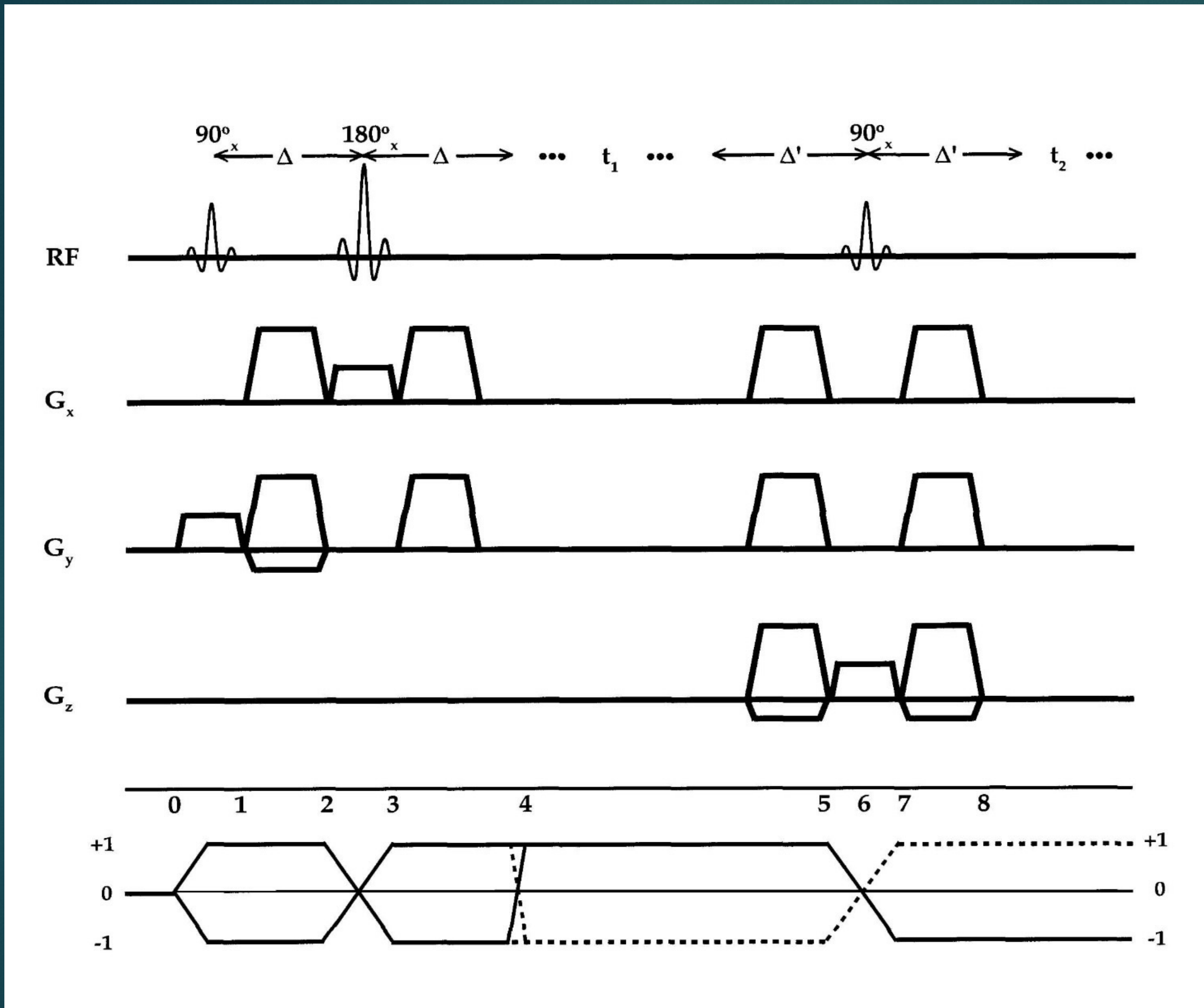

- Based on a spin-echo and a coherence-transfer-echo
Hahn (1952) / Maudsley, Wokaun and Ernst (1978)

Thomas et al. (MRM2001)

F1

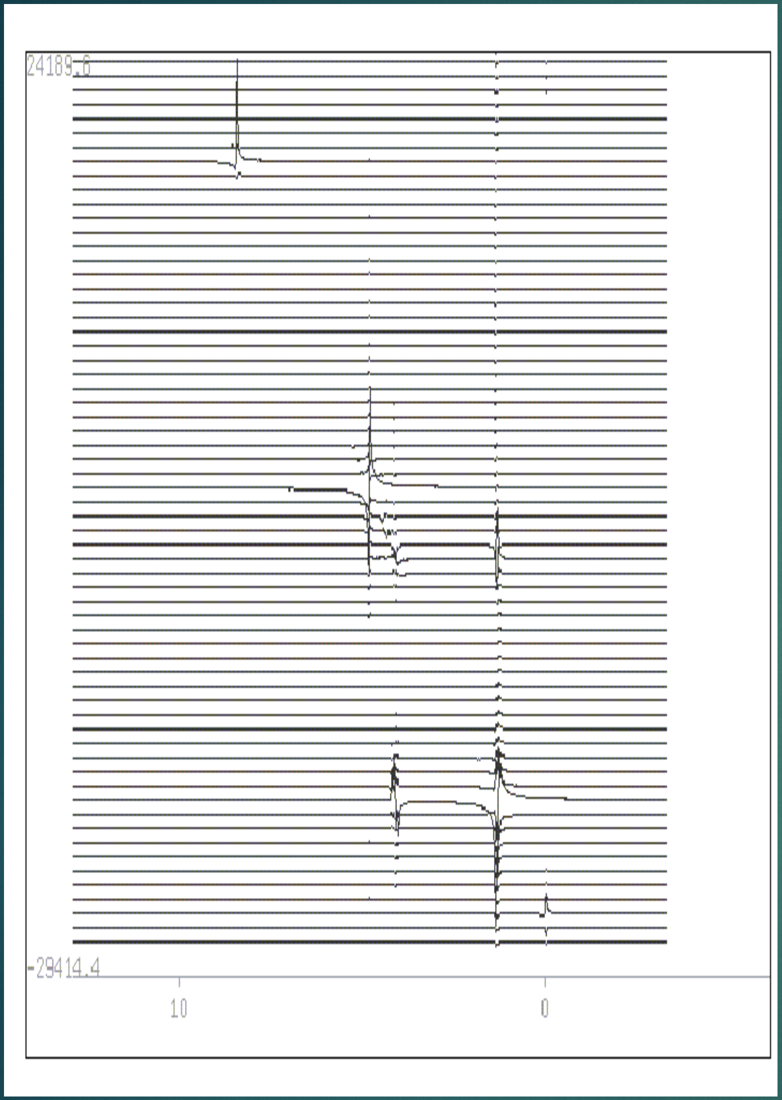
24189.6
-29414.4
10
0

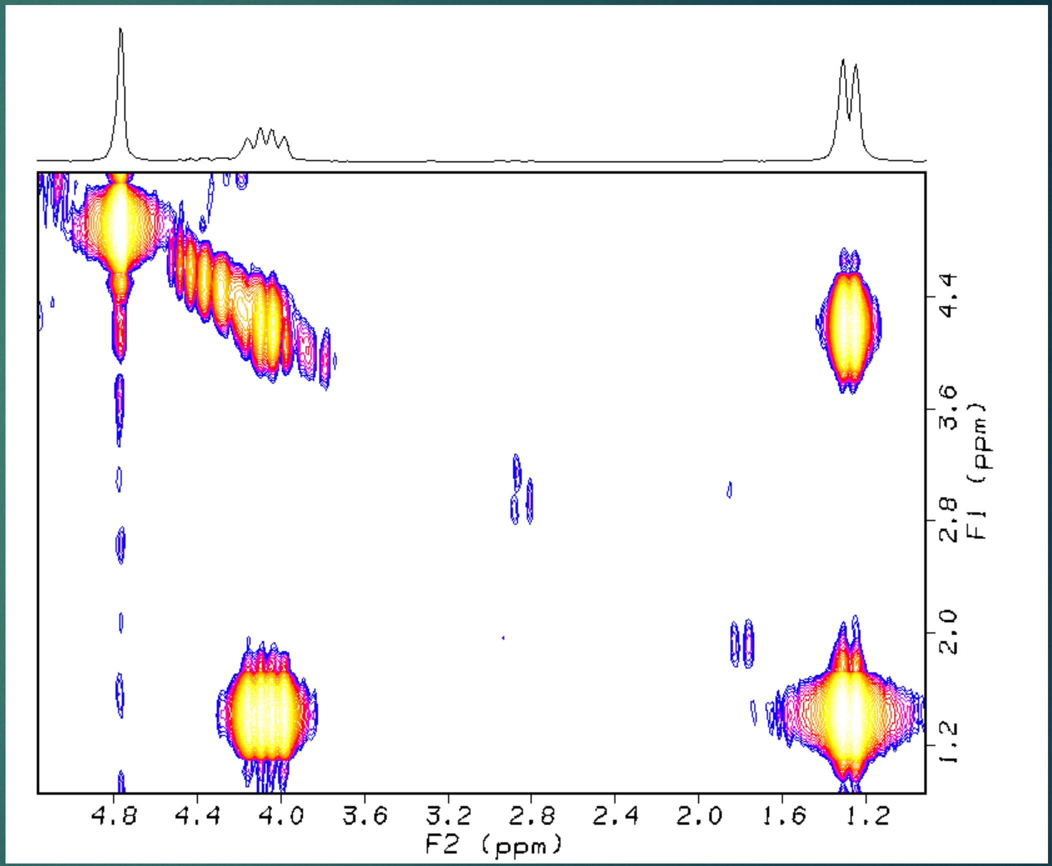
4.8
4.4
4.0
3.6
3.2
2.8
2.4
2.0
1.6
1.2
F2 (ppm)
4.4
3.6
2.8
2.0
1.2
F1 (ppm)

F2

Brain Phantom 3T MRI/MRS Scanner

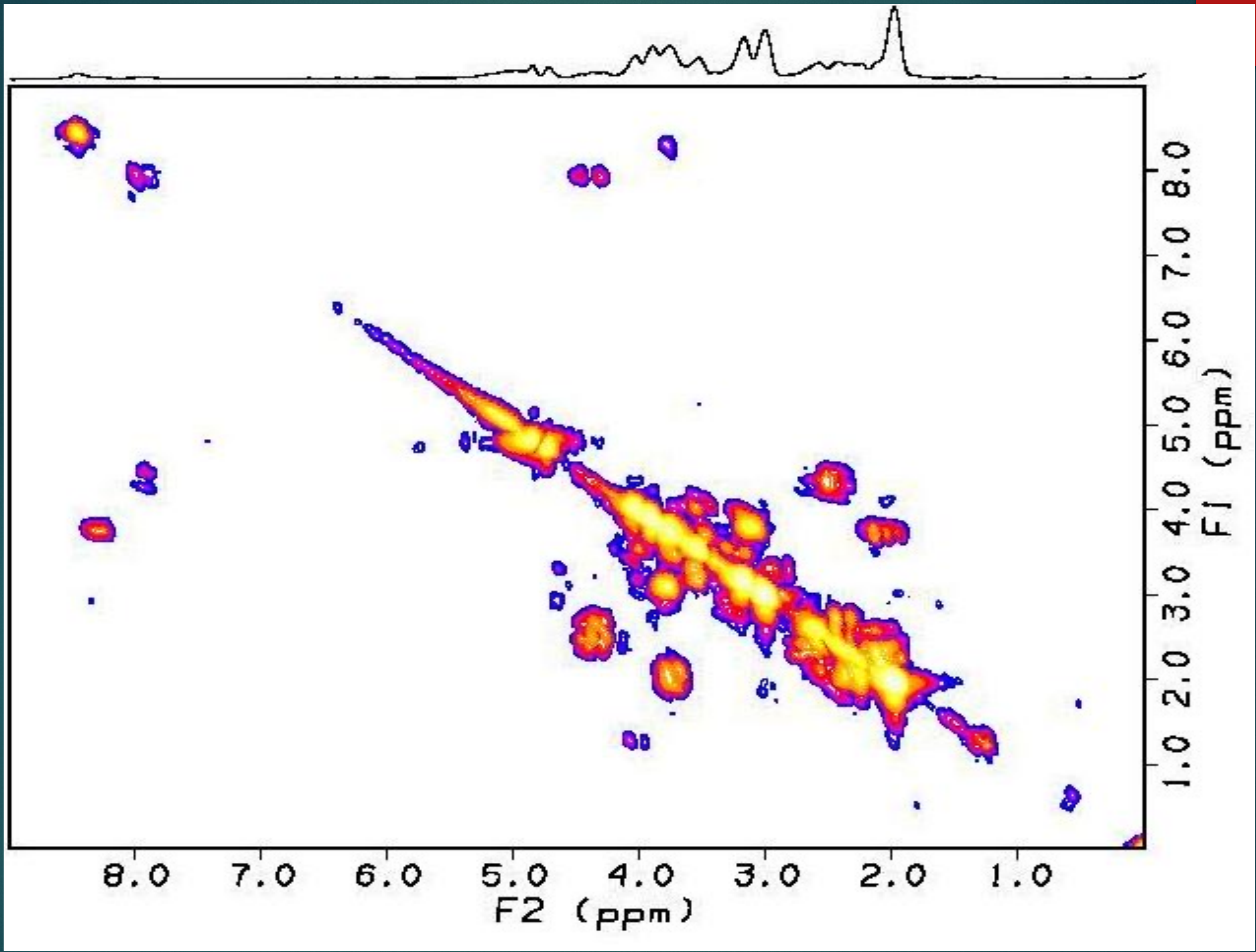

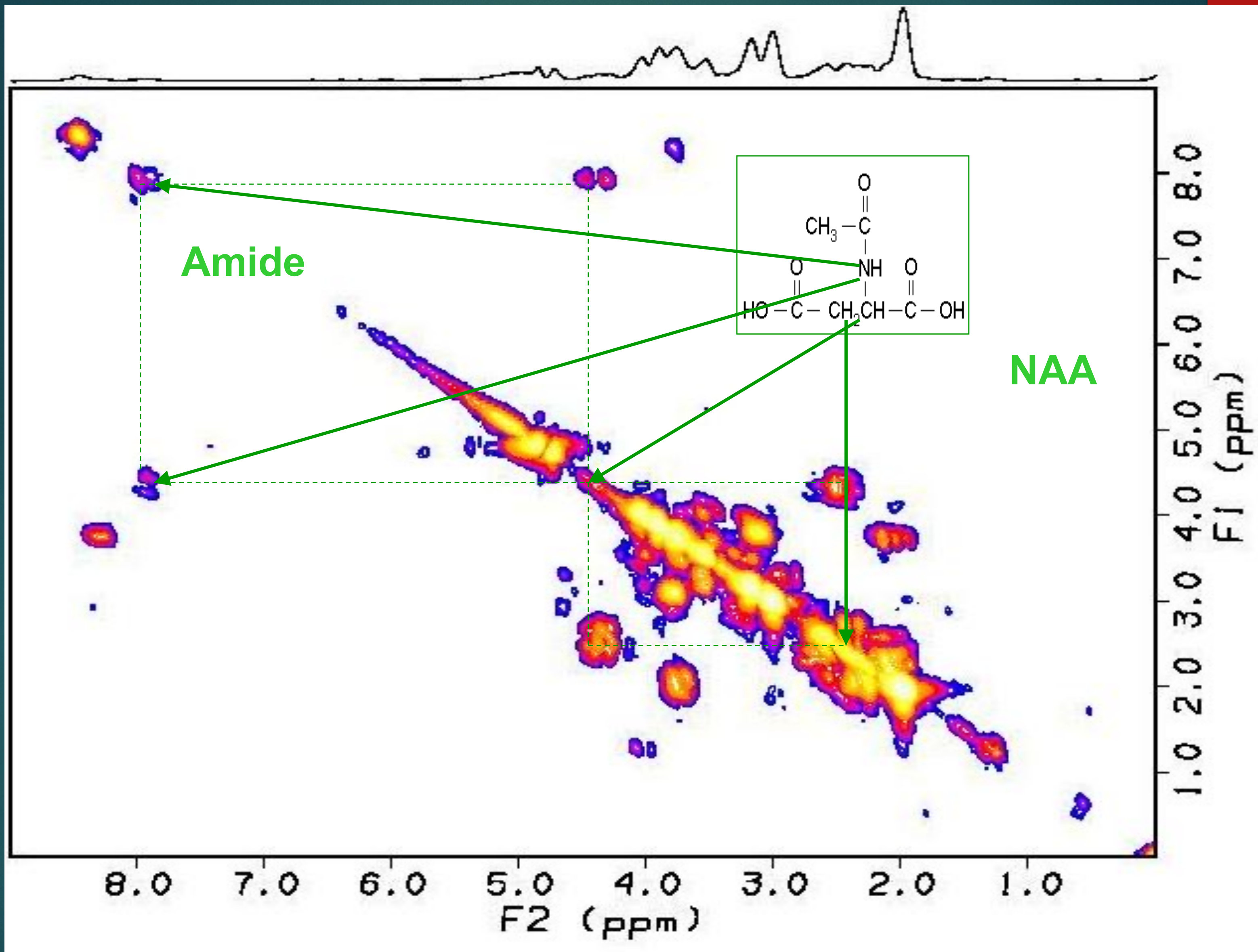

Amide
NAA
CH3 – C
NH
HO – C – CH2CH – C – OH
F2 (ppm)
F1 (ppm)
8.0
7.0
6.0
5.0
4.0
3.0
2.0
1.0

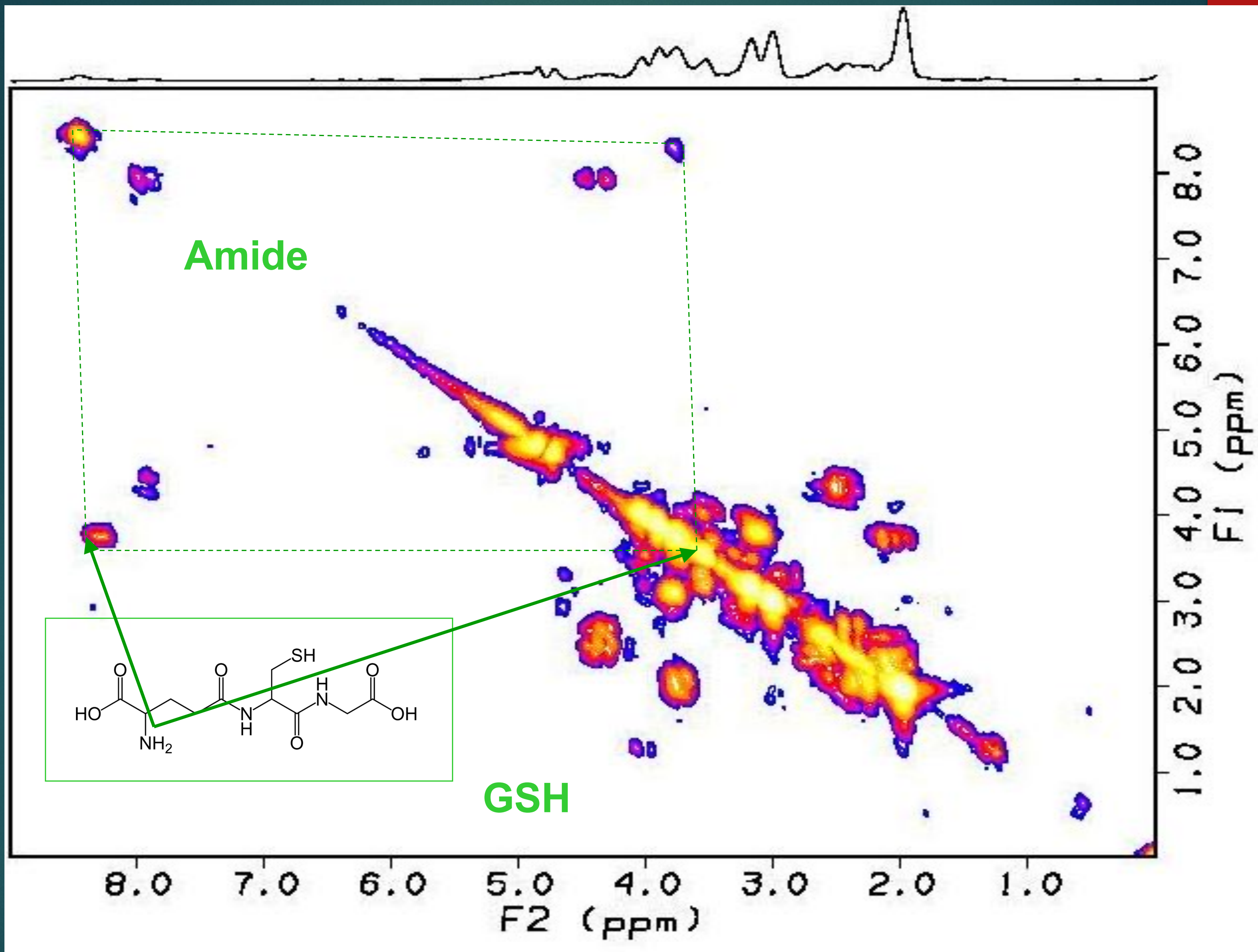

Amide
GSH
SH
HO
O
NH2
N
H
OH
F2 (ppm)
F1 (ppm)
8.0
7.0
6.0
5.0
4.0
3.0
2.0
1.0

2D MRS – Gray Matter Metabolites

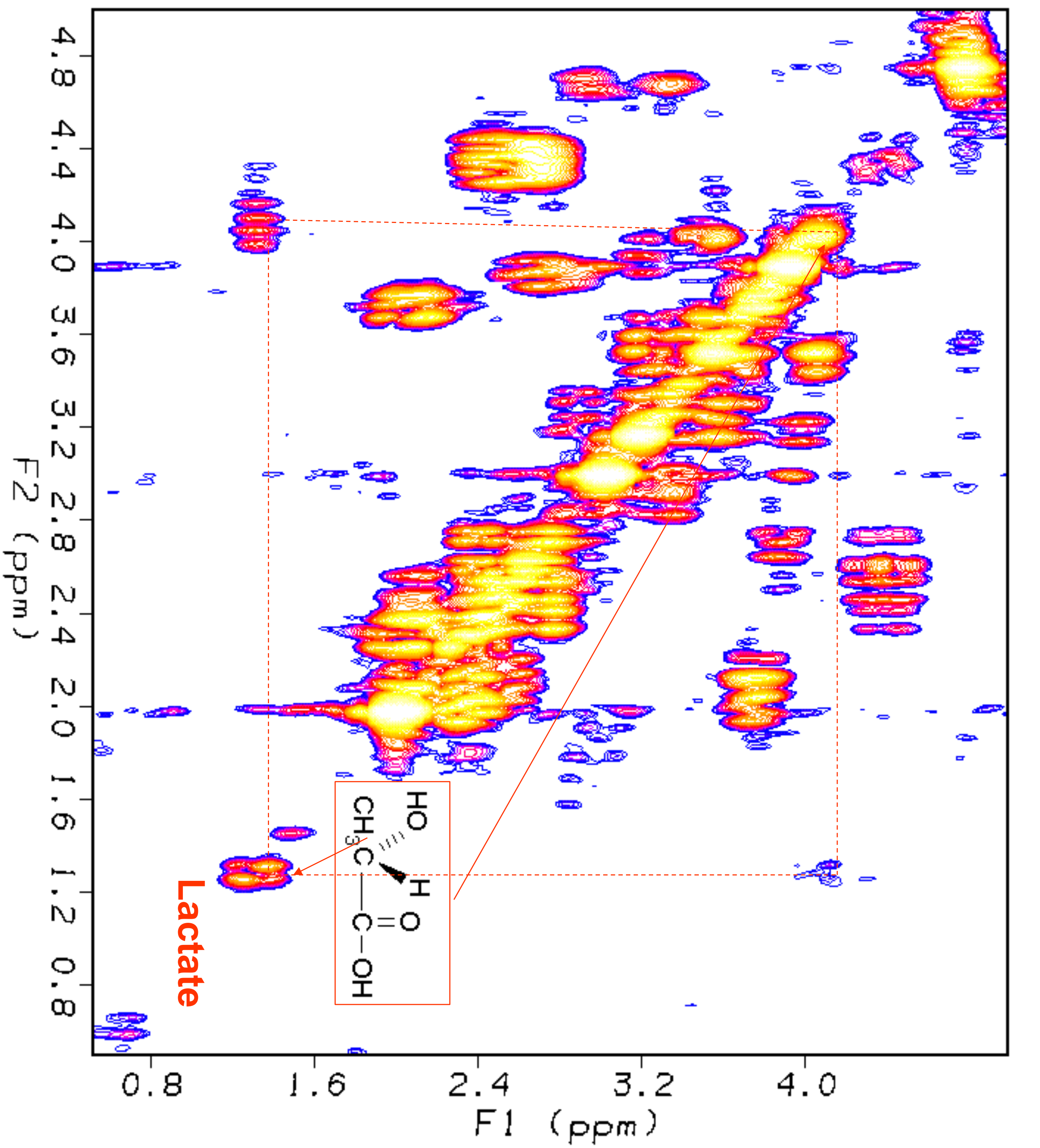

2D MRS – Gray Matter Metabolites

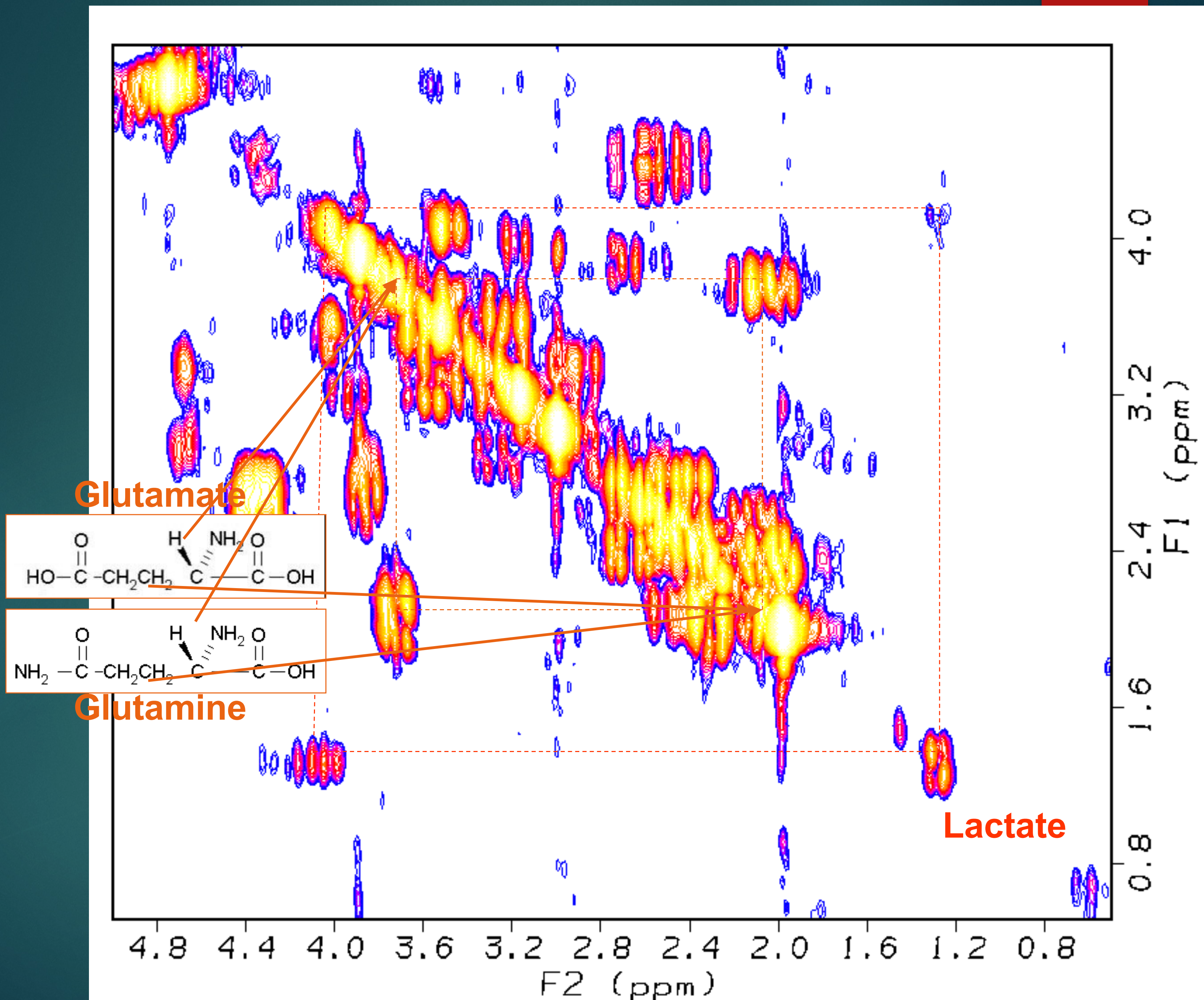

Localized 2D COSY Spectra of a 27yo healthy breast

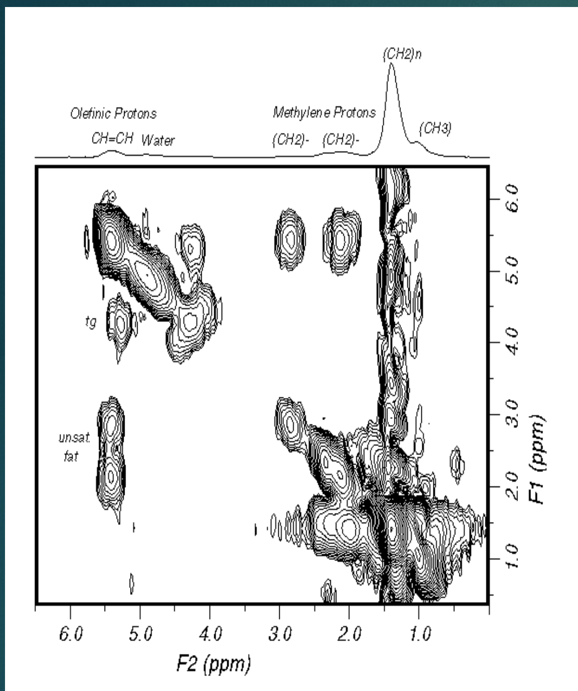

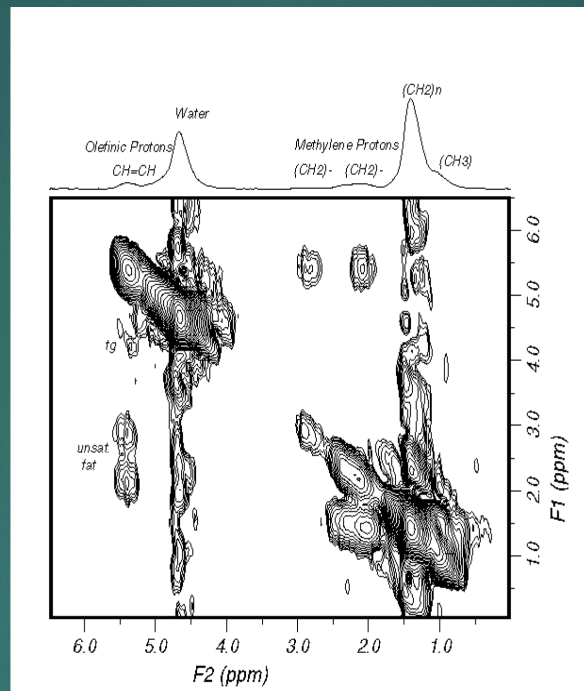

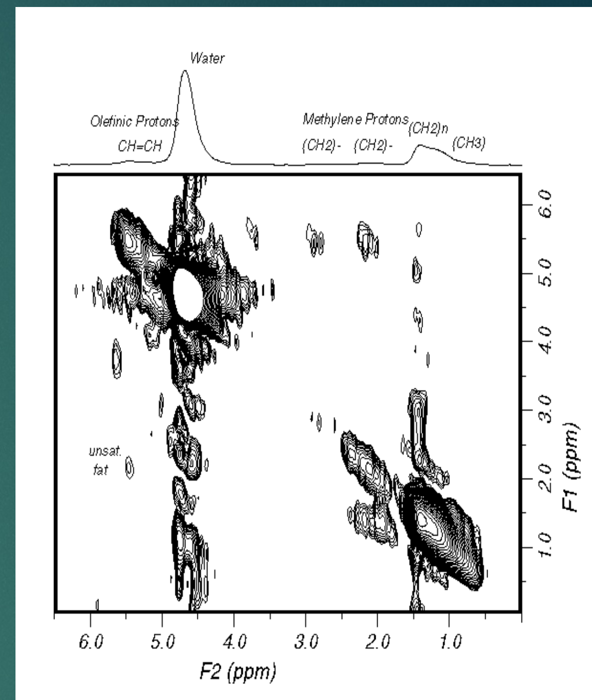

- $1 \times 1 \times 1$ cm^3
- 40 t_1 incr.
- 8NEX/ Δ t_1

¯10 minutes

-1.5T

¯30 minutes for 3 locations

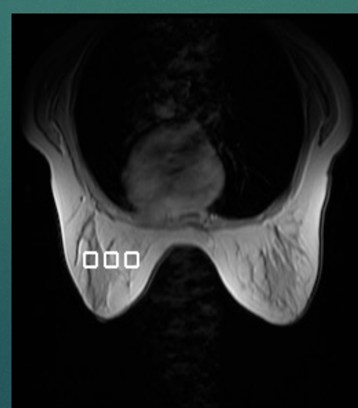

(Thomas JMRI2001)

DCE-MRI

- Graphs of DCE-MRI curves for malignant patients
- Plots show uncertainty in enhancement curves
- Patient I shows a plateau shaped curve which cannot differentiate malignant from benign lesion

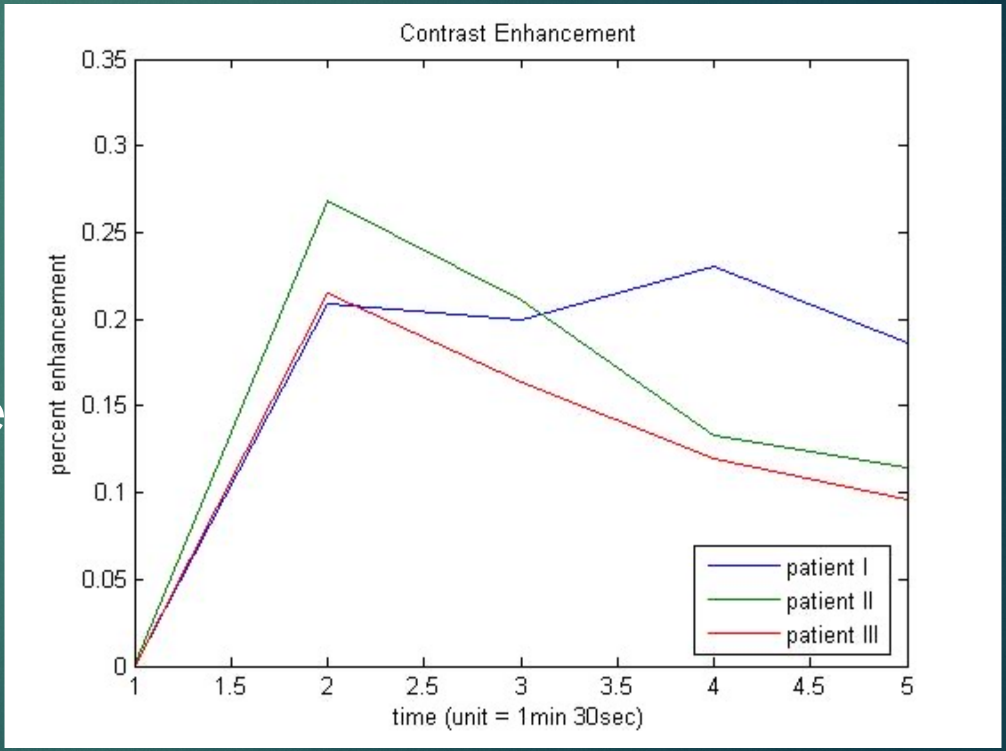

Malignant Patient with Type II enhancement

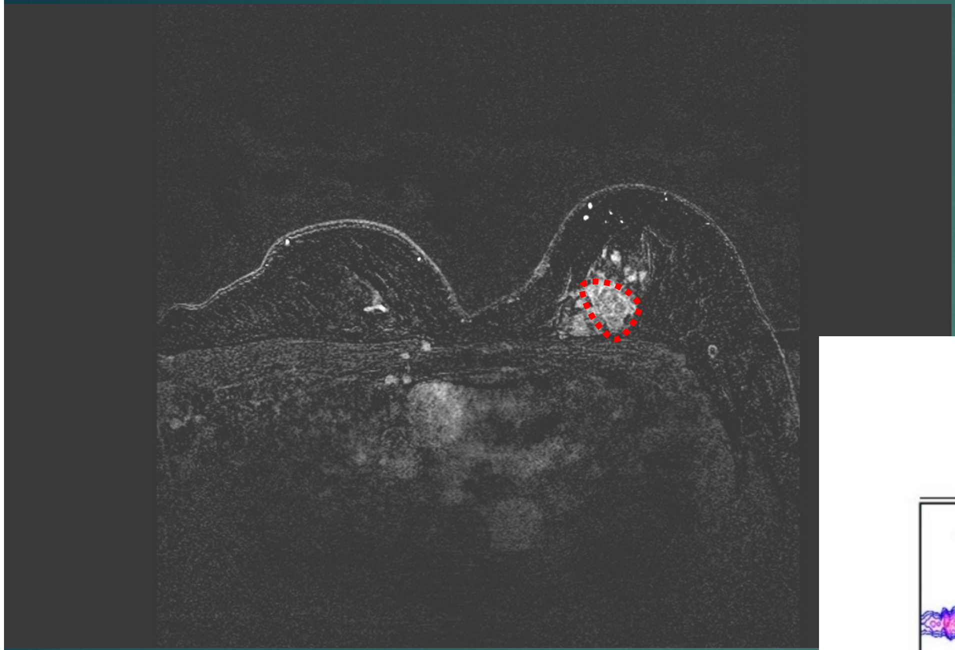

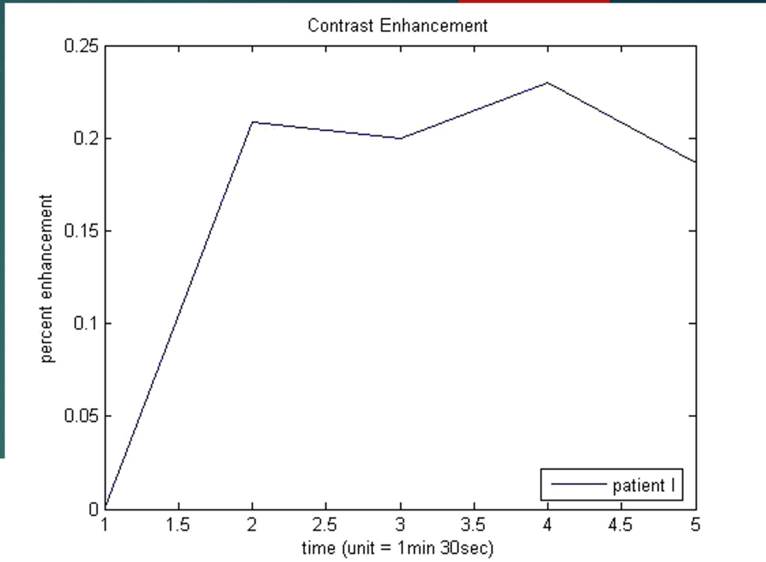

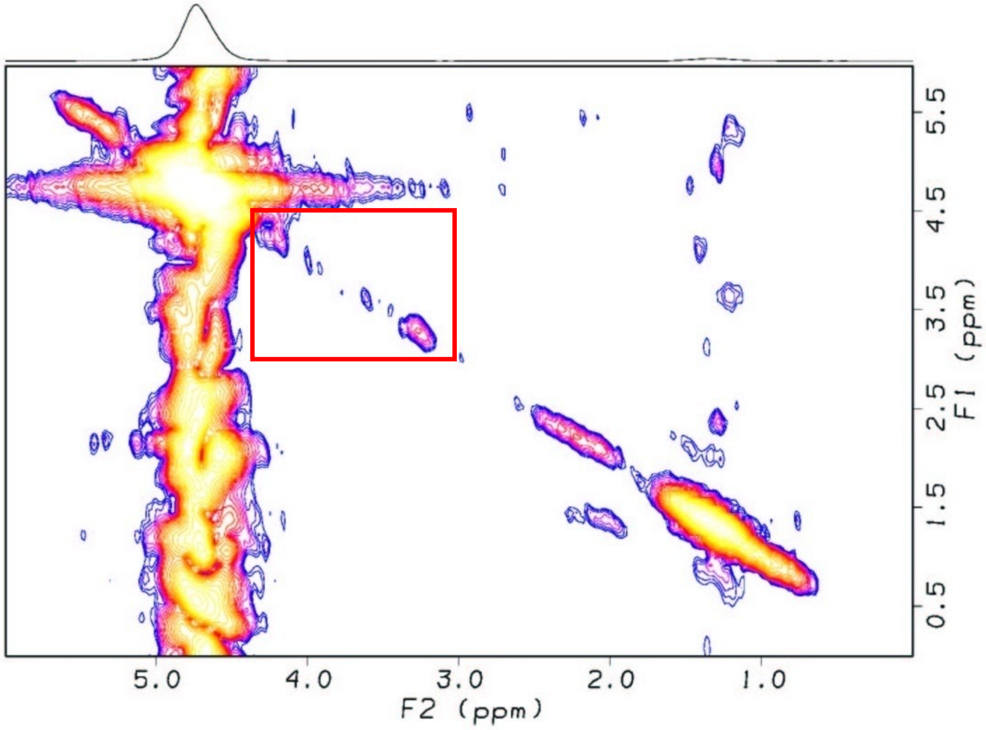

-56 yo malignant patient
-1x1x1 cm3
-45 t1 incr.
-8NEX/ Δ t1
-12 minutes

Lipnick 2010

2D L-COSY of Breast Cancer

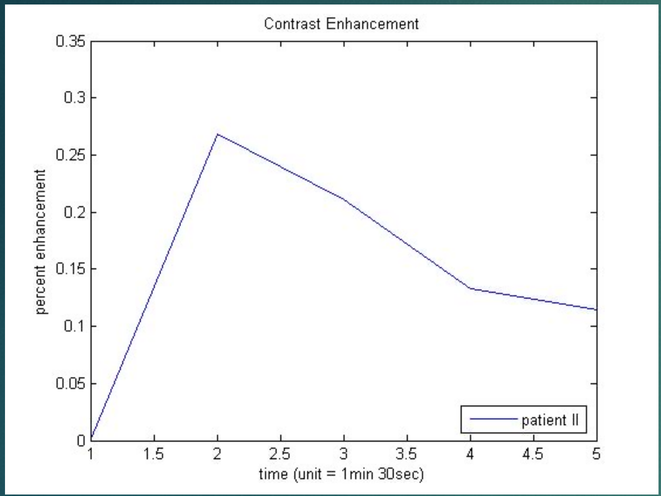

A 55 yo malignant patien

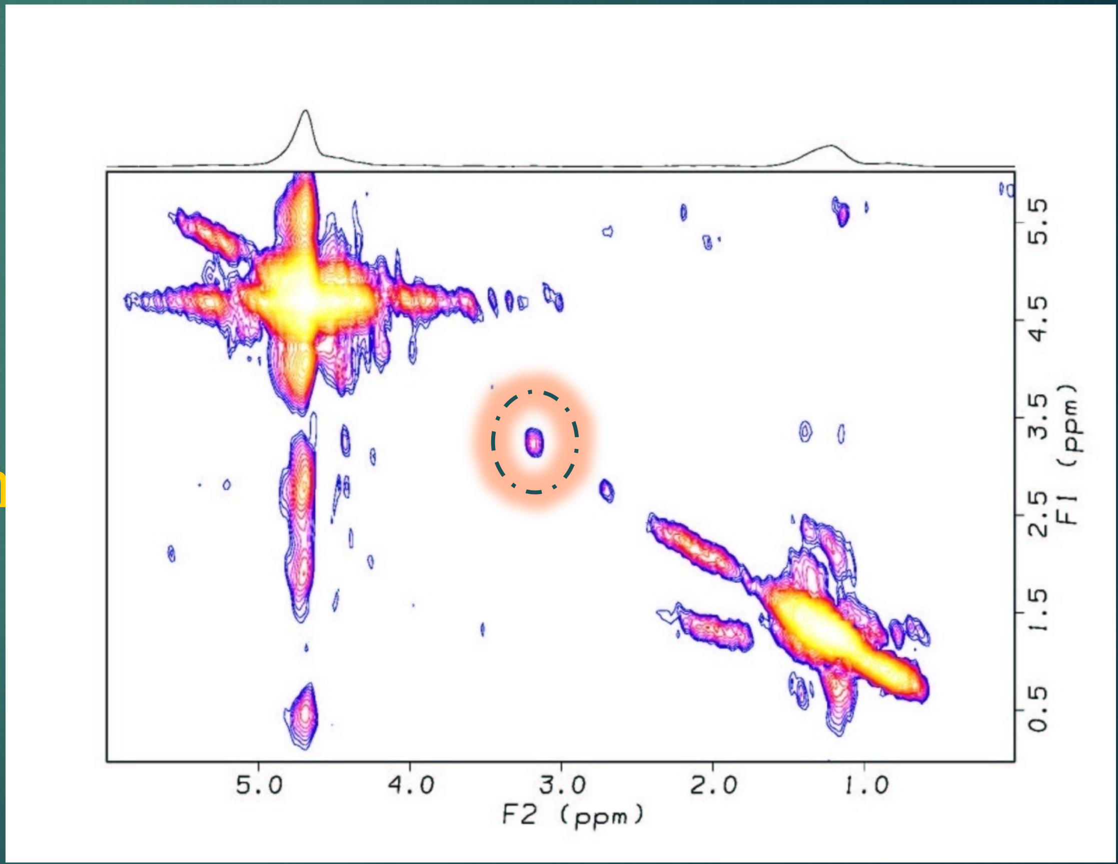

- $1 \times 1 \times 1$ cm^3
- 45 t_1 incr.
- 8NEX/ Δt_1
- 12 minutes

Lipnick 2010

2D L-COSY of Breast Cancer

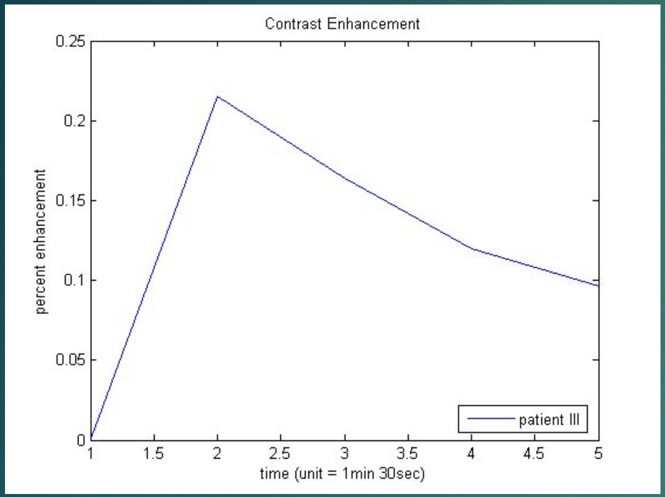

A 55 yo malignant patien

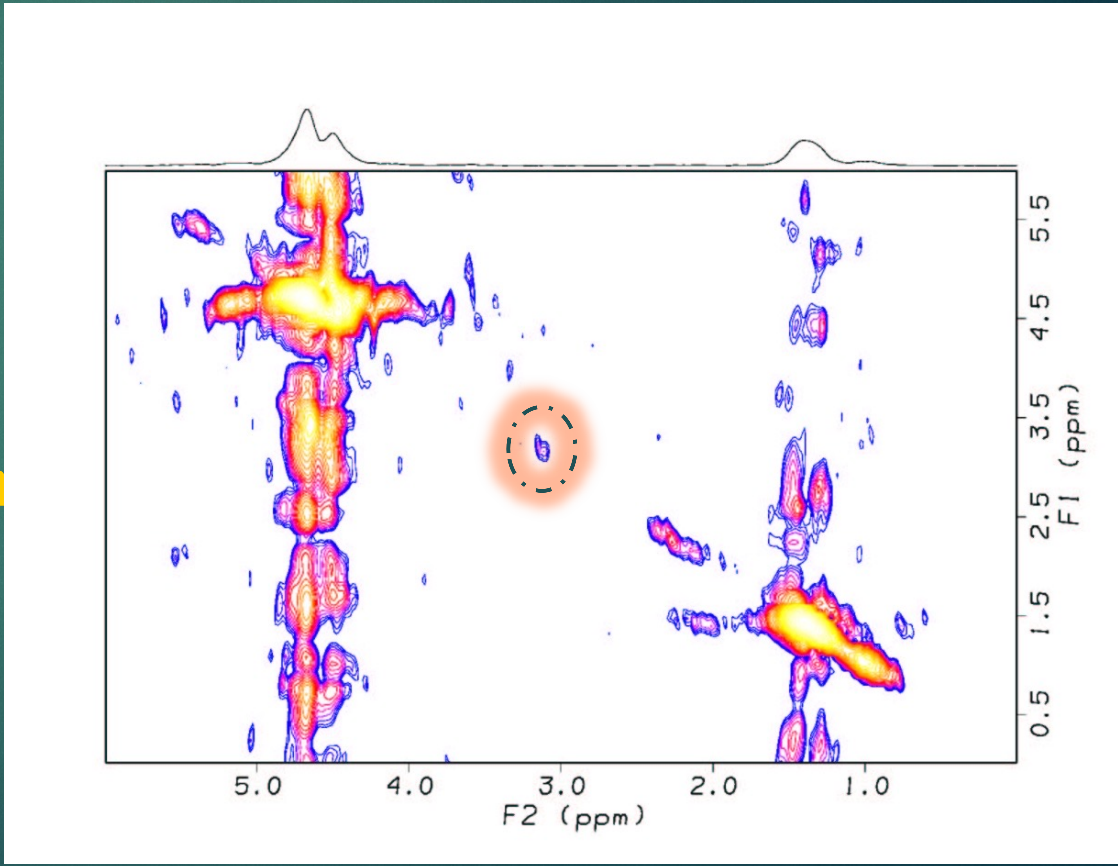

-1x1x1 cm^3

-45 t_1 incr.

-8NEX/ Δ t_1

-12 minutes

4D ^{1}H MR Spectroscopic Imaging: 2 Spectral + 2 Spatial Dimensions

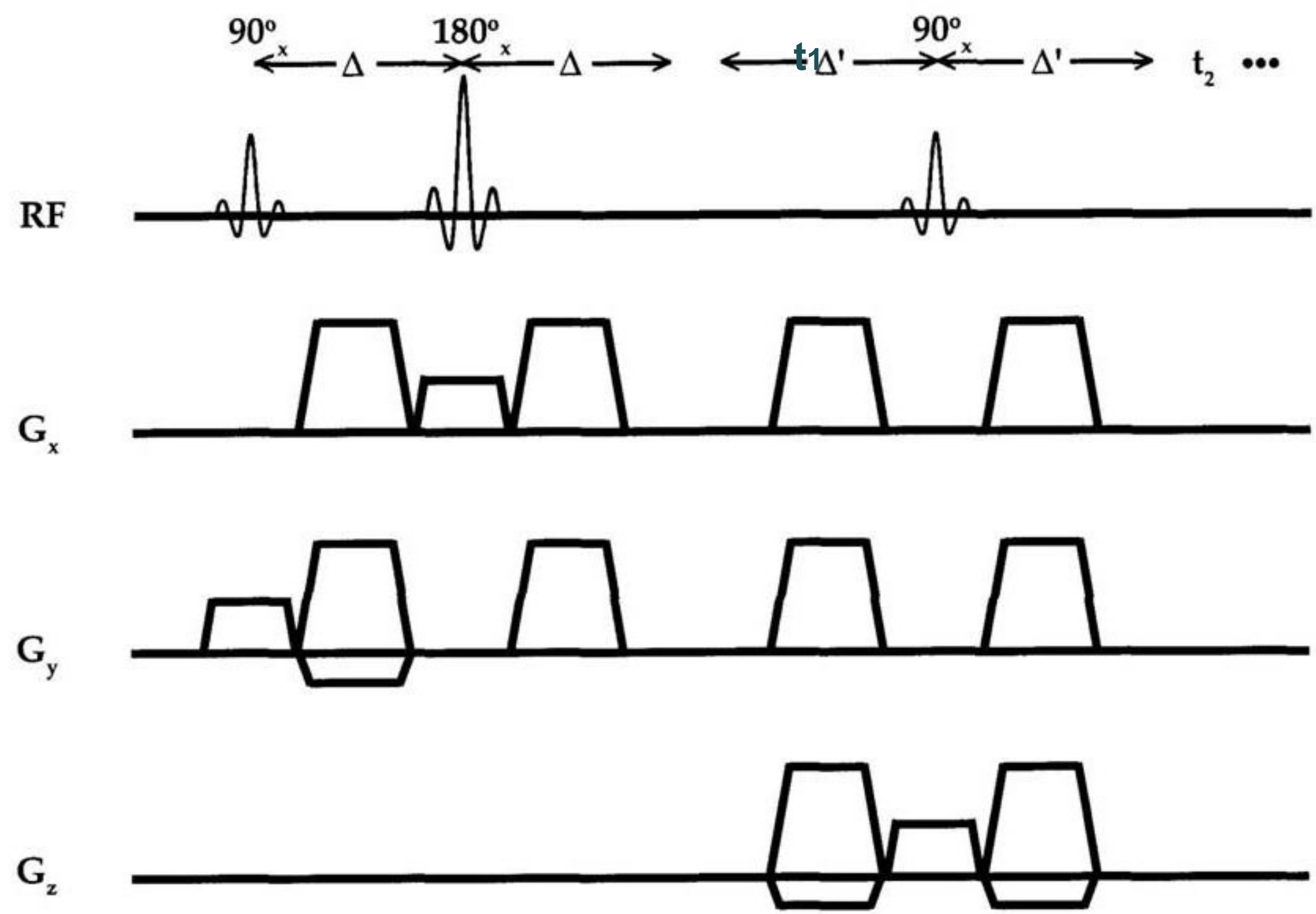

Total Scan time

TR * N $_{(t_1\ \text{Encodings})}$ * Averages

= 2s*128*8= 34minutes

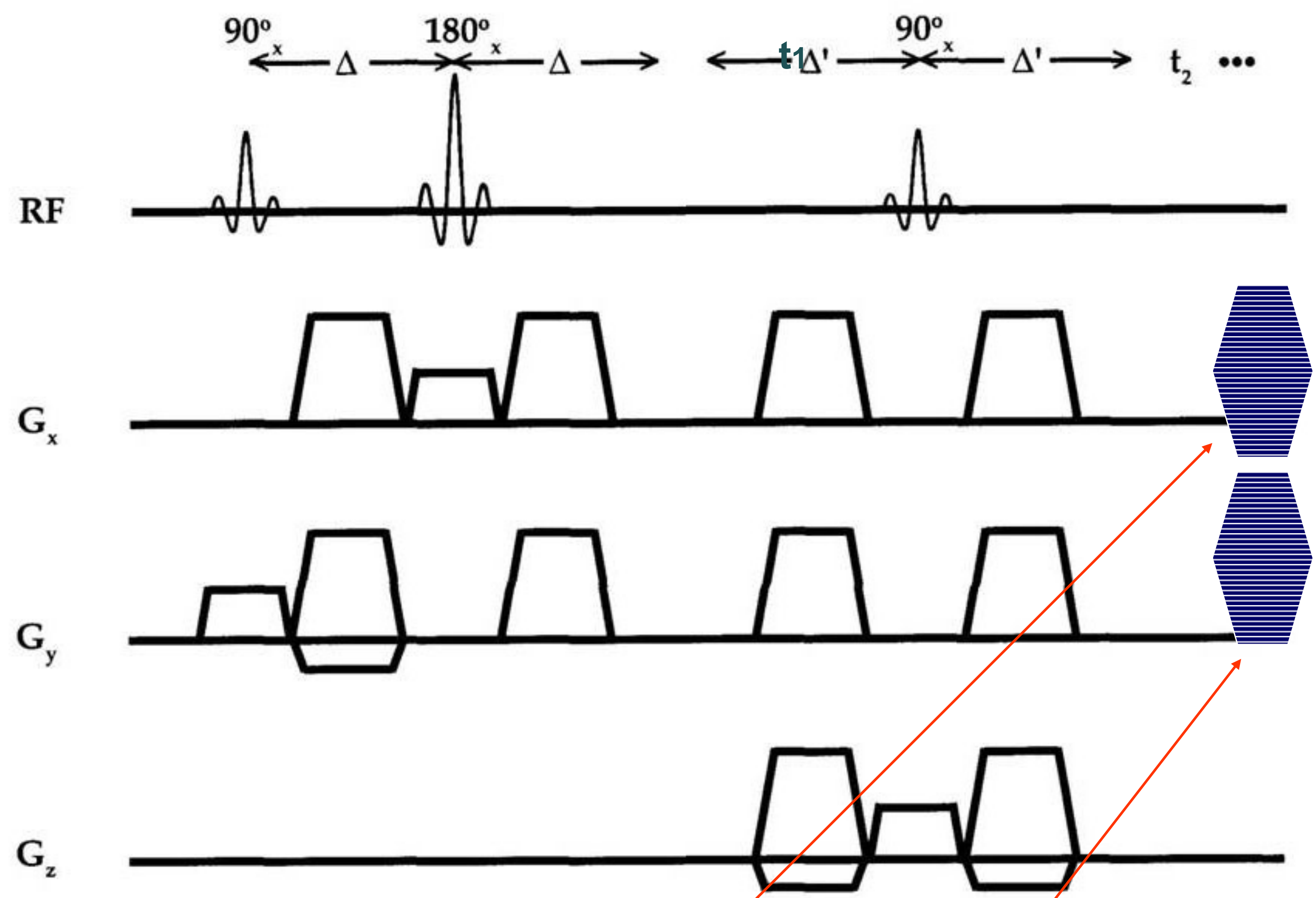

=
2s*128*1*16*1
6
= 546minutes
Or
=2s*128*1*16
= 18.2 hours

Total Scan time

TR* N (t1 Encodings) *N $_{\text{(y-Phase Encodings)}}$ N $_{\text{(X-Phase Encodings)}}$ * N $_{\text{(t1 Encodings)}}$ * Averages

Echo-Planar Correlated Spectroscopic Imaging (EP-COSI)

Scan time = N $_{\text{(X-Phase Encodings)}}$ *** N** $_{(t_1 \text{ Encodings})}$ *** TR**

= 2s*128*1*16 = 68minutes

Lipnick et al, MRM 2010

EP-COSI of Human Calf *in vivo*

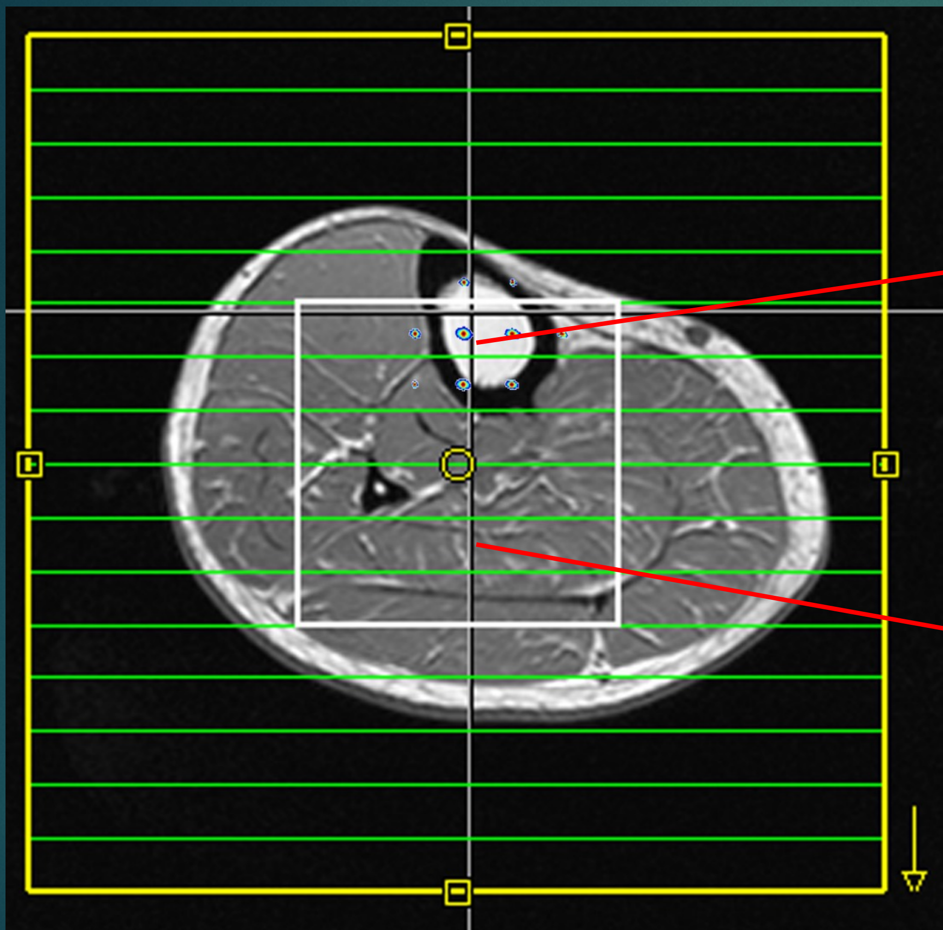

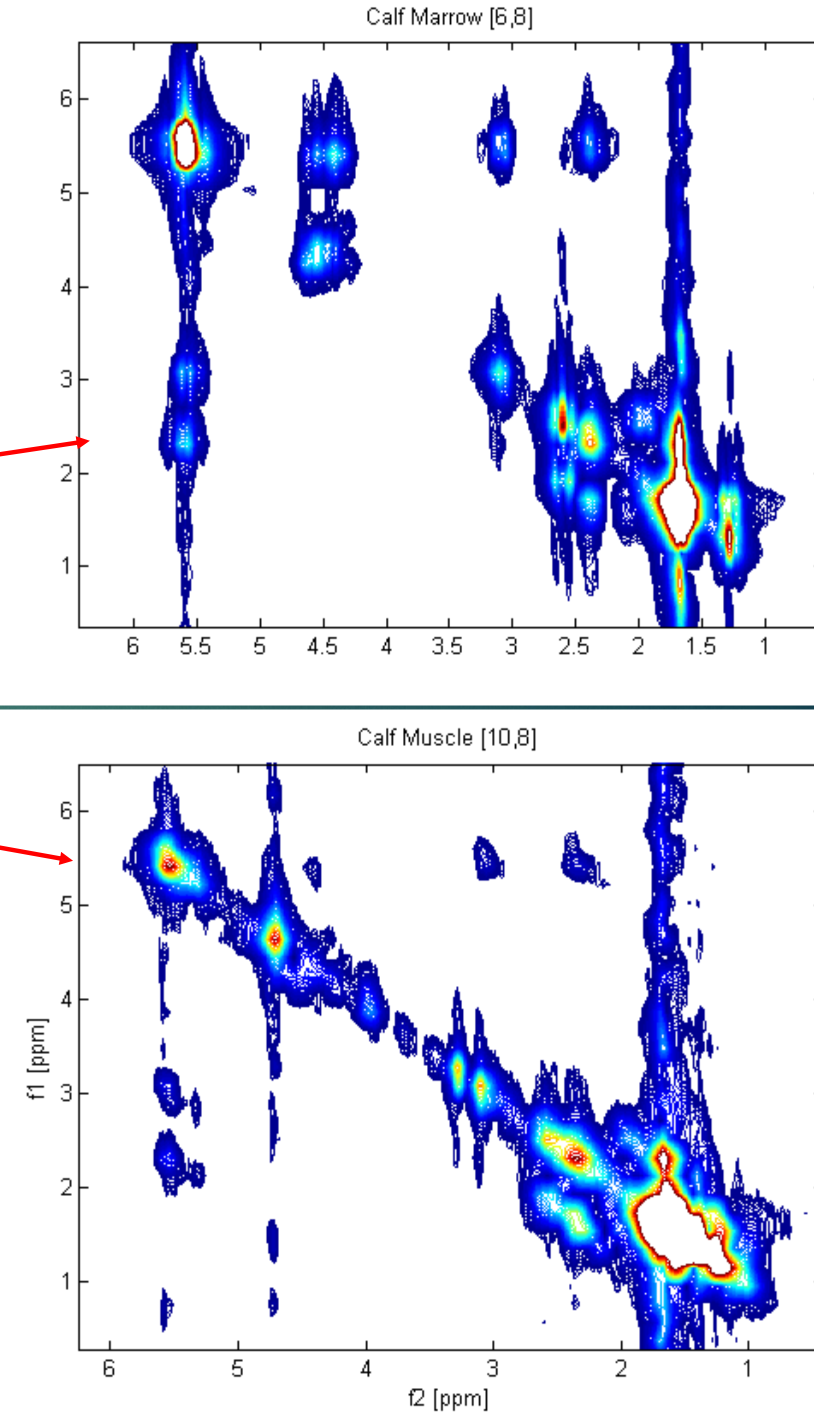

3T MRI, TR/TE=1.5s/30ms,
CP-Ext (T/R), 16x16 (x,y), FOV 16cm,
Extracted VOI of 1x1x2cm^3 and
Total Duration of 20 minutes

5. 2D spectral+ 3D Spatial Encoding

5D Echo-Planar J-resolved Spectroscopic Imaging *with NUS*

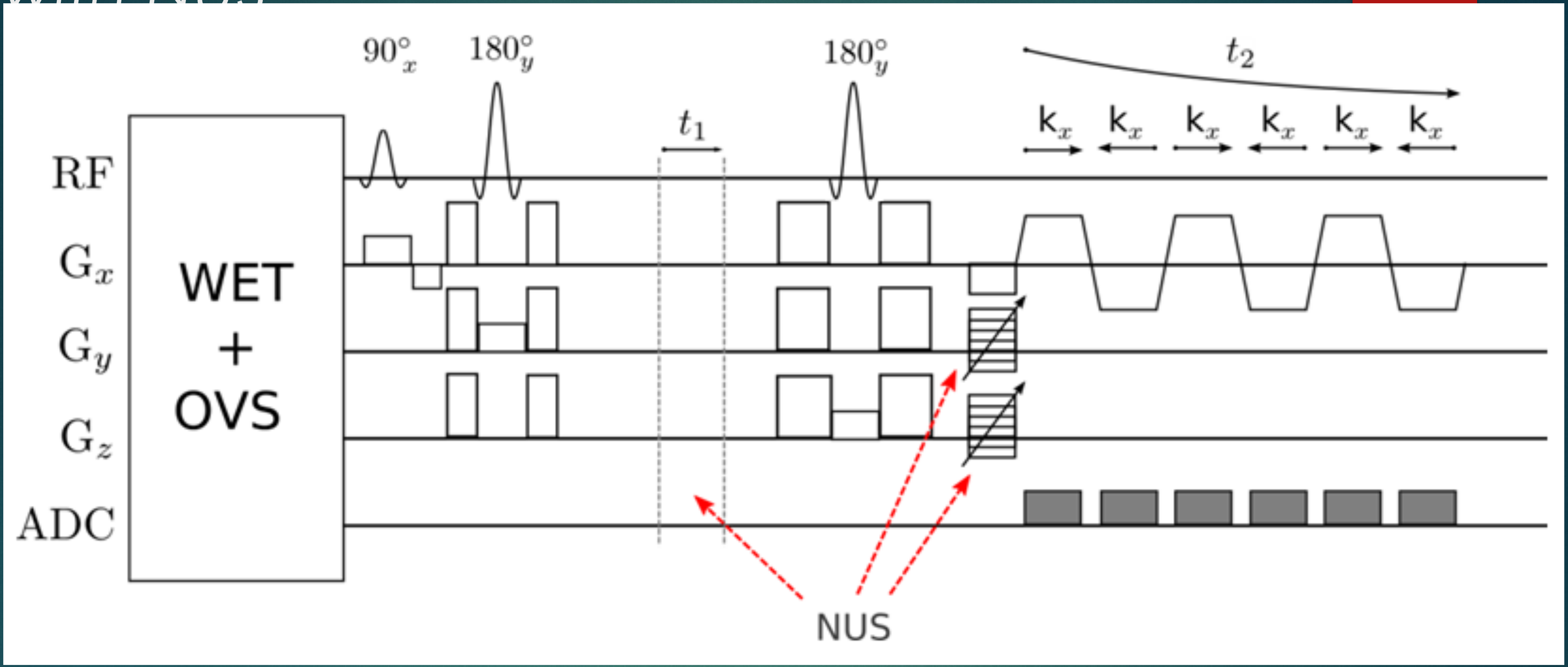

- 3D CSI/MRSI (32x32x16) -410 minutes
  - 3D EPSI (32x16) – 12.8 minutes
- 3D EPSI+2DJRES (32x16x64)- 819 minutes
- 5D EPJRESI (16x8x64) 8X NUS- 21 minutes

Wilson et al, MRM 2016

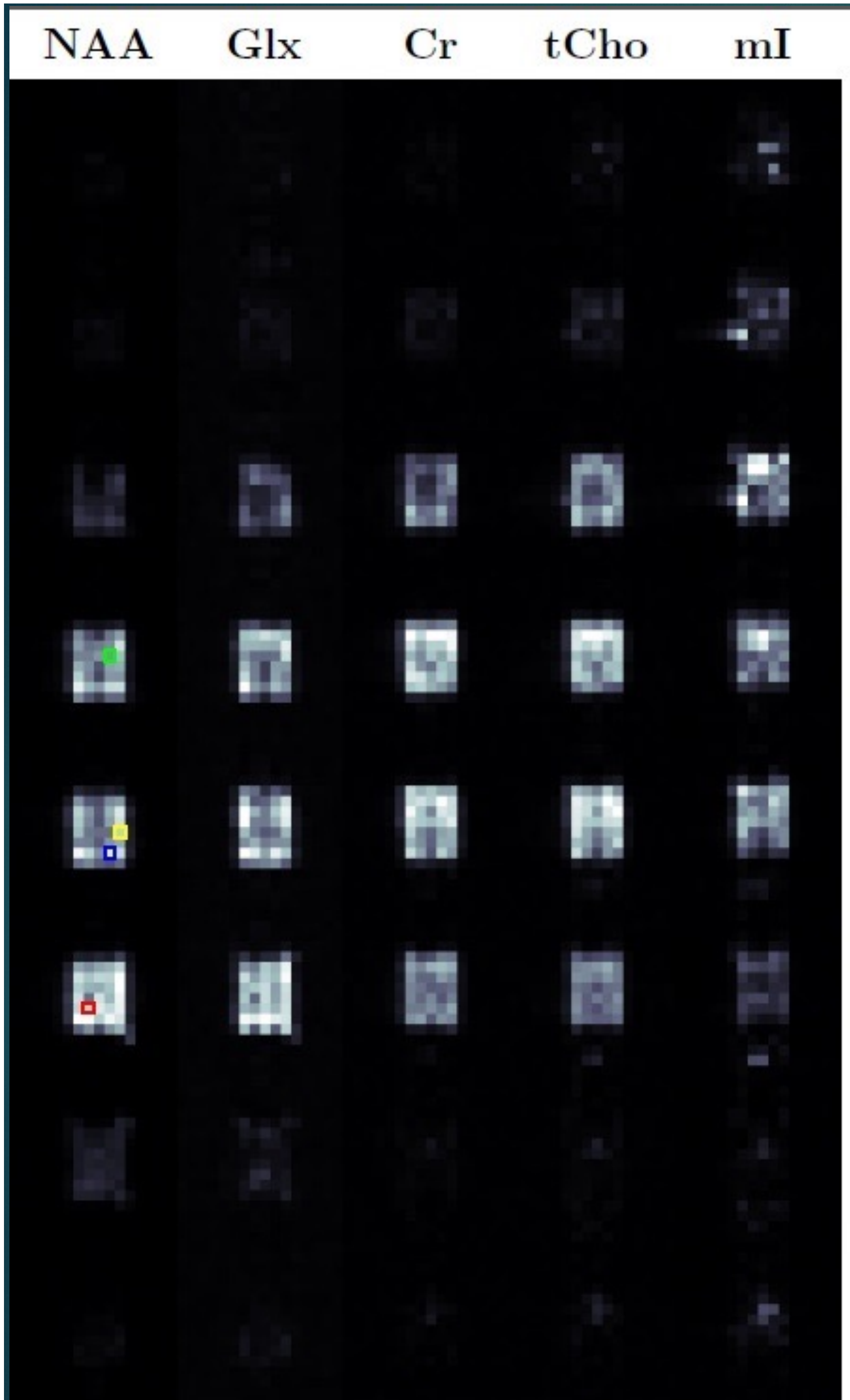

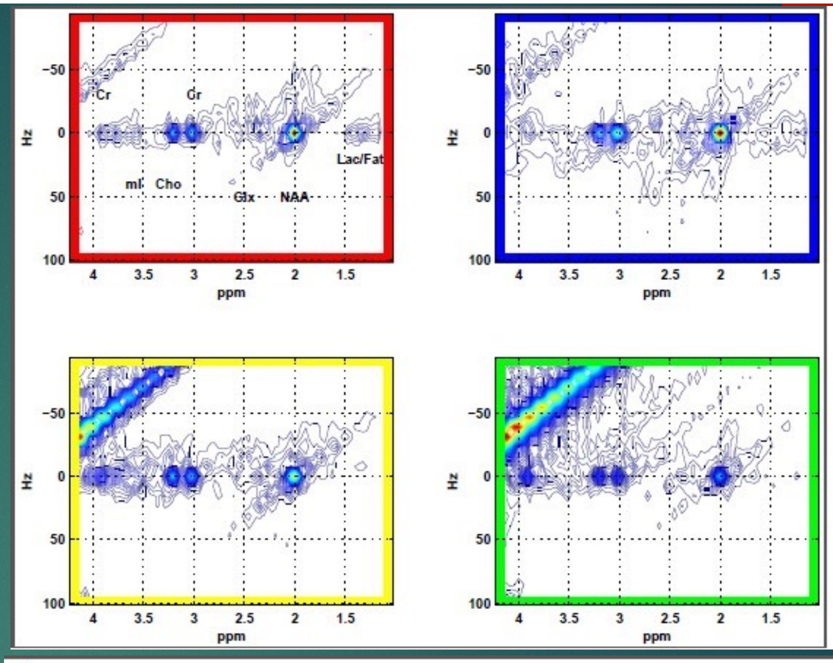

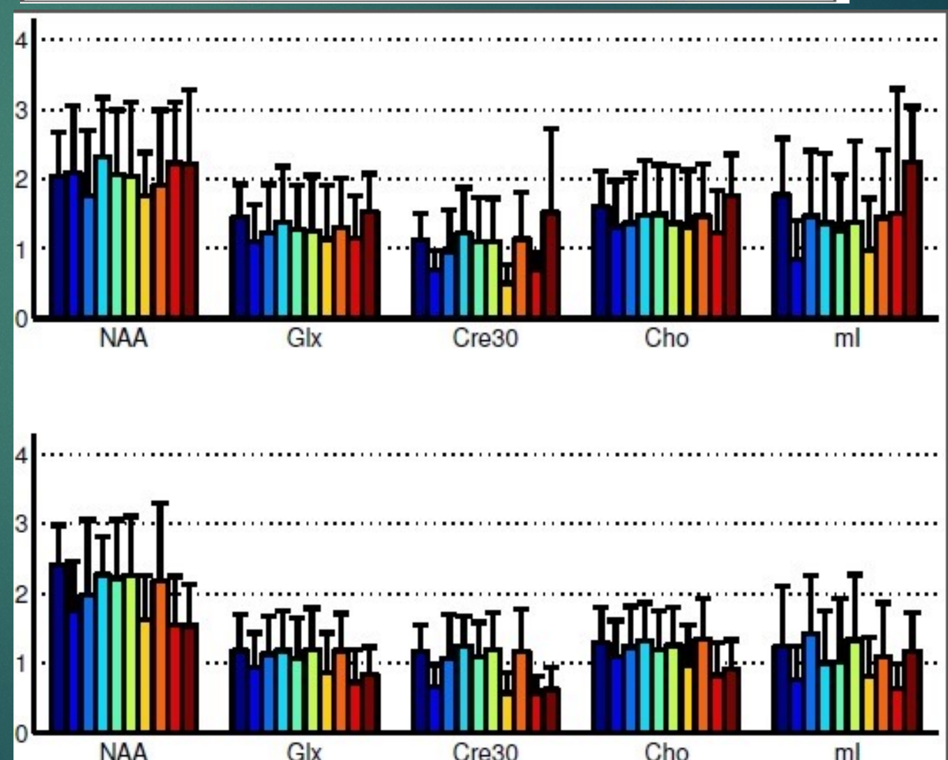

5D EP-JRESI 8X NUS-21 min

Wilson et al, MRM 2016

5D EP-JRESI 8X- OSA

Metabolites →	NAA	Ch	ml	Glx
Healthy Controls				
Occipital White	16.94	8.52	14.33	6.08
Occipetal Gray	1.62	1.56	2.79	10.82
Left Insular Cortex	7.30	6.53	5.19	2.90
Left Parietal Insular Cortex	1.17	8.82	10.31	6.58
OSA patients post CPAP				
Occipital White	9.20	4.92	8.70	14.50
Occipetal Gray	6.03	3.20	4.00	10.00
Left Insular Cortex	2.70	1.22	18.69	1.40
Left Parietal Insular Cortex	2.70	1.97	14.81	9.56

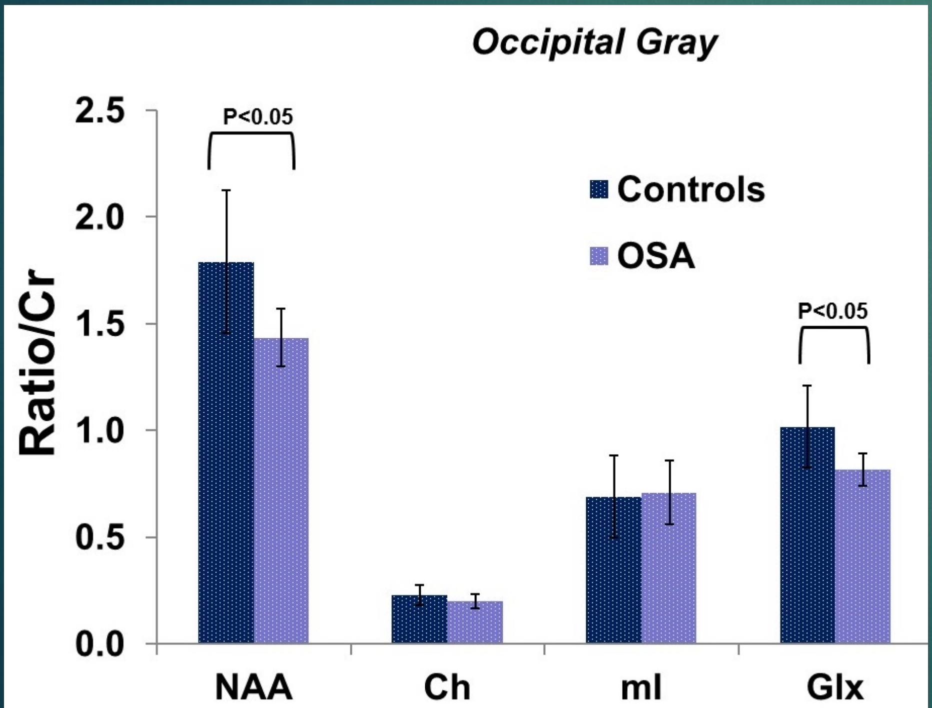

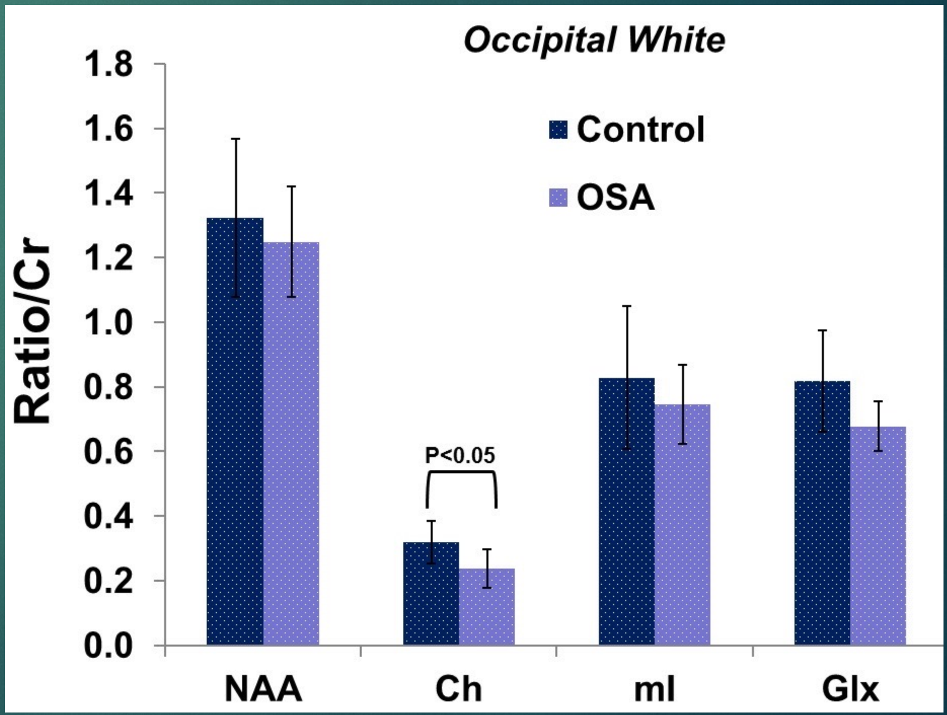

Thomas ISMRM 2016

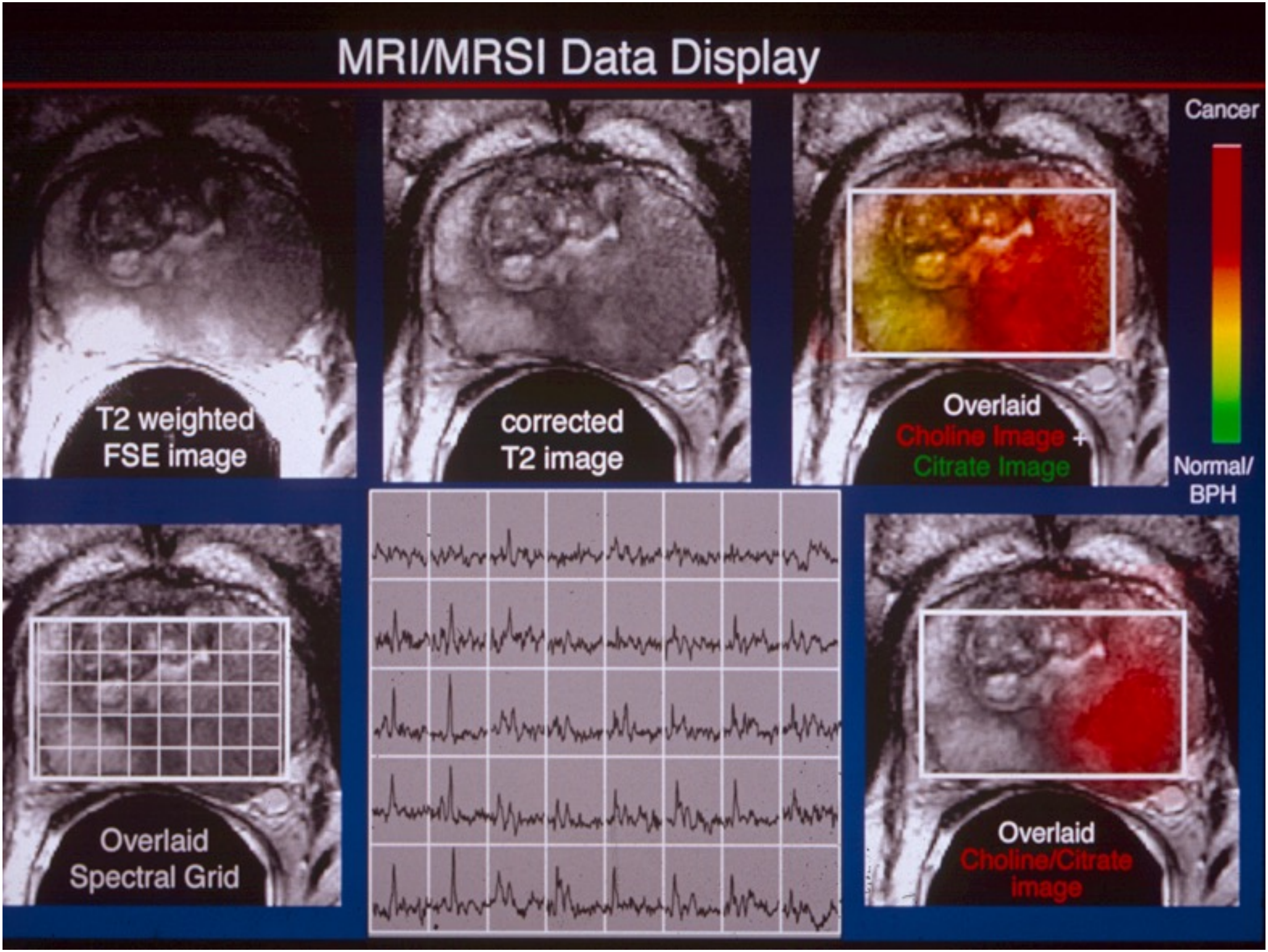
MRI/MRSI Data Display
T2 weighted
FSE image
corrected
T2 image
Overlaid
Choline Image +
Citrate Image
Cancer
Normal/
BPH
Overlaid
Spectral Grid
Overlaid
Choline/Citrate
image

5D MR Spectroscopic Imaging: 3 spatial and 2 spectral dimensions

[redacted]

(a)

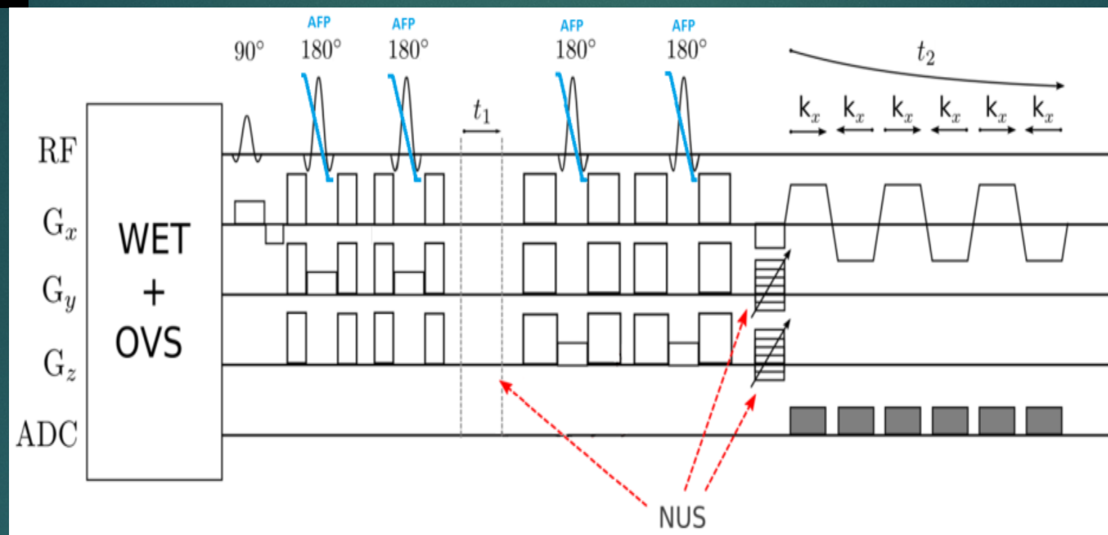

(b) 8x undersampling pattern

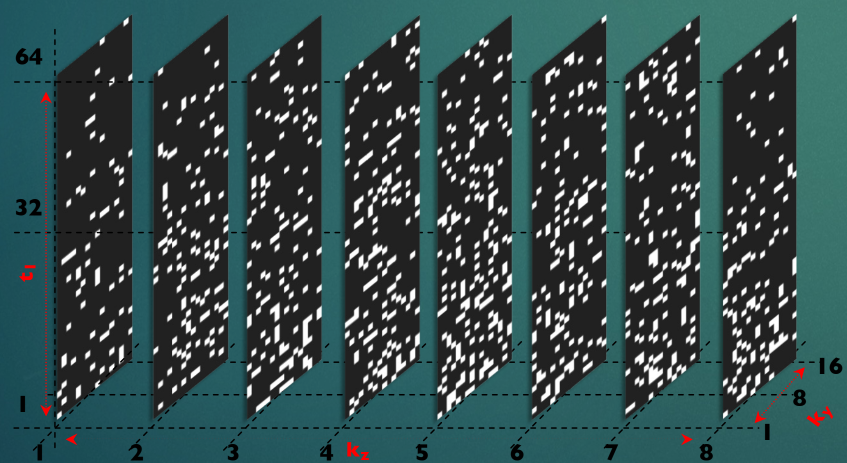

(c) 12x undersampling pattern

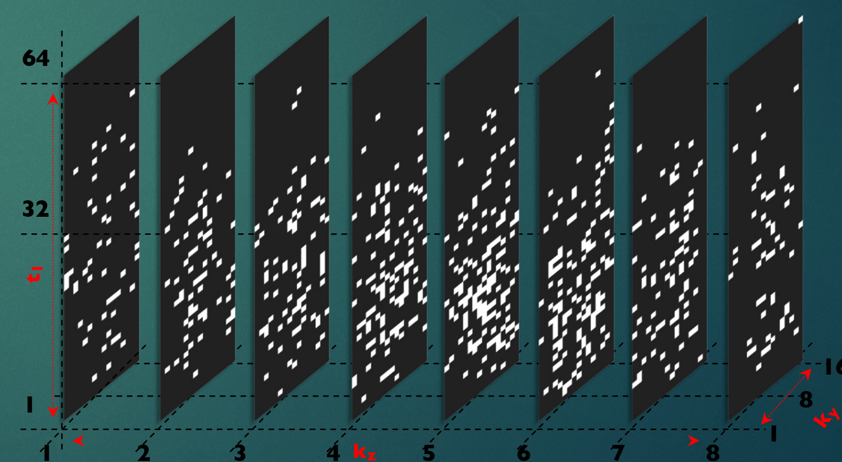

A. Joy, A. Saucedo, Z. Iqbal, et al., MAGMA 2022

Reconstruction results of a prospectively undersampled (8x) 5D EP-JRESI data acquired in a 26-year-old healthy volunteer

[redacted]

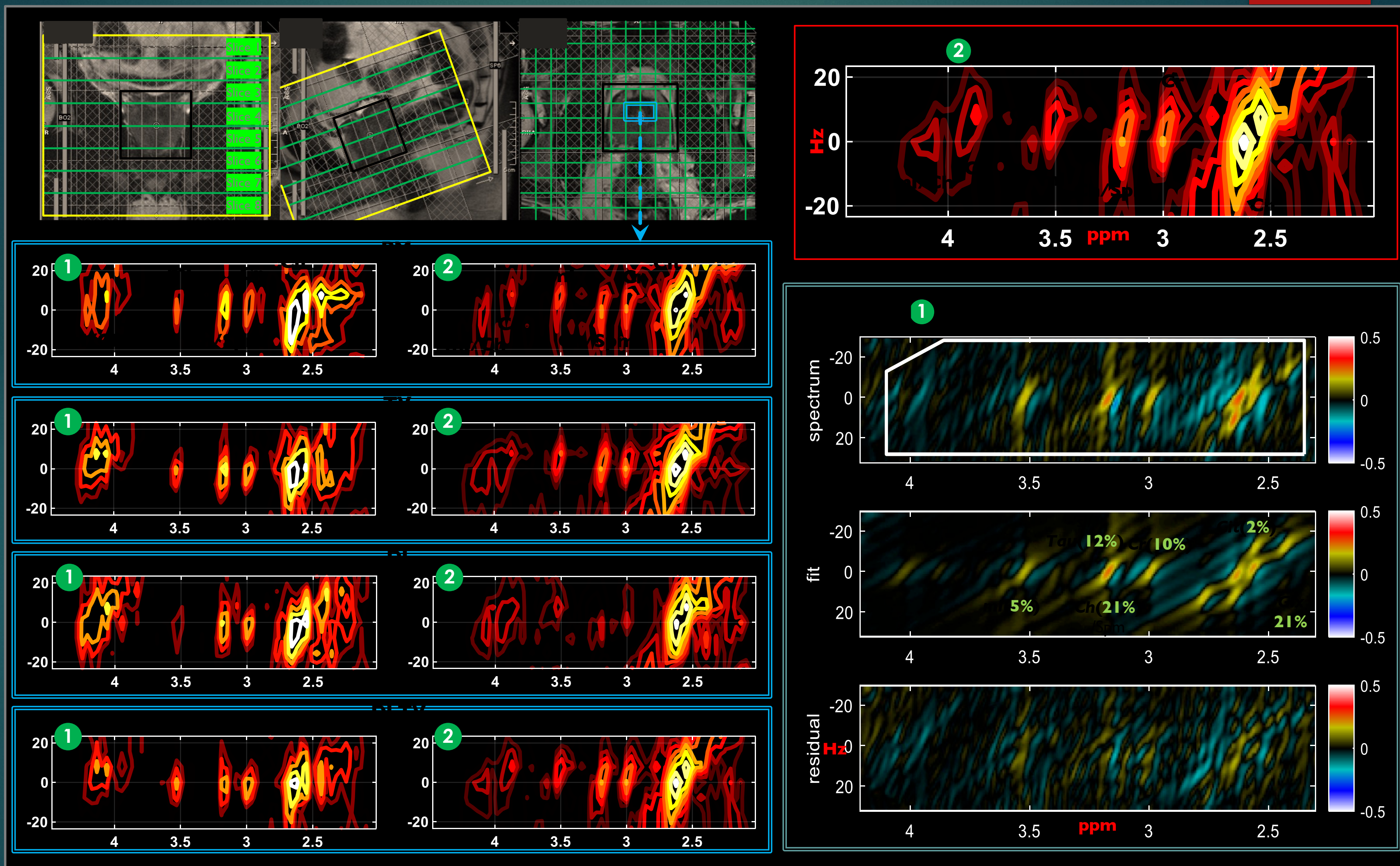

A. Joy, A. Saucedo, Z. Iqbal, et al., MAGMA 2022

Overview of an MRI scanner

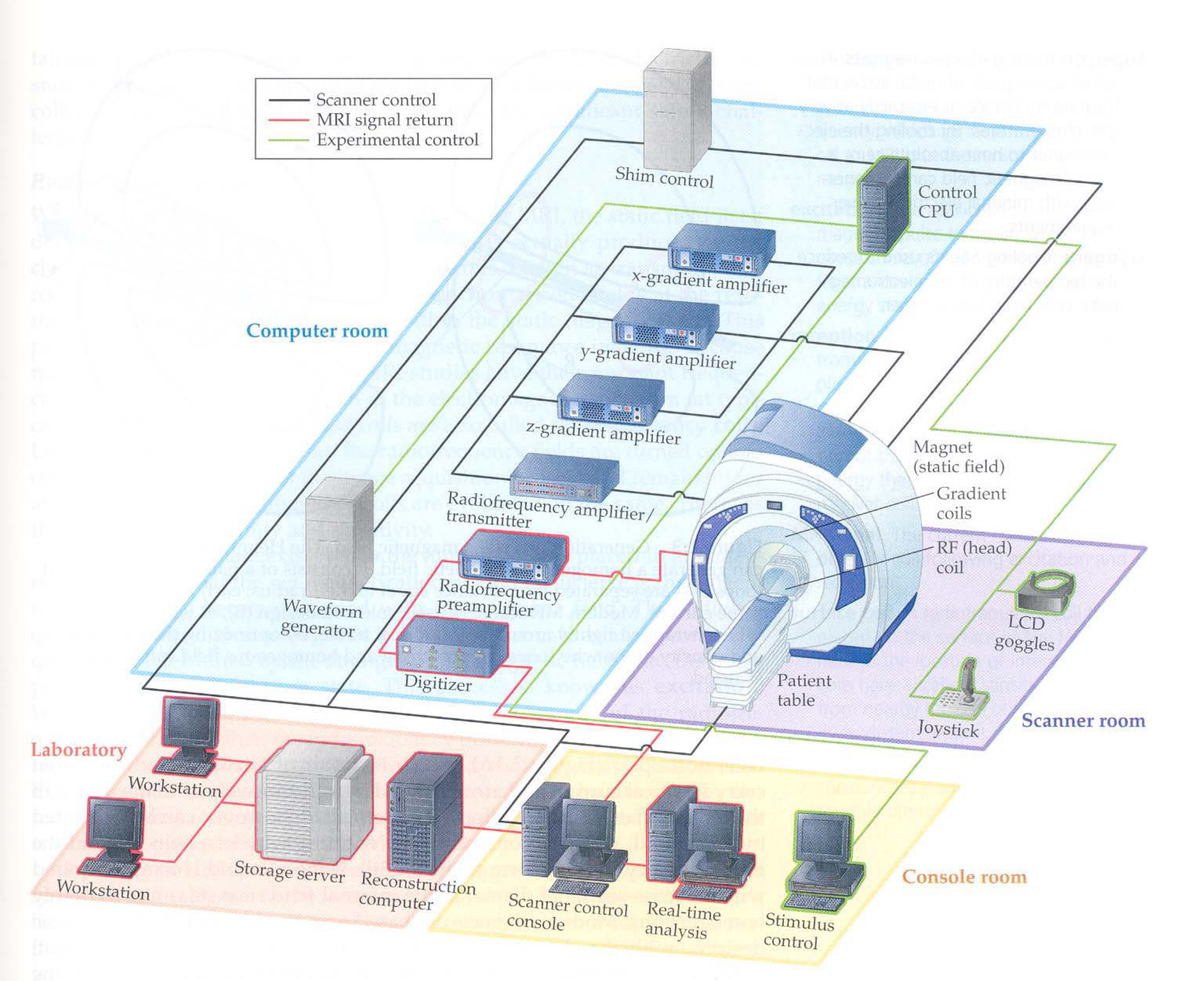

Conclusions

- MRI has become a revolution in Medicine during our time, thanks to NMR!
  - MRI sequences can be easily translated into MR Spectroscopic Imaging
- EPSI, Spiral, SI-CONCEPT and Radial EPSI have been implemented on MRI scanners on 3T, 7T and 9.4T MRI scanners
- Accelerated Polar and Radial MRSI data need gridding to Cartesian; acquisition less than 5 minutes may facilitate functional MRSI
- 3spatial+2 spectral accelerated acquisition & the MRSI data can be post-processed using linear and non-linear reconstruction (Compressed Sensing)
- 6D MRSI (3spatial+3 spectral) and more……………….

PBM222

“Advances in Medical Magnetic Resonance: Clinical MR Spectroscopy and Fast MR techniques”

Course Instructors:
M. Albert Thomas Ph.D.
+
MRRL Faculty

Fall Quarter 2025


THANK YOU
Copyright 2004, WorldStart.com